USGS
science for a changing world

Prepared in cooperation with the County of Maui Department of Water Supply

Groundwater Availability in the Lahaina District, West Maui, Hawai‘i

Scientific Investigations Report 2012–5010

U.S. Department of the Interior
U.S. Geological Survey

COVER:
Aerial view, looking east, of the Ukumehame area, west Maui, Hawai‘i
(Photograph © by Ron Dahlquist Photography. Used with permission.)

USGS
science for a changing world

Groundwater Availability in the Lahaina District, West Maui, Hawai‘i

By Stephen B. Gingerich and John A. Engott

Prepared in cooperation with the County of Maui Department of Water Supply

Scientific Investigations Report 2012–5010

U.S. Department of the Interior
U.S. Geological Survey

U.S. Department of the Interior
KEN SALAZAR, Secretary

U.S. Geological Survey
Marcia K. McNutt, Director

U.S. Geological Survey, Reston, Virginia: 2012

Suggested citation:
Gingerich, S.B., and Engott, J.A., 2012, Groundwater availability in the Lahaina District, west Maui, Hawai‘i: U.S. Geological Survey Scientific Investigations Report 2012–5010, 90 p.

Executive Summary

Much of the public water supply in the Lahaina District, west Maui, Hawai‘i, is pumped from a freshwater lens in volcanic rocks. Because of population growth, groundwater withdrawals from wells in this area are expected to increase from about 5.8 million gallons per day (Mgal/d) in 2007 to more than 11 Mgal/d by 2030. Currently (2011), the salinity of water pumped from some of the wells in the area is higher than acceptable for drinking water. The expected increasing demand for water in an area in which the salinity is already elevated has led to concern over the long-term sustainability of withdrawals from existing and proposed wells. To aid in management of groundwater resources and to plan for sustainable growth on the island, in 2008 the Maui County Department of Water Supply (MDWS) entered into a cooperative agreement with the U.S. Geological Survey (USGS) to study the groundwater availability in the Lahaina District. The objectives of the 4-year study were to estimate the effects of several hypothetical withdrawal scenarios within the District on water levels, the transition zone between freshwater and saltwater, and surface-water/groundwater interactions. For management purposes, the State of Hawai‘i Commission on Water Resource Management delineated the Lahaina area of Maui as an aquifer-management sector (Lahaina Aquifer Sector) containing six hydrologically connected systems; Honokōhau, Honolua, Honokōwai, Launiupoko, Olowalu, and Ukumehame Aquifer Systems (figure ES1). The most intensely developed groundwater body in this area comprises a lens-shaped freshwater body, an intermediate brackish-water transition zone, and underlying saltwater.

Groundwater Recharge and Discharge

Recharge to the Lahaina Aquifer Sector was estimated for six sub-periods: 1926–79, 1980–84, 1985–89, 1990–94, 1995–99, and 2000–04. Estimated recharge for the study area declined 43 percent between the periods 1926–79 and 2000–04. The period 1926–79 had the highest estimated recharge [199 Mgal/d], and recharge from irrigation (mainly for sugarcane) during this period was at least 50 percent higher than in any other period considered. The period 2000–04 had the lowest estimated recharge (113 Mgal/d) because irrigation and thus return flows from irrigation decreased, and rainfall was the lowest of any period. After 1980, recharge has been augmented by direct injection of treated sewage effluent near the coast.

Discharge from the aquifer in the study area occurs as withdrawals from wells, base flow to streams, and diffuse seepage to the ocean. Average withdrawals in the Lahaina Aquifer Sector in 2000–10 were about 4 Mgal/d.

Numerical Groundwater Model

A three-dimensional numerical groundwater model capable of simulating density-dependent solute transport was developed as part of this study. Simulated water levels, the salinity of pumped water, and salinity profiles (values of salinity relative to depth) generally were in agreement with measured water levels, pumped-water salinities, and salinity profiles from representative wells in the modeled area during 1926–2008.

Future Withdrawal and Recharge Scenarios

The groundwater model was used to simulate changes in water levels and salinity under several hypothetical withdrawal and recharge scenarios. Simulated salinities at selected MDWS and private well fields after 30 years (a generally accepted planning horizon) of withdrawal are classified, for the purposes of this study, as acceptable if they are below 1-percent seawater salinity, cautionary if they are between 1- and 2.5-percent seawater salinity, and threatened if they are greater than

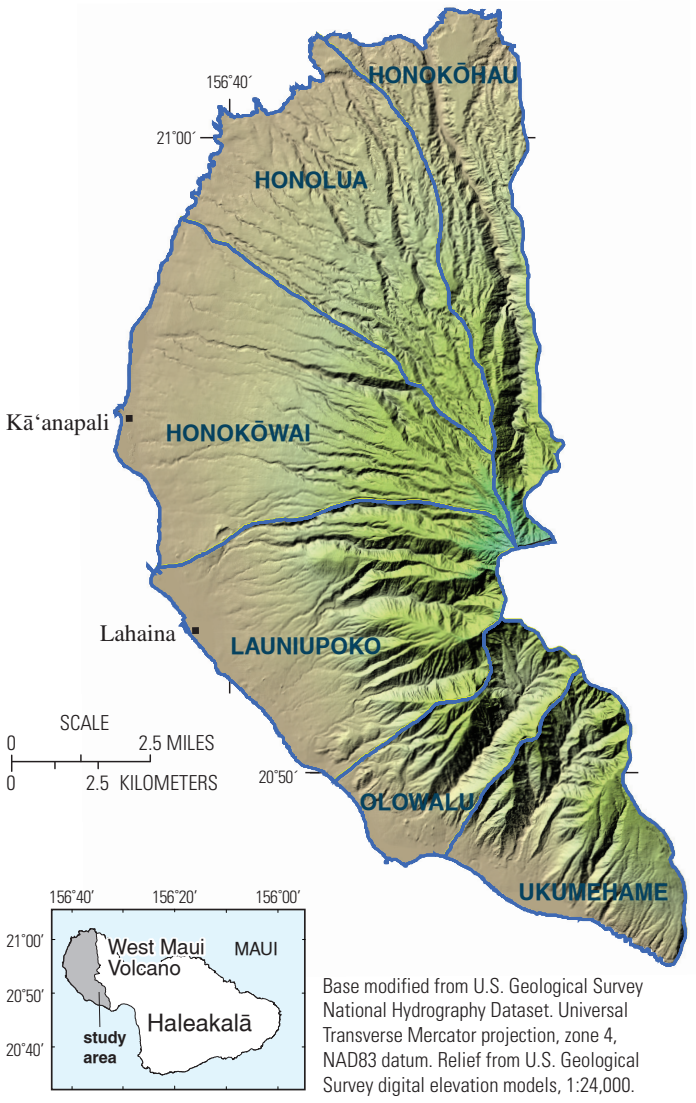

Figure ES1. Location of study area and State of Hawai‘i Commission on Water Resource Management aquifer systems within the Lahaina Aquifer Sector, Maui, Hawai‘i.

2.5-percent seawater salinity. This classification was developed cooperatively by the MDWS and USGS to provide a basis for comparing the various scenarios. Estimated future recharge is lower than historical recharge for the study area owing mainly to decreased irrigation relative to that when sugarcane and pineapple cultivation in the area was widespread. All future recharge estimates are based on continuation of historical average climate conditions, or, in one case, drought rainfall conditions, and do not include potential effects of climate change on rainfall amounts or distribution. The State of Hawai‘i Commission on Water Resource Management typically calculates sustainable-yield estimates based on historical rainfall conditions and land use without irrigation.

Simulations included either 2008–09 withdrawals or proposed withdrawal distributions continued for 30 years into the future. Proposed withdrawal amounts and locations were based on input from the major water users in the area. Model results indicate the following:

1. Projected withdrawals will result in many wells pumping water in excess of 1-percent seawater salinity, and in some cases, in excess of recommended drinking-water standards.
2. Discontinuing diversion of surface water and restoring streamflow in the Lahaina area will enhance groundwater recharge from stream channels and will freshen water pumped by wells, particularly those closest to the streams.
3. A promising area for future groundwater development is the Launiupoko aquifer system, where as much as 10 Mgal/d of freshwater can be developed.
4. Drought conditions may cause increased salinity in water pumped by wells, but the effects of drought will be temporary if rainfall returns to normal following the drought.
5. Injection of treated wastewater in Lahaina affects the groundwater flow system by creating a barrier to inflow of saltwater from the ocean. The effects of wastewater injection on the nearshore ocean environment were not evaluated in this study.

Table ES1. Withdrawal and recharge used in various simulation scenarios, Lahaina District, west Maui, Hawai‘i.

[All simulations are from 2010–2039; Mgal/d, million gallons per day; yr, year]

Scenario	Recharge condition	Pumping condition
1	89 Mgal/d: 2000–04 land use without agriculture; 1926–2004 rainfall	6.3 Mgal/d: 2008–09 withdrawal rates; 2.0 Mgal/d injection
2	89 Mgal/d: 2000–04 land use without agriculture; 1926–2004 rainfall	11.2 Mgal/d: 30-yr projected withdrawal rates; 7.0 Mgal/d injection
3	89 Mgal/d: 2000–04 land use without agriculture; 1926–2004 rainfall	11.2 Mgal/d: 30-yr projected withdrawal rates; no injection
4	89 Mgal/d: 2000–04 land use without agriculture; 1926–2004 rainfall	17.1 Mgal/d: 30-yr projected withdrawal rates with full Hawaii Water Service Company projection; 7.0 Mgal/d injection
5	89 Mgal/d: 2000–04 land use without agriculture; 1926–2004 rainfall	20.7 Mgal/d: Redistributed withdrawal; 7.0 Mgal/d injection
6	105 Mgal/d: 2000–04 land use without agriculture; 1926–2004 rainfall;	11.2 Mgal/d: 30-yr projected withdrawal rates; 7.0 Mgal/d injection added 16 Mgal/d from streambed recharge
7	89 Mgal/d: 2000–04 land use without plantation-scale agriculture; 1926–2004 rainfall with worst historic drought (65 Mgal/d; 1998–2002 rainfall) during 2025–29	11.2 Mgal/d: 30-yr projected withdrawal rates; 7.0 Mgal/d injection

Contents

Figures

Tables

Conversion Factors, Abbreviations, and Datums

Multiply	By	To obtain
Length		
inch (in.)	25.4	millimeter (mm)
foot (ft)	0.3048	meter (m)
mile (mi)	1.609	kilometer (km)
Area		
acre	4,047	square meter (m^2)
square foot (ft^2)	0.09290	square meter (m^2)
square mile (mi^2)	2.590	square kilometer (km^2)
Volume		
million gallons (Mgal)	3,785	cubic meter (m^3)
cubic foot (ft^3)	0.02832	cubic meter (m^3)
Flow rate		
foot per day (ft/d)	0.3048	meter per day (m/d)
foot per year (ft/yr)	0.3048	meter per year (m/yr)
cubic foot per second (ft^3/s)	0.02832	cubic meter per second (m^3/s)
million gallons per day (Mgal/d)	0.04381	cubic meter per second (m^3/s)
inch per hour (in/h)	0 .0254	meter per hour (m/h)
inch per year (in/yr)	25.4	millimeter per year (mm/yr)
Mass		
pound, avoirdupois (lb)	0.4536	kilogram (kg)
Pressure		
atmosphere, standard (atm)	101.3	kilopascal (kPa)
bar	100	kilopascal (kPa)
pound per square foot (lb/ft^2)	0.04788	kilopascal (kPa)
pound per square inch ($lb/in.^2$)	6.895	kilopascal (kPa)
Density		
pound per cubic foot (lb/ft^3)	16.02	kilogram per cubic meter (kg/m^3)
Hydraulic conductivity		
foot per day (ft/d)	0.3048	meter per day (m/d)
Hydraulic gradient		
foot per mile (ft/mi)	0.1894	meter per kilometer (m/km)
Dynamic viscosity		
Slug per foot per second (slug/ft/s)	47.88	Pascal-sec (Pa-s)

Temperature in degrees Celsius (°C) may be converted to degrees Fahrenheit (°F) as follows: °F = (1.8 × °C)+32

Temperature in degrees Fahrenheit (°F) may be converted to degrees Celsius (°C) as follows: °C = (°F-32)/1.8

Vertical coordinate information is referenced to local mean sea level

Horizontal coordinate information is referenced to the North American Datum of 1983 (NAD83).

Altitude, as used in this report, refers to distance above the vertical datum.

Specific conductance is given in microsiemens per centimeter at 25 degrees Celsius (µS/cm at 25 °C).

This page left intentionally blank.

Groundwater Availability in the Lahaina District, West Maui, Hawai‘i

By Stephen B. Gingerich and John A. Engott

Abstract

Most of the public water supply in the Lahaina District, west Maui, Hawai‘i, is pumped from a freshwater lens in volcanic rocks. Because of population growth, groundwater withdrawals from wells in this area are expected to increase from about 5.8 million gallons per day in 2007 to more than 11 million gallons per day by 2030. Currently (2011), the salinity of water pumped from some of the wells in the area exceeds acceptable limits for drinking water. The expected increasing demand for water in an area in which the salinity of water is already unacceptable has led to concern over the long-term sustainability of withdrawals from existing and proposed wells.

A three-dimensional numerical groundwater flow and transport model was developed to simulate the effects of hypothetical withdrawal and recharge scenarios on water levels and on the transition zone between freshwater and saltwater. The model was constructed using time-varying recharge, withdrawals, and ocean levels. Hydraulic characteristics used to construct the model were initially based on published estimates but ultimately were varied to obtain better agreement between simulated and measured water levels and salinity profiles in the modeled area during 1926–2008. Scenarios included groundwater withdrawal at 2008–09 rates and locations with projected recharge (based on 2000–04 land use, no agricultural irrigation, and the rainfall record for the period 1926–2004) and withdrawal at redistributed rates and locations with several different recharge scenarios.

Simulation results indicate that continuing the 2008–09 withdrawal rates and distribution (6.3 million gallons per day from 21 wells) into the future would result in decreased water levels, a thinner freshwater lens, and increased salinity of water pumped from wells. Groundwater demand projections and proposed new well sites were used to produce a projected withdrawal rate and distribution during 2010–39. Simulation results from this projected withdrawal scenario (11.2 million gallons per day from 28 wells, including 10 proposed wells) also indicate decreased water levels, a thinner freshwater lens, increased water salinity, and unacceptable salinity at several current withdrawal sites, mainly in the Honokōwai Aquifer System; however, more groundwater is available than in the previous scenario. A simulation in which injection of treated wastewater is stopped indicates that several wells will have increased salinities compared to the scenario in which injection continues.

A scenario in which increased groundwater withdrawal was redistributed in an attempt to maximize withdrawal while maintaining acceptable salinities in the withdrawn water was simulated. The redistributed withdrawal simulates 20.7 million gallons per day of withdrawal from 26 wells or well fields in the Lahaina District. Simulation results indicate the following: (1) average water levels decrease by about 0.5–1 feet and the transition zone rises 20–50 feet in some areas after 30 years, mainly in the Launiupoko Aquifer System near the proposed wells, and (2), all wells produce water with salinities in the acceptable class (less than one-percent seawater salinity) after 30 years.

Introduction

The resident population on the island of Maui, Hawai‘i, grew from 38,691 in 1970 to 144,444 in 2010, which represents an increase of more than 250 percent (State of Hawai‘i Department of Business, Economic Development, & Tourism, 2011). The total population on Maui grew about 23 percent during 2000–10. Because of the increase in population, the demand for groundwater for domestic supply also increased, and groundwater withdrawals likely will continue to increase in the future. Demand for groundwater provided by the County of Maui Department of Water Supply (MDWS) in the Lahaina area is estimated to increase from about 2.1 million gallons per day (Mgal/d) in 2007 to 3.5 Mgal/d in 2030 (Carl Freedman, Haiku Design and Analysis, written commun., 2010). Accounting for groundwater pumped by several private water systems in the area, the total demand for groundwater is expected to increase from 5.8 Mgal/d in 2007 to 11.1 Mgal/d in 2030. However, the amount of groundwater that is available in the Lahaina area to meet future water demands is uncertain.

For management purposes, the State of Hawai‘i Commission on Water Resource Management (CWRM) delineated the Lahaina area of Maui as an aquifer-management sector (Lahaina Aquifer Sector), and further divided the sector into six hydrologically connected aquifer systems: Honokōhau, Honolua, Honokōwai, Launiupoko, Olowalu, and Ukumehame Aquifer Systems (fig. 1).

In a near-shore, freshwater-lens system with steady recharge, increased withdrawals will, in the long term, result in water-level decline, a shallowing of the transition zone between freshwater and saltwater, and a reduction of natural groundwater discharge to streams or to the ocean. The extent to which water levels decline and the transition zone rises is dependent on factors including the distribution and rates of withdrawals and the hydraulic

Figure 1. Location of Lahaina District and State of Hawai‘i Commission on Water Resource Management aquifer systems within the Lahaina Aquifer Sector, Maui, Hawai‘i.

characteristics of the aquifer system. In some cases, pumping from a well also may induce brackish water to enter the well if the withdrawal rate is too high or the well is too deep.

The chloride concentrations of water pumped from wells in the Lahaina area increase in response to increased withdrawals on a monthly basis (MDWS, unpub. data). Chloride concentrations in water pumped from several MDWS wells has exceeded 250 mg/L, which is the recommended secondary standard for drinking water (U.S. Environmental Protection Agency, 2011). Chloride concentrations in the pumped water have been as high as 877 mg/l in 1992 and were recently as high as 349 mg/l in 2006. Data are insufficient, however, to determine whether a long-term regional change in the transition zone has taken place. Data from a deep monitoring well in the area show no rise in the middle of the transition zone during 2001–06 (Commission on Water Resource Management, 2008); however, movement in the future may take place as the aquifer adjusts to changes in withdrawals (Rotzoll and others, 2010). The potential rise in the transition zone between freshwater and saltwater and increases in chloride concentrations in pumped water, and the large increase in expected withdrawals have led to concern over the long-term sustainability of withdrawals from existing wells in the Lahaina area. That concern lead the MDWS to enter into a cooperative agreement in 2008 with the U.S. Geological Survey (USGS) to conduct a groundwater-availability study in the Lahaina area of west Maui. The objective of this 4-year study is to estimate the effects of several hypothetical withdrawal scenarios within the Lahaina area, on water levels, the transition zone between freshwater and saltwater, and surface-water/groundwater interactions using a numerical groundwater flow and transport model.

This report describes (1) information related to the regional hydrologic system of the Lahaina area of west Maui, (2) development of a numerical groundwater flow and transport model, and (3) results of model simulations assessing the hydrologic effects of various recharge and withdrawal conditions on the hydrologic system.

Acknowledgments

The authors are grateful to MDWS Director David Taylor and former Director Jeffrey Eng and the MDWS staff for their cooperation and assistance, especially in discussing potential withdrawal and recharge scenarios. Carl Freedman of Haiku Design and Analysis provided valuable assistance in developing the withdrawal scenarios. Art Oughton, Terry Tamble, James Smith, and the staff at Hawaii Water Service Company (HWSC), Jeffrey Pearson of Maui Land & Pineapple Co., Inc. (ML&P), and David Minami and Ryan Grether of West Maui Land Company, Inc. provided pumping and salinity data and arranged access and cooperation for collecting water-level data in their wells. Other well owners who kindly provided access to their wells include the County of Maui Department of Parks and Recreation and CWRM. Jeff Perreault of the USGS provided support in resurveying measuring points and collecting valuable water-level data during the study. Ed Carlson of the National Geodetic Survey led the effort to resurvey benchmarks and measuring points for wells throughout the study area. The authors thank ML&P, Kā‘anapali Land Management Corporation, Kā‘anapali Farms, West Maui Land Company, Inc., and Kamehameha Schools for permission to access their land to measure streamflow. Finally, the authors thank the concerned citizens of Maui who continued asking questions and providing feedback and encouragement at our presentations throughout the study.

Setting of Study Area

Maui, the second largest of the Hawaiian Islands, lies between lat 20º32' N and 21º03' N and long 155º57' W and 156º47' W (fig. 1). The island is composed of two shield volcanoes, the older West Maui Volcano, which reaches 5,788 ft in altitude at Pu‘u Kukui, and the younger Haleakalā (East Maui Volcano), which reaches an altitude of 10,025 ft. The two volcanoes are connected by an isthmus as much as 5 mi wide and at altitudes generally less than 300 ft, which is covered with terrestrial and marine sedimentary deposits (Stearns and Macdonald, 1942). The main area of interest for this study is the Lahaina District, which covers the western half of West Maui Volcano. West Maui Volcano is deeply dissected by numerous streams, which originate near its summit. Topography within the study area ranges from a gently sloping surface rising away from the coast to steep interior mountains.

Land Use

Gently sloping areas around west Maui have been used for agriculture for more than a century. The urban areas mainly are along the coast and include numerous resorts. The west Maui interior is mostly forested conservation land. Historically, the principal agricultural crops (fig. 2) have been sugarcane and pineapple, but recently the types of crops planted have become more diversified. The historical changes in agricultural practices within the study area were characterized by Engott and Vana (2007) to estimate changes in irrigation-water application, and the following section on land use is summarized from their work. From the early 1900s until about 1999, land use was mostly unchanged except for some minor urban development along the coast. However, as large-scale plantation agriculture declined after 1999, land-use changes became pronounced, and during 2000–04, plantation-scale agricultural land (mainly sugarcane acreage) decreased by about 79 percent relative to land use prior to 1999.

The Pioneer Mill Co. was a major sugarcane cultivator from the late 1800s until 1999, when it ceased sugarcane production, and the land was subsequently bought by ML&P and other private investors. ML&P grew pineapple on the northwest slope of West Maui Mountain, where pineapple had a long history of cultivation, and in a small area of former Pioneer Mill Co. sugarcane lands. However, the extent of pineapple cultivation in west Maui decreased considerably since the late 1990s and ceased in 2009.

Climate

The topography of Maui and the location of the north Pacific anticyclone relative to the island affect its climate, which is characterized by mild and uniform temperatures, seasonal variation in rainfall, and great geographic variation in rainfall (Blumenstock and Price, 1967). During the warmer dry season (May–September), the stability of the north Pacific anticyclone produces persistent northeasterly winds, known locally as trade winds, which blow 80–95 percent of the time. During the cooler rainy season (October–April), migratory weather systems commonly travel past the Hawaiian Islands, resulting in less persistent trade winds that blow 50–80 percent of the time. Low-pressure systems and associated southerly winds can bring heavy rains to the island and the dry coastal areas can receive most of their annual rainfall from these systems.

The variation in mean annual rainfall with altitude is extreme on Maui, with differences of more than 130 inches within one mile of Pu‘u Kukui (fig. 3) (Giambelluca and others, 1986). At Pu‘u Kukui, average annual rainfall during 1928–2010 exceeded 366 in/yr but during 2000–10, average rainfall was about 280 in/yr (U.S. Geological Survey, 2011). Mean annual rainfall at the coast in the dry leeward areas is lower than 15 in. In a recharge study for Central and West Maui, Engott and Vana (2007) determined that fog interception, which can provide additional precipitation not measured by standard rain gages, could be as much as 20 percent of measured annual rainfall.

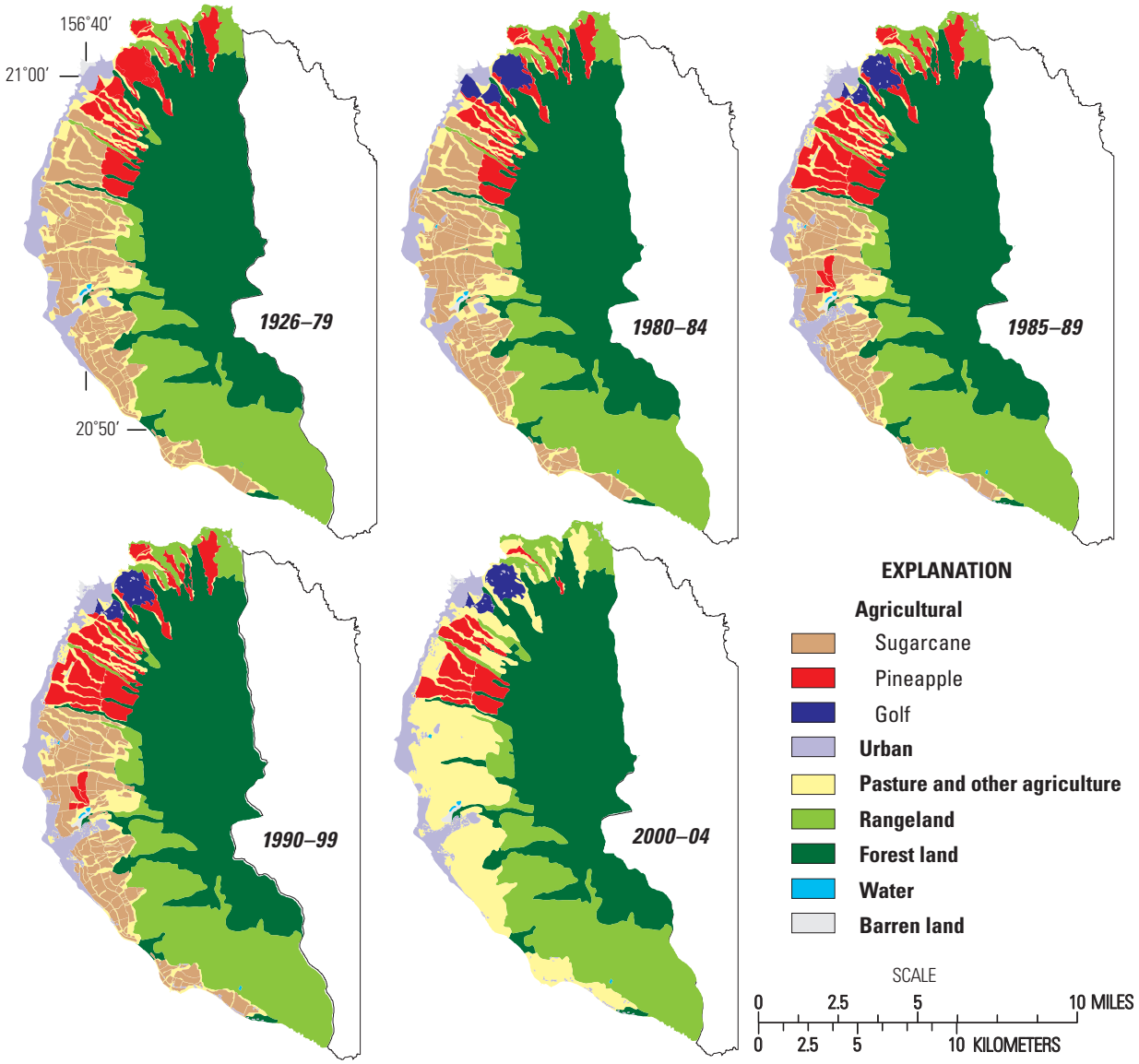

Base modified from U.S. Geological Survey National Hydrography Dataset, 1:24,000, Universal Transverse Mercator projection, zone 4, NAD83 datum.

Figure 2. Land use during 1926–2004 in the Lahaina District, west Maui, Hawai‘i (modified from Engott and Vana, 2007).

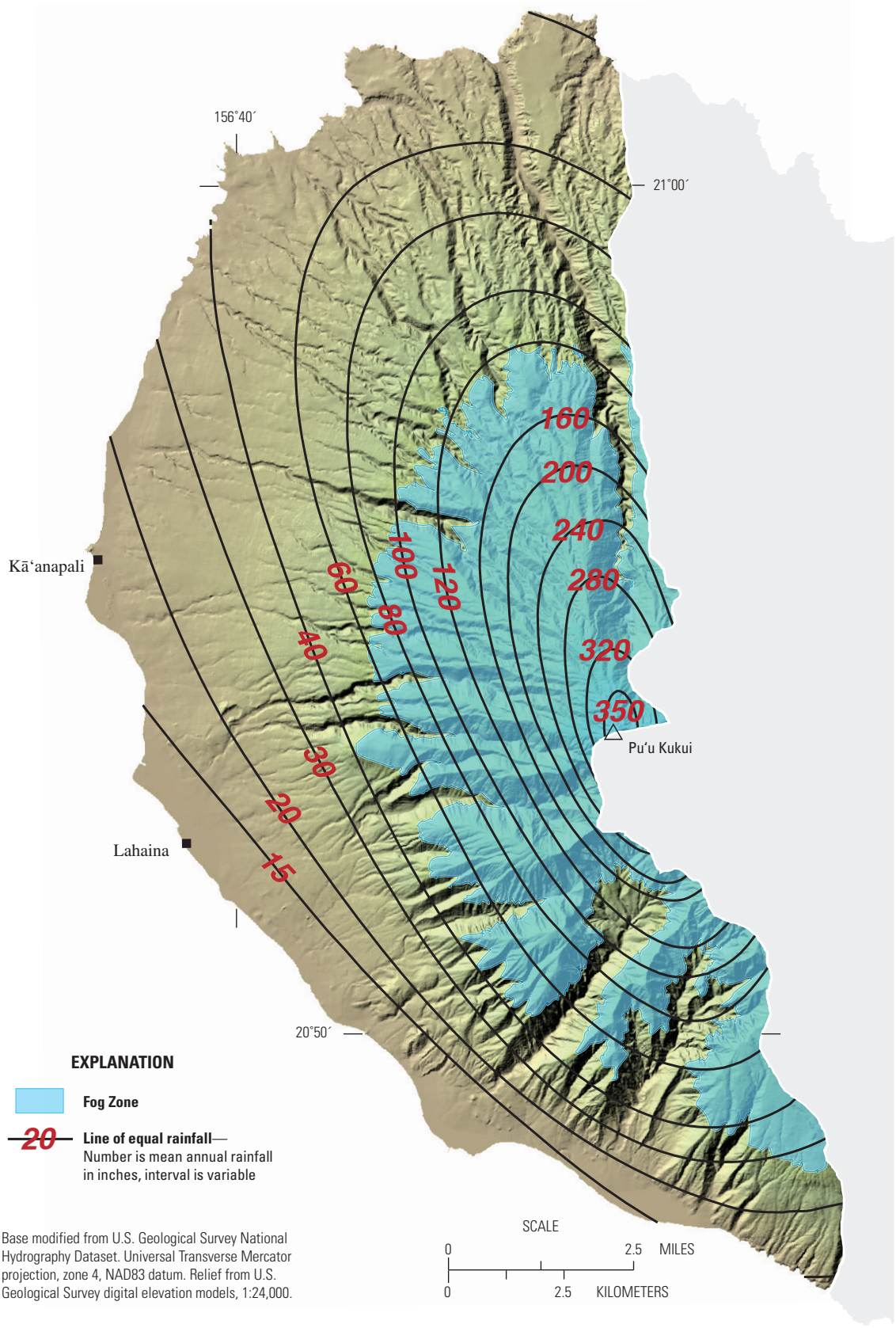

Figure 3. Mean annual rainfall in the Lahaina District, west Maui, Hawai‘i (modified from Giambelluca and others, 1986).

Geology

The geology of Maui was described in detail by Stearns and Macdonald (1942), and some of the geologic units were subsequently reclassified by Langenheim and Clague (1987). West Maui Volcano has a central caldera and two main rift zones that trend in northwestern and southeastern directions from the caldera (fig. 4). Thousands of dikes exist within the rift zones, with the number of dikes increasing toward the caldera and with depth. Additional dikes exist outside the trends of the rift zones, creating a radial pattern of dikes emanating from the caldera (Macdonald and others, 1983). Thousands of lava flows have erupted from vents in and near the caldera and rift zones.

The rocks of West Maui Volcano consist of the mostly shield-stage Wailuku Basalt, which is overlain by the postshield-stage Honolua Volcanics and rejuvenated-stage Lahaina Volcanics. The Wailuku Basalt consists of tholeiitic basalt, olivine-tholeiitic basalt, and picritic tholeiitic basalt, and postshield-stage caldera-filling lava of alkalic basalt, and includes lava flows with associated intrusive rocks and pyroclastic and sedimentary deposits (Langenheim and Clague, 1987, p. 79). Individual lava flows range from 1 to 100 ft in thickness and dip between 5–20 degrees away from their sources (Stearns and Macdonald, 1942, p. 161). The Honolua Volcanics consist of mugearite, trachyte, and hawaiite, and include lava flows and associated domes, dikes, and pyroclastic deposits (Langenheim and Clague, 1987, p. 79). The thickness of individual flows ranges from 25 to 300 ft and may reach 500 ft near vents (Stearns and Macdonald, 1942, p. 173). These flows average about 75 ft thick and generally form a veneer on the older Wailuku Basalt. Isotopic analyses indicate a Pleistocene age for the Wailuku Basalt and Honolua Volcanics (McDougal, 1964; Naughton and others, 1980). The Lahaina Volcanics consist of Pleistocene-age basanite and picritic basanite, and include lava flows and associated pyroclastic deposits (Langenheim and Clague, 1987, p. 79). These rock types are not widespread and all lie on the west side of West Maui Volcano (Stearns and Macdonald, 1942, p. 180).

Wedges of sedimentary deposits are present at several areas along the coast, mainly at the mouths of stream valleys. Sedimentary deposits throughout Maui have been divided into consolidated earthy deposits, calcareous sand dunes, and unconsolidated deposits (Stearns and Macdonald, 1942). The consolidated earthy deposits are primarily older alluvium, which forms the bulk of the alluvial fans stretching from the lower elevations to the coast. The consolidated earthy deposits are composed primarily of poorly sorted conglomerates. Unconsolidated deposits are found in streambeds and in the coastal areas, and are primarily composed of younger, poorly sorted alluvium.

Because the sedimentary deposits are hydrologically significant owing to their relatively low permeability compared to that of the volcanic rocks, the subsurface extent of these deposits may be important; however, drilling information or other evidence that would help define the extent of these features is sparse. Lithologic information from 15 wells (appendix A) was analyzed in concert with existing geologic maps to construct a map of the top of the Wailuku Basalt for the study area and extending offshore (fig. 5). Where no lithologic information was available, the broad topographic slope of the West Maui Volcano was extended (extrapolated) offshore to determine the approximate position of the buried surface. The subsurface extent of valley-filling deposits was estimated from borehole data and extrapolation below sea level of the slope of the stream valley walls.

Rock Hydraulic Properties

The hydraulic properties of the various rock types control the occurrence and flow of groundwater in the study area. Groundwater is withdrawn primarily from a freshwater-lens system in the dike-free volcanic rocks outside of the dike-intruded rift zones. Some rocks tend to impede groundwater flow more than others, thereby creating barriers to flow and areas of steeper hydraulic gradient.

Hydraulic Conductivity

Hydraulic conductivity is a quantitative measure of the capacity of a rock to transmit water. Rock hydraulic conductivity depends on the rock permeability and the properties of the fluid in the rock. Permeability describes the ease with which fluid can move through rock. The permeability of volcanic rocks is variable and depends on many factors, including the mode of emplacement and amount of weathering. Lava viscosity and the topography over which lava flows travel also can affect permeability. Thicker flows generally are less permeable and form from highly viscous lava or on flat topography (Gingerich and Oki, 2000).

Dike-free Volcanic Rocks

The permeability of the subaerial, shield-building, dike-free lava flows in the study area generally is high. The main elements of lava flows contributing to the permeability are (1) clinker zones associated with a‘a flows, (2) voids along the contacts between flows, (3) cooling joints normal to flow surfaces, and (4) lava tubes associated with pahoehoe flows. The regional horizontal hydraulic conductivity of the dike-free volcanic rocks generally ranges from hundreds to thousands of feet per day (Burnham and others, 1977; Oki, 2005; Rotzoll and others, 2007; Hunt, 2007) (fig. 6). Because of the high permeability of the dike-free volcanic rocks, horizontal water-table gradients in these rocks are small (on the order of a foot per mile). Horizontal hydraulic conductivity in the lava flows may be anisotropic—several times greater parallel to the lava flows than perpendicular to the flows (Nichols and others, 1996, p. A14).

In general, the vertical hydraulic conductivity of the dike-free lava flows may be tens to hundreds of times less than the horizontal hydraulic conductivity. In the Kahului area, Bowles (1970) suggested that horizontal permeability might be as great as ten times the vertical permeability on the basis of aquifer tests on stormwater disposal wells. Burnham

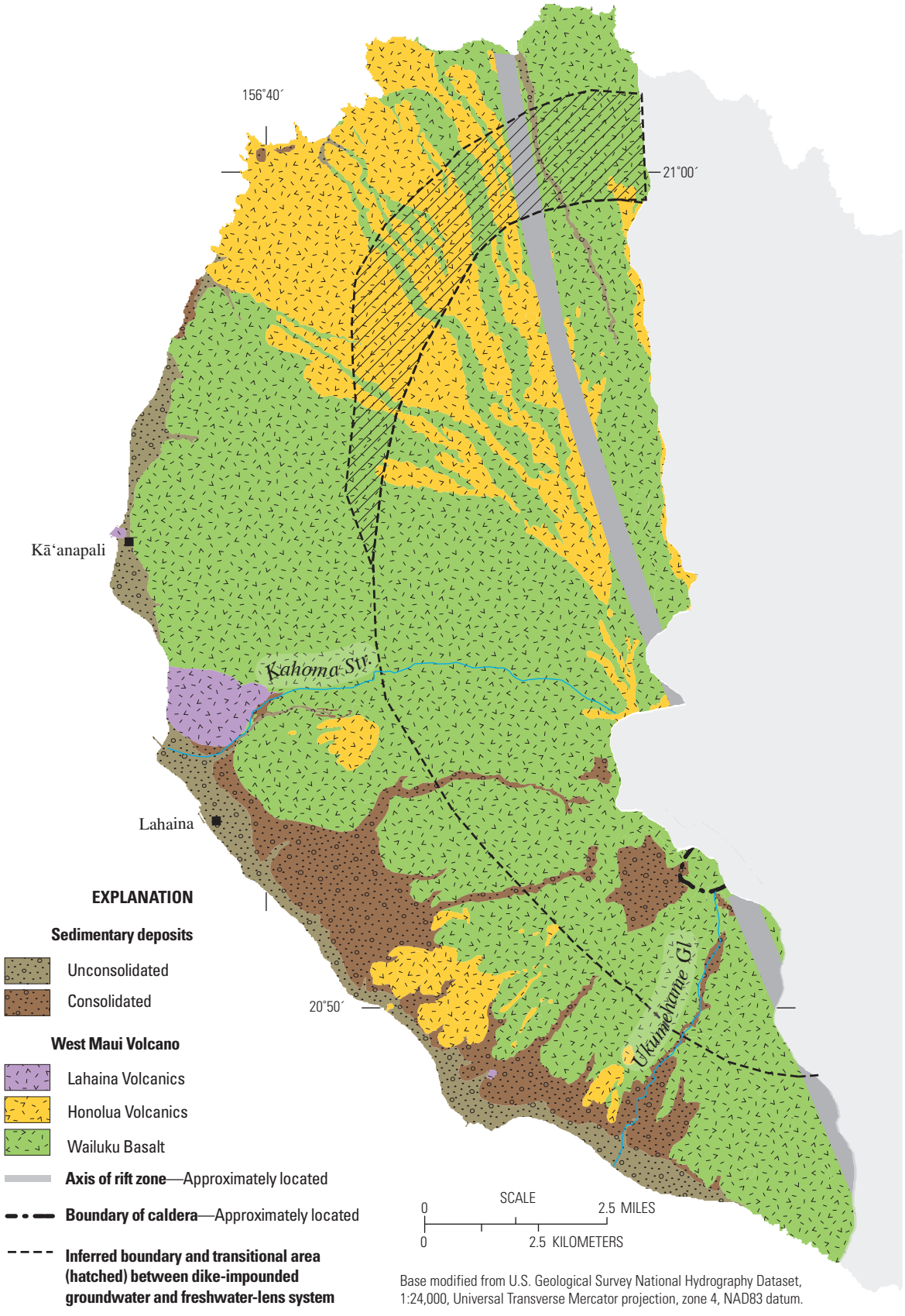

Figure 4. Generalized surficial geology in the Lahaina District, west Maui, Hawai‘i (modified from Stearns and Macdonald, 1942; Sherrod and others, 2003).

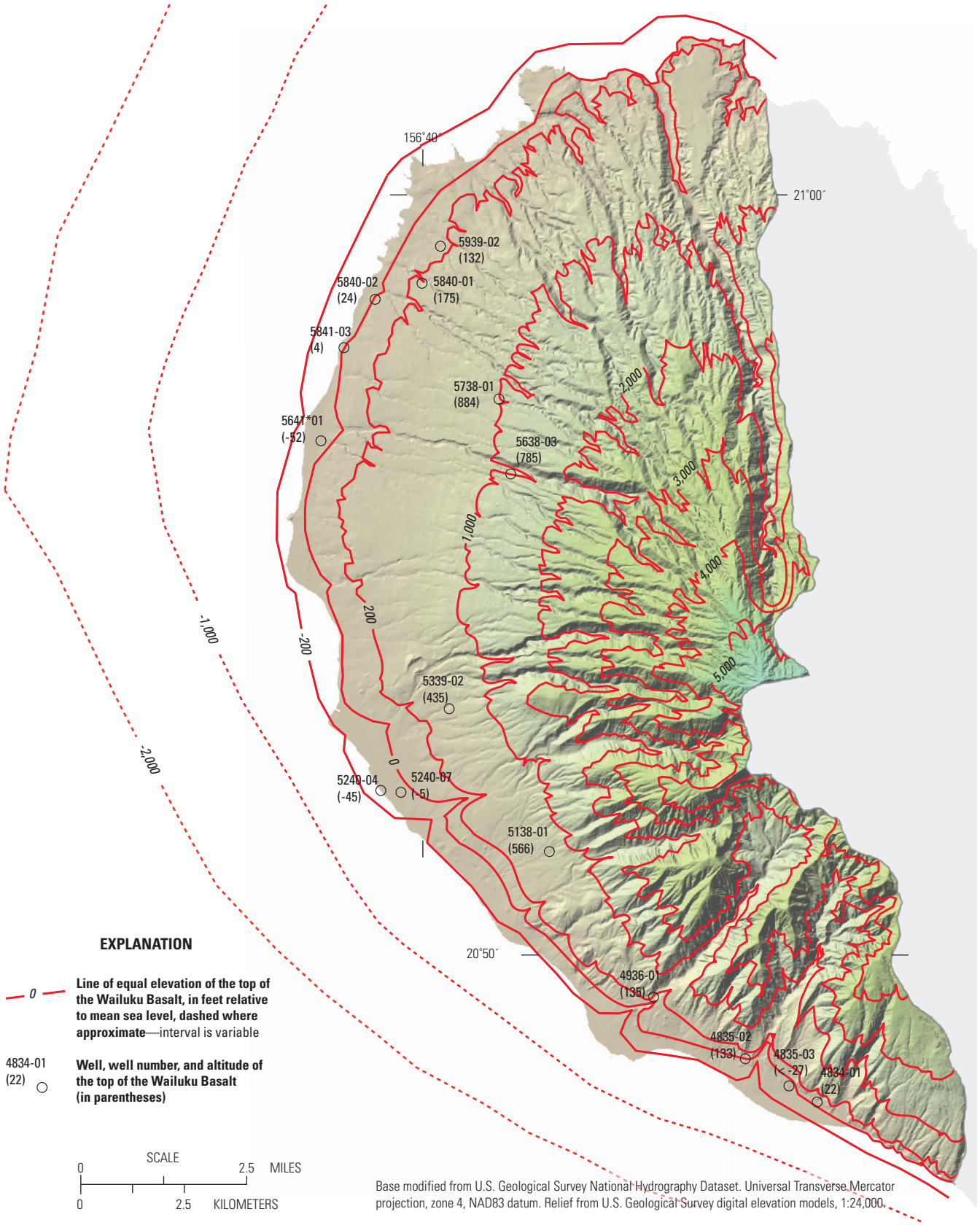

Figure 5. Structural contours of the top of the Wailuku Basalt and wells with stratigraphic information in the Lahaina District, west Maui, Hawai‘i.

and others (1977) obtained acceptable results in simulations made with their numerical model using horizontal hydraulic conductivity 10–100 times the vertical hydraulic conductivity near Kahului. Hunt (2007) used a ratio of horizontal to vertical hydraulic conductivity of 200 to 1 for a numerical modeling study of the Kīhei, Maui area. Souza and Voss (1987) also estimated the ratio of horizontal to vertical hydraulic conductivity to be 200 to 1 in their modeling study on O‘ahu. Gingerich (2008) used ratios ranging from 200–800 to 1 to achieve acceptable modeling results in the Wailuku area, Maui based on water-level and salinity measurements in wells.

Dikes

Intrusive volcanic rocks include rocks such as dikes, sills, and stocks that formed by magma that cooled below the ground surface. Dikes associated with the rift zones of the West Maui Volcano are the dominant intrusive rocks in the study area, and are most abundant within the central area of the rift zones and

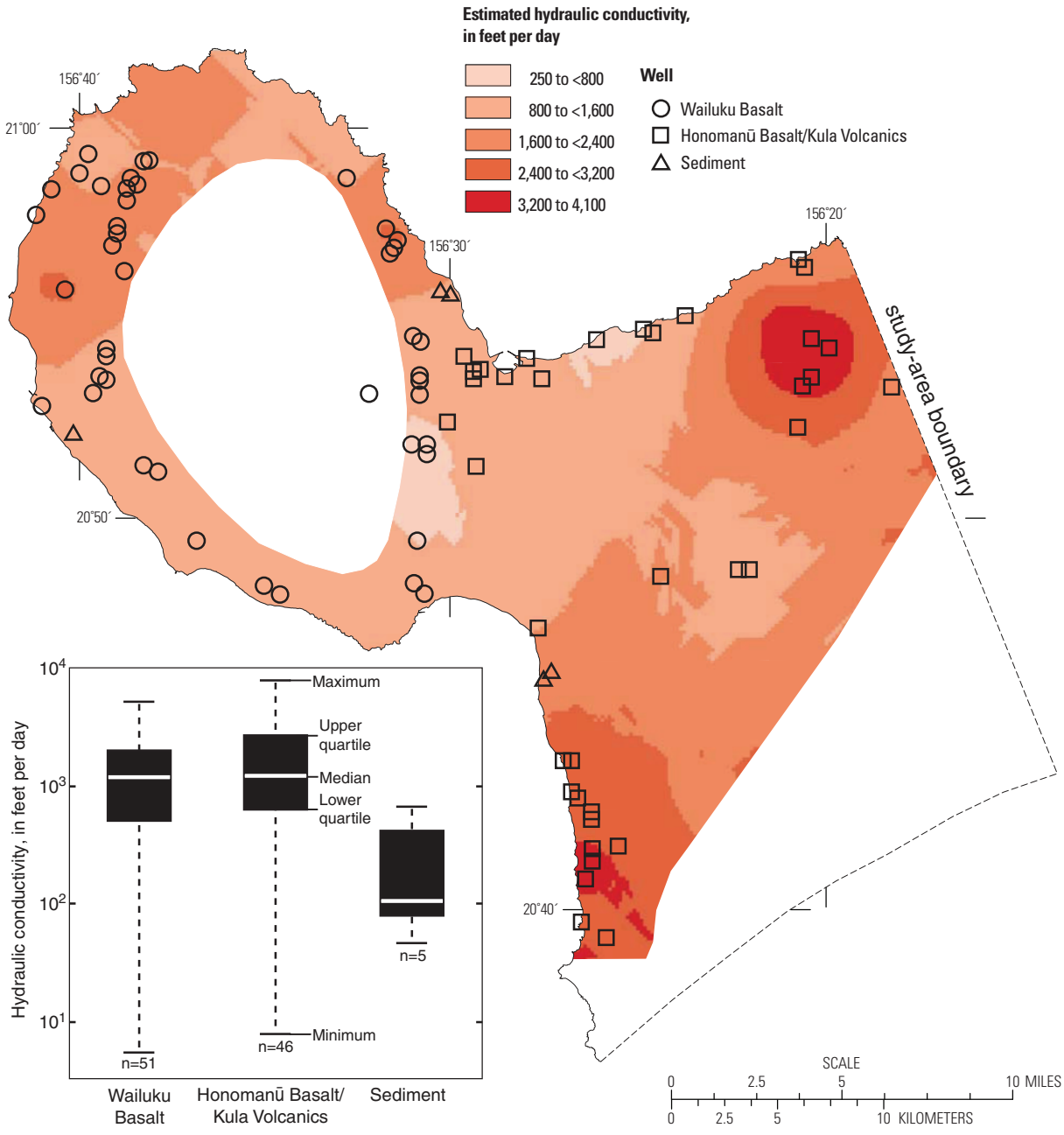

Figure 6. Distribution of regional aquifer hydraulic conductivity in central and west Maui, Hawai‘i (modified from Rotzoll and others, 2007).

the caldera complex. Although the thickness of individual dikes generally is less than 10 ft, dikes are hydrologically important because of their low permeability and their impounding effect on groundwater. Groundwater levels in the West Maui Volcano interior may be as high as 3,000 ft above sea level as evidenced by tunnels tapping dike compartments (Stearns and Macdonald, 1942, p. 195).

In general, the average hydraulic conductivity of a rift zone decreases as the number of dike intrusions within the rift zone increases. In addition, hydraulic conductivity is expected to be higher in a direction along the strike of the dikes rather than perpendicular to the strike. Rotzoll and others (2007) report a hydraulic conductivity of about 20 ft/d from an analysis of an aquifer test made on a well in ‘Īao Valley in the dike complex; however, not enough detail is available to determine the number, orientation, or spacing of dikes in the area of the test. On the basis of a numerical model analysis, Meyer and Souza (1995) suggested that the average effective hydraulic conductivity of a dike complex ranges from about 0.01 to 0.1 ft/d. These values reflect the influence of the intrusive dikes as well as the lava flows between dikes. The hydraulic conductivity of the intrusive dike material was estimated to range from 10^{-5} to 10^{-2} ft/d (Meyer and Souza, 1995).

Weathering

Weathering reduces the permeability of all types of volcanic rocks. The permeability reduction may be attributed to secondary mineralization that clogs the original open spaces, or clays and colloids that precipitate from percolating water (Mink and Lau, 1980). Burnham and others (1977, p. 6) report that the buried lava surface beneath the Kahului, Maui area contains a residual clay that indicates a long period of exposure, soil formation, and erosion prior to burial. On the basis of laboratory permeameter tests on core samples, Wentworth (1938) estimated the hydraulic conductivity of weathered basalt to be from 0.083 to 0.128 ft/d. An injection test conducted in weathered basalt beneath Waiawa Stream valley on O‘ahu yielded a hydraulic conductivity of 0.058 ft/d (R.M. Towill Corporation, 1978). Miller (1987) used the water-retention characteristics of core samples collected beneath central O‘ahu pineapple fields to estimate the saturated hydraulic conductivity of saprolite and found values ranging from 0.0028 to 283 ft/d. The wide range of hydraulic-conductivity values estimated by Miller was attributed to the variability in macroporosity among samples.

Sedimentary rocks

The sediments of greatest hydrologic significance because of their relatively low permeability are the older consolidated alluvial deposits, which were created during the period of extensive erosion that carved deep valleys in the original volcanoes. These deposits are in deeply incised valleys, beneath the isthmus of Maui, and along parts of the Lahaina District coast. The low permeability of consolidated alluvial deposits is caused by a reduction of pore space during the weathering process as well as mechanical compaction of the deposits (Wentworth, 1951). Wentworth (1938) estimated the hydraulic conductivity of three weathered alluvium samples from O‘ahu with the use of a laboratory permeameter. Two of the samples had a hydraulic conductivity of less than 0.013 ft/d, and the third sample had a hydraulic conductivity of 1.08 ft/d. Eight samples classified as alluvium, without reference to their degree of weathering, produced a range of hydraulic conductivity from 0.019 to 0.37 ft/d (Wentworth, 1938).

The sedimentary deposits and underlying weathered volcanic rocks of the isthmus and coastal plains form a low-permeability confining unit, called caprock, which overlies high-permeability volcanic rocks and impedes seaward freshwater discharge at the coast. Although the permeability of the various components of the caprock may vary widely, from low-permeability in older alluvium and saprolite to high permeability in buried coral reef deposits and sand dunes, overall the caprock has lower regional permeability than the volcanic-rock aquifers. Rotzoll and others (2007) show a range of hydraulic conductivity from about 30 to 650 ft/d estimated on the basis of data from five aquifer tests in sediments of central Maui. Little information about the anisotropy or vertical hydraulic conductivity of the caprock is available. Burnham and others (1977) modeled a clay layer overlying the volcanic-rock aquifer beneath Kahului with a vertical hydraulic conductivity from about 1 to 10 ft/d. Gingerich (2008) used values ranging from 6.9 to 17 ft/d for horizontal hydraulic conductivity and 0.38 to 0.69 ft/d for vertical hydraulic conductivity of the sedimentary and valley-filling deposits to achieve acceptable model simulation results in the ‘Īao and Waihe‘e areas. Valley-fill deposits on O‘ahu were modeled with horizontal and vertical hydraulic conductivities ranging from 0.058 to 30 ft/d (Oki and others, 1998; Oki, 2005).

Effective Porosity and Specific Storage

The effective porosity and specific storage of the rocks forming an aquifer affect the timing and amount of the water-level response to natural or human-induced changes. The effective porosity represents that part of the total rock porosity that contributes to flow and is roughly equal to the aquifer specific yield for this discussion. Specific storage is a measure of the compressive storage of the rocks and fluid. Small values of effective porosity or specific storage result in relatively large and typically rapid water-level changes in response to changes in pumping or recharge, whereas large values of these properties result in relatively smaller and typically slower water-level changes.

Total porosity of a rock is the ratio of the volume of void spaces to the total rock volume. Pore spaces in a layered sequence of lava flows may result from (1) vesicles (small spaces formed by the expansion of gas bubbles during the solidification of cooling lava), (2) joints and cracks, (3)

separations between lava flows, (4) void spaces between fragmented rock, including a‘ā clinker, and (5) lava tubes. Total porosity of the volcanic rocks on O‘ahu was measured at different spatial scales using rock samples (Wentworth, 1938; Ishizaki and others, 1967), borehole photographic logs (Peterson and Sehgal, 1974), and density logs from gravity surveys in underground tunnels (Huber and Adams, 1971). Total porosity estimates for O‘ahu volcanic rocks range from less than 5 to more than 50 percent. Low porosity values may be associated with massive features, including dense flows, ‘a‘ā cores, dikes, and thick lava flows, and high values may be associated with ‘a‘ā clinker zones. Effective porosity, which includes only the hydraulically interconnected pore spaces, may be as much as an order of magnitude less than total porosity. Estimates of effective porosity from modeling studies range from 0.04 to 0.15 for volcanic-rock aquifers (Gingerich and Voss, 2005; Oki, 2005; Hunt, 2007; Gingerich, 2008). Rotzoll and others (2007) estimated specific storage and specific yield from one test to be 2.0×10^{-6} ft^{-1} and 0.07, respectively, on the basis of analysis of aquifer-test data from wells in central Maui.

Dispersion Characteristics

The mixing of freshwater with underlying saltwater in an aquifer creates a brackish-water transition zone. The extent of such mixing in an aquifer depends on several factors, including the groundwater velocity and the aquifer dispersivity. High dispersivity values, all other factors being equal, result in greater mixing. Dispersivity values generally are larger in the (longitudinal) direction of flow relative to directions transverse to flow, and may be controlled by aquifer anisotropy. Few reported dispersivity values are available for volcanic-rock aquifers. Gingerich (2008) used longitudinal dispersivity values of 250 and 25 ft for maximum and minimum estimates and 3.3 ft for a transverse dispersivity estimate to obtain the best match to observed data in central Maui. Meyer and others (1974) estimated the dispersivity to be about 200 ft for the volcanic-rock aquifer in the Honolulu, Oÿahu area, and this value likely represents a longitudinal dispersivity. Using a cross-sectional numerical model, Souza and Voss (1987) estimated the longitudinal and transverse dispersivities of the Pearl Harbor area, O‘ahu to be 250 and 0.82 ft, respectively. Liu (2006) estimated transverse dispersion values ranging from 0.2 to 2.0 ft^2/d from salinity profiles measured in deep monitoring wells throughout the Pearl Harbor area, O‘ahu.

Groundwater Flow System

Fresh groundwater moves mainly from inland recharge areas to coastal discharge areas, where springs and seeps exist above and below sea level. Water moving westward from the center of West Maui Volcano flows radially to discharge areas along the coast. Fresh groundwater in the Lahaina area occurs mainly in freshwater-lens systems and dike-impounded systems (Yamanaga and Huxel, 1969).

Freshwater Lens

Currently, the most important source of fresh groundwater in the Lahaina area is the freshwater lens in dike-free volcanic rocks (fig. 7). The main groundwater system in this area consists of a lens-shaped freshwater body, an intermediate brackish-water transition zone, and underlying saltwater. Several geologic features form boundaries of the freshwater-lens system or impede groundwater flow within the system. Features that form boundaries of the freshwater-lens system include dikes in the West Maui Volcano interior; features that may impede flow within the system include valley-fill barriers and the discontinuous coastal sedimentary caprock that thickens in a seaward direction.

The freshwater lens in the study area forms because of the density difference between freshwater and underlying saltwater. The lens thickness can be estimated using the Ghyben-Herzberg relation (for example, Freeze and Cherry, 1979, p. 375-376). This relation assumes that freshwater and saltwater do not flow or mix. Although freshwater and saltwater do flow and mix in freshwater-lens systems, the Ghyben Herzberg relation can be used where the flow is primarily horizontal to estimate the depth at which salinity is about 50 percent that of seawater. For these conditions, the freshwater-lens thickness below sea level is directly proportional to the height of the top of the freshwater above sea level. In principle, at a place where the water table stands 1 foot above sea level, for example, freshwater will extend to 40 feet below sea level, and the freshwater lens will thus be 41 feet thick. This relation exists because the ratio of the density of saltwater to freshwater is 41:40. In the dike-free volcanic rocks of the Lahaina area, freshwater mixing with underlying saltwater creates a brackish-water transition zone that may be tens of feet thick. (For the purposes of this report, brackish water is considered water with salinity that ranges from greater than 2-percent to less than 100-percent seawater salinity.)

The water table in the dike-free volcanic rocks is as high as a few feet above sea level. In general, the water-table altitude in the dike-free volcanic rocks is lowest near the coast and increases in an inland direction at a rate of about 1.7–2.5 ft/mi, but local variations may exist near areas of converging flow caused by pumping from wells. Although freshwater flow is predominantly horizontal in the dike-free volcanic rocks, the flow may have an upward or downward component in some areas.

The low permeability sedimentary material stretching from south of Ukumehame Stream to north of Kahoma Stream (fig. 4) acts as a confining unit that impedes fresh groundwater discharge to the coast. The caprock extends offshore, beyond the seaward extent of the freshwater lens. Beneath the caprock groundwater flow is confined. The freshwater-lens system in the dike-free volcanic rocks is mainly unconfined inland from the caprock. Within the caprock, the freshwater lens is unconfined.

Low permeability valley-filling sediments also are expected to impede groundwater flow to the north and south. Water levels are commonly an indicator of a low-permeability barrier to flow if

abrupt differences in groundwater levels are present on either side of the suspected hydrologic barrier. Low-permeability valley-filling sediments were found to create such water-level differences in the ‘Īao area of central Maui. No water-level data, however, have shown that valley-filling deposits create pronounced water-level differences in the Lahaina study area.

A saltwater-circulation system is present beneath the freshwater lens. Saltwater flows landward in the deeper parts of the aquifer, flows upward, and then mixes with seaward-flowing fresher water (fig. 7). This mixing creates the brackish-water transition zone. When water is pumped from a freshwater-lens system in equilibrium, water levels will decrease and the transition zone will rise until a new equilibrium is reached between the amount of recharge to the system and the amount of base flow to streams and discharge to wells and the coast. The coastal caprock that impedes freshwater discharge also impedes the flow of seawater into the aquifer. This causes the balance between freshwater and saltwater to be out of equilibrium as seawater moves slowly into the aquifer to balance the freshwater that has been removed. Hence, in these areas the midpoint of the freshwater lens (where the water has 50-percent seawater salinity) could be deeper than would be expected by applying the Ghyben-Herzberg principle. Only after a new equilibrium is reached will the depth of the midpoint of the transition zone be about 40 times the head (above sea level) at the water table.

Dike-Impounded System

Dike-impounded systems are found near the caldera and rift zones of the volcanoes, where low-permeability dikes have intruded other rocks. Near-vertical dikes tend to compartmentalize areas of more permeable volcanic rocks. Dikes impound water to altitudes as great as 3,000 ft in the West Maui Volcano interior as evidenced by tunnels tapping dike compartments (Stearns and Macdonald, 1942, p. 195). In some stream valleys, where extensive erosion has exposed dike compartments, groundwater discharges directly to streams.

The extent of the dike-impounded water body in West Maui is inferred from the dikes exposed in valley walls, tunnels, water levels in wells, and streamflow and has been interpreted

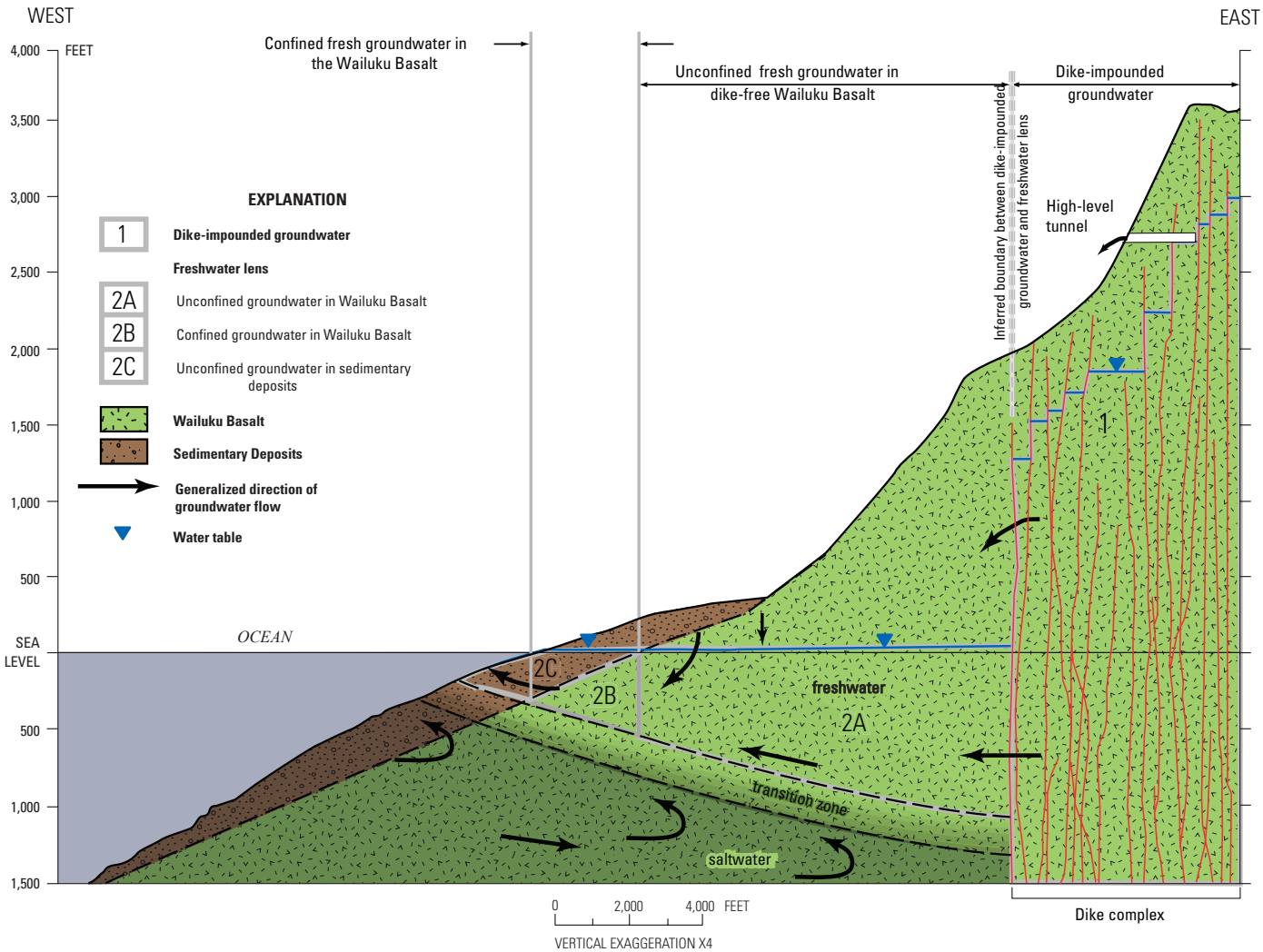

Figure 7. Geologic section of the Lahaina area showing groundwater occurrence and movement, west Maui, Hawai‘i.

differently in various studies (Yamanaga and Huxel, 1969, fig. 6; Yamanaga and Huxel, 1970, fig. 7; Takasaki, 1978). The boundary used in this report was drawn considering water-level data from wells that were not available to previous investigators (fig. 4). No data from wells are available for determining the depth to which freshwater extends below sea level within the dike-impounded system. Where erosion extends to below the water level in the stream valleys, groundwater discharges directly to the streams as base flow. Fresh groundwater that does not discharge to streams or tunnels or is not withdrawn from wells in the dike-impounded system flows to downgradient areas in the freshwater-lens system. Although preferential flow to downgradient areas in some parts of the West Maui Volcano is likely, no evidence is available to indicate where these areas might be.

Recharge

Groundwater recharge generally is greatest in the inland mountainous regions, where rainfall is highest, but the plantation-scale sugarcane cultivation (and, to lesser degrees, pineapple cultivation) has profoundly affected the amount and location of recharge to the groundwater system in agricultural areas (Engott and Vana, 2007). Typically, water-budget calculations for areas with sugarcane irrigation assume that 5–70 percent of irrigation water is not used by the crop and most of this unused water "returns" to groundwater as recharge. Since the early 20th century, about 21 billion gallons of surface water have been diverted each year from study-area streams for crop irrigation within the area. Irrigation rates in the study area have been steadily decreasing since the 1970s, when large sugarcane plantations began converting from furrow irrigation to more efficient drip irrigation methods and began reducing the acreage dedicated to sugarcane production. Some stream diversions were reduced during this period. In 1999, sugarcane cultivation in the area ceased, and in 2009, pineapple cultivation ceased. Decreasing irrigation coincided with recent periods of below-average rainfall, leading to substantially reduced recharge rates in many areas. Although streamflow diversion for irrigation water is continuing, irrigation records for the various landowners and the amount and distribution of diversified and continually changing crops are unavailable or even nonexistent in some cases. Therefore, current and future irrigation estimates and contributions to recharge are less certain.

Groundwater recharge for central and west Maui, including the Lahaina District, was estimated by Engott and Vana (2007) for six periods spanning the years 1926 to 2004. These estimates incorporated historical rainfall and accounted for changes in land cover and irrigation practices. Recharge also was estimated for several hypothetical rainfall and land-cover scenarios, including drought conditions and cessation of agriculture. Modifications to the water-budget model in Engott and Vana (2007) were made for this study to (1) give consideration to canopy-interception processes in forests, (2) distinguish between native and non-native forest, and (3) account for differences in the transpiration properties of forests depending on their location with respect to the fog zone. A discussion of the salient changes made to the earlier water-budget model and the resulting new groundwater-recharge estimates used in this study is included in appendix B.

Estimated recharge for the study area declined by 43 percent during 1926–2004. The period 1926–79 had the highest estimated recharge—at least 50 percent higher than in any other period considered. The period 2000–04 had the lowest estimated recharge because irrigation decreased and rainfall was the lowest of any period.

Recharge from Streams

Downstream from the area of dike-impounded water, where the water table of the freshwater-lens system is below the streambed, the potential exists for streamflow infiltration to recharge the freshwater-lens system. In many of the streams, the only water flowing in these diverted streams is runoff immediately after rainfall, because at other times all dry-weather flow is captured by the diversion ditches for irrigation. The water-budget estimates calculated for this study did not account for historical recharge through streambed seepage, because streams were dry most of the time. In the past decade, the flow in Honolua Stream has been fully restored (no diversion) and partially restored in Ukumehame Stream. In the future, the flow of additional streams may be fully or partially restored to natural conditions, potentially changing future recharge.

Most water diverted from study-area streams is transported to agricultural areas above the freshwater lens, and a fraction of this irrigation water eventually recharges the freshwater lens. However, if the water were left in the streams, much of it would still recharge the aquifer by seeping through the streambed. The potential recharge from the streambeds to the freshwater lens was estimated on the basis of streamflow gaging-station and flow-measurement data. Streamflow measurements were made in study-area streams during periods when streamflow was not completely diverted (fig. 8). The flow measurements (wading measurements made with an acoustic doppler velocity meter, assumed to have an average error of plus or minus 5 percent) and the length of stream channel between measurement sites were used to calculate streamflow loss, in gallons per day per foot of stream channel (table 1). These rates were extrapolated to nearby reaches on the same stream where flow measurements were not available. Seepage-loss rates for Wahikuli and Launiupoko Streams were estimated using rates from Kahana Stream because of similar observed conditions in these streams. The estimated potential loss to recharge was capped at the estimated average base flow determined from historical gaging station data originally presented in Gingerich (2008). Base flow is groundwater discharge to the stream that commonly occurs even in the absence of recent rainfall and runoff. The estimate of total streamflow loss under undiverted streamflow conditions, which becomes recharge to the underlying groundwater system, is about 16 Mgal/d (table 1).

Table 1. Potential streamflow loss contributing to groundwater recharge, Lahaina District, west Maui, Hawai‘i.

[Mgal/d, million gallons per day; NA, not available; Honokōhau Stream measurements from Fontaine (2003)]

Stream name	Date of measurement	Flow at measurement site (Mgal/d)		Streamflow loss (Mgal/d)	Length of measurement section (feet)	Loss per foot of channel length (gallon per day per foot)	Estimated length of losing section (feet)	Estimated potential loss to recharge (Mgal/d)
		Upstream	Downstream					
Honokōhau	various			1.53	12,400	123	12,400	1.53
Honolua	5/13/2008	0.28	0.0	0.28	7,390	38	16,500	0.93
Honokahua	5/14/2008	0.21	0.0	0.21	1,900	111	16,900	0.63
Kahana	4/1/2009	0.27	0.0	0.27	1,000	270	19,400	0.76
Honokōwai	1/7/2010	0.03	0.0	0.03	1,240	24	18,800	2.48
Wahikuli	1/6/2010	0.0	0.0	0.00	NA	NA	15,700	0.42
Kahoma	1/8/2010	1.18	0.0	1.18	14,200	83	18,900	2.49
Kaua‘ula	9/2/2008	0.98	0.7	0.28	2,180	128	16,400	2.16
Kaua‘ula	9/17/2008	0.13	0.0	0.13	2,440	53		
Launiupoko	7/28/2008	0.0	0.0	0.00	NA	NA	16,400	0.65
Olowalu	8/15/2008	0.19	0.0	0.19	6,000	32	15,000	1.98
Ukumehame	5/25/2006	3.9	3.34	0.56	3,100	181	10,800	1.95
Ukumehame	9/20/2006	0.59	0.4	0.18	3,100	58		
Total								**15.99**

Recharge from Injection Wells

Groundwater recharge is augmented by injection of treated sewage effluent at the Lahaina Sewage Treatment Plant (well 5641*01 on fig. 5). Daily injection records are available since 1996 and earlier estimates are based on plant operator recollections (Scott Rollins, Maui County Department of Environmental Management, written commun., 2009). Injection rates were about 3.5 Mgal/d in 1980 when full injection began and averaged from 4 to 6 Mgal/d through four injection wells through 2009 (appendix C).

Discharge

Discharge from the study area is in the form of groundwater withdrawals from wells, discharge to streams as base flow, and diffuse seepage to the ocean. Withdrawals from wells and base flow in streams have been measured in most locations, although records are incomplete for some periods and locations. Diffuse seepage to the ocean has not been measured directly.

Withdrawals from Wells

Groundwater withdrawals in the study area began after the first Maui-type skimming shaft was constructed in 1897 (Stearns and Macdonald, 1942). Reported withdrawals were compiled from published records (Stearns and Macdonald, 1942; Yamanaga and Huxel, 1969; Souza, 1981), information contained in USGS files (USGS Pacific Islands Water Science Center, unpub. data), and a CWRM digital database (CWRM unpub. data, 2010). Stearns and Macdonald (1942) present withdrawal records from individual wells starting in 1918. Earlier withdrawal records are not available. During the early period of groundwater development, most of the water was used for sugarcane cultivation.

Groundwater withdrawals increased steadily during the 1920s, and averaged 33 Mgal/d during the period 1918–29 (fig. 9). During 1930–79, average withdrawals were about 44 Mgal/d, mostly from the Honokōwai and Launiupoko Aquifer Systems. After 1979, sugarcane irrigation decreased and domestic withdrawals began to increase and spread into the Honolua Aquifer System. Average withdrawals during 1980–2000 were about 21 Mgal/d. During 2000–08, however, average withdrawals decreased to about 4 Mgal/d. The CWRM, sustainable-yield estimate for the Lahaina Aquifer Sector is 34 Mgal/d (State of Hawai‘i, 2008).

Base Flow to Streams

Base flow represents groundwater discharge to streams. Groundwater discharge from the dike-impounded water body contributes to the flow of nearly all perennial streams on West Maui Volcano (Stearns and Macdonald, 1942, p. 195). The base-flow component of streamflow was estimated from daily streamflow records for gaging stations operated on nine streams in the study area by adjusting each record to a common base period (Gingerich, 2008). Some streamflow records are from gaging stations that measured streamflow upstream of any diversion, and others were reconstructed from records collected on ditches and tunnels diverting the streams of interest. Flow from ungaged streams was considered a minor part of the total streamflow and was not included. Total average base flow during 1913–2005 from the nine gaged streams was about 35 Mgal/d (Gingerich, 2008; table 2).

Sixteen tunnels were constructed during 1900–26 to increase streamflow by developing water from the dike-impounded water body in West Maui Volcano, and nine of

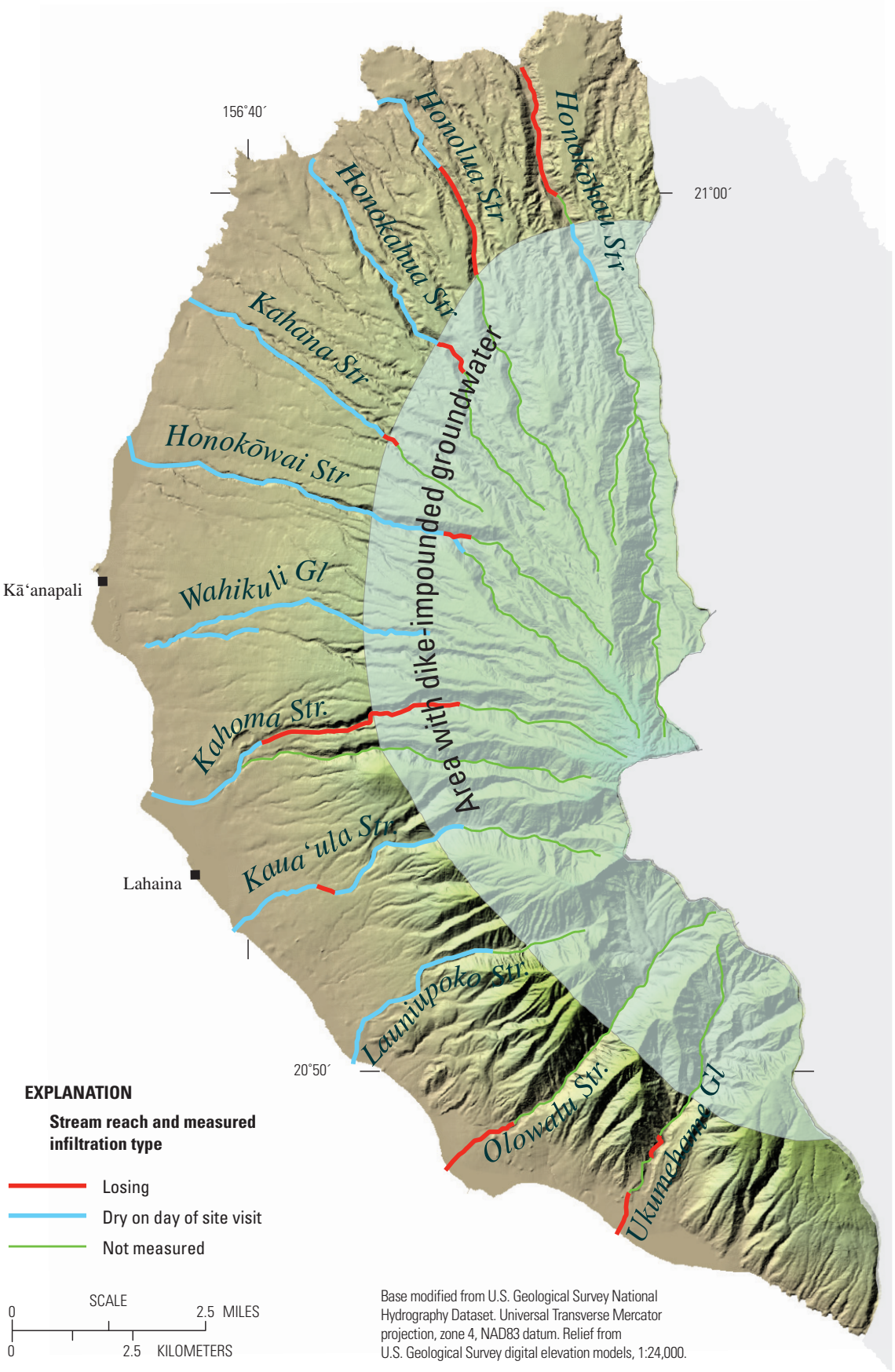

Figure 8. Measured losing and dry reaches in Lahaina District streams, west Maui, Hawai'i.

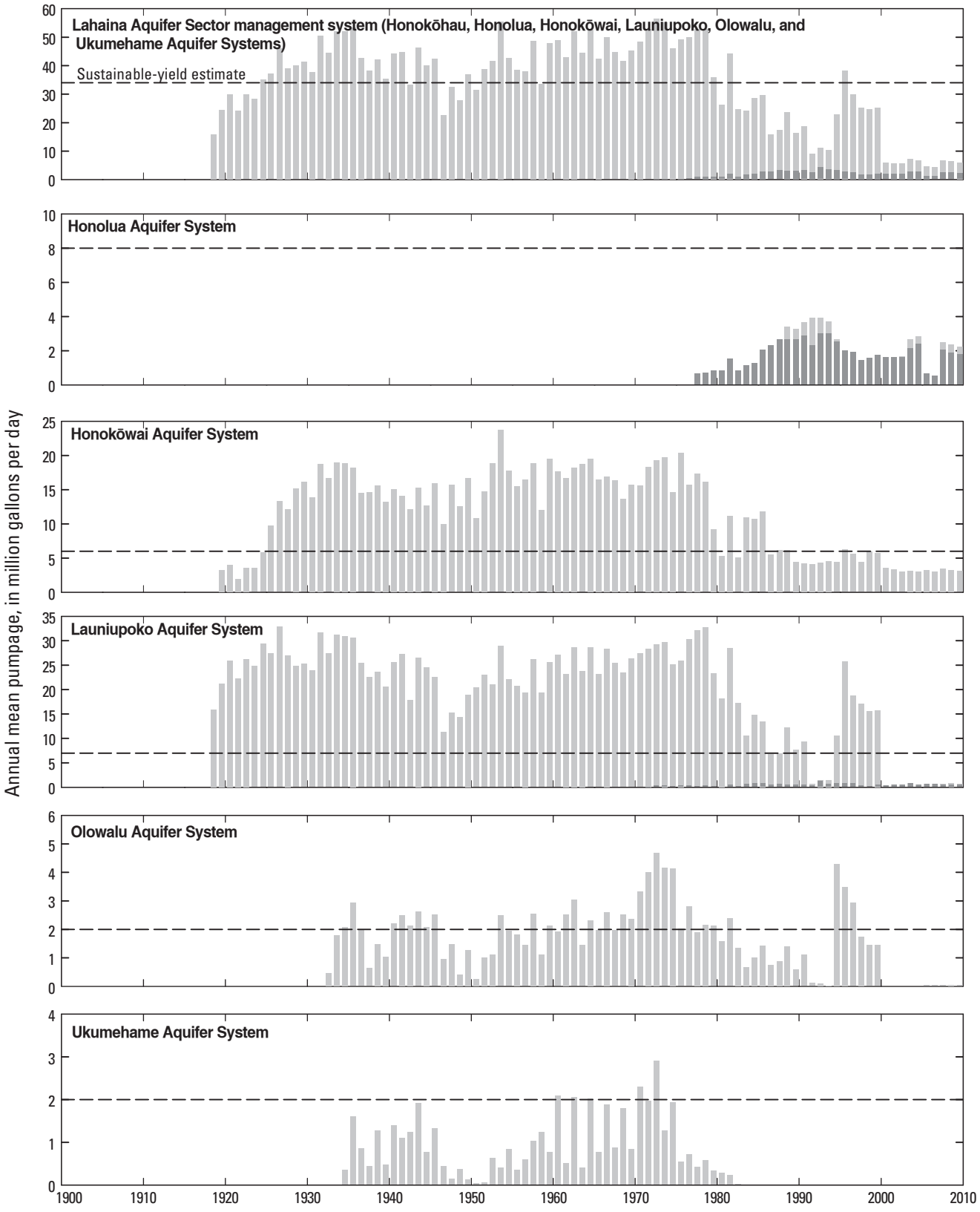

Figure 9. Groundwater withdrawals from the Lahaina Aquifer Sector, 1900–2010, west Maui, Hawai‘i. Sustainable-yield values (dashed lines; as of 2008) are from the State of Hawai‘i Commission on Water Resource Management. No pumpage is reported for the Honokōhau Aquifer System. Pumpage for public supply shown in dark gray.

these tunnels are in the study area (Stearns and Macdonald, 1942, p. 195). Little evidence is available to determine whether these tunnels increased streamflow by capturing additional water not discharging to any stream or if they just redistributed streamflow by capturing water that would eventually discharge into the streambed farther downstream.

Water Levels

Groundwater-flow directions commonly are inferred from water levels measured in wells. Changes in those levels also are an indicator of changes in recharge or withdrawals from the groundwater system, and can be an indicator of freshwater-lens thickness. In the west Maui study area, groundwater levels vary spatially (horizontally and vertically) and temporally.

The first successful well drilled on Maui was completed in the Lahaina area in 1883 (McCandless, 1936), the first shaft or skimming tunnel (tunnel and sump constructed at or near sea level to collect water from the top of the freshwater lens) in the study area was constructed in 1897, and the first inclined shaft in Hawai‘i was constructed near Olowalu in 1933 (Stearns and Macdonald, 1942). However, published water levels from wells are not available earlier than 1935. Water levels in the Lahaina area ranged from 3 to 6 ft above mean sea level at the time of these first recorded measurements (fig. 10). No apparent upward or downward trend is evident in the long-term record of water-level data from the ‘Alaeloa well (5840-01) (regression analysis indicates less than 0.1-ft increase in 37 years). Variations in monthly water levels are mainly due to similar variations in monthly ocean level (fig. 11).

In general, measured water levels in the study area are lowest near the coast and increase (in altitude) inland toward the recharge areas of West Maui Volcano (Yamanaga and Huxel, 1969, Souza, 1981). Water levels measured in February 1979 and again in February 1980 (Souza, 1981) ranged from 2.3 to 6.5 ft above mean sea level (fig. 12). An additional synoptic water-level survey was made on September 10, 2008, on seven wells as part of this study by the USGS using either a calibrated steel tape or continuously recording pressure transducers mounted in the wells. Hourly water levels were averaged over the entire day to remove possible tidal and barometric variations during the survey, the measured wells were relatively remote from actively pumped wells. The only available long-term water-level record shows mainly the effects of ocean-level change and not seasonal variations (fig. 11), thus the measured water levels likely represent the regional water-table configuration throughout the year. Water levels ranged from 1.8 ft above sea level in the north to about 6.1 ft above mean sea level in the south upgradient of the low-permeability coastal sediments (fig. 12). An additional measurement was made on April 2, 2009, when the Honokōwai B well (5638-03) became available and the water level of 5.4 ft indicated that this well was tapping part of the coastal freshwater-lens system and not dike-impounded groundwater.

Measuring points for each of the wells measured in the 2008 synoptic survey were resurveyed, and all wells were tied into a common sea-level datum. Existing measuring-point elevations changed as much as 4 ft as a result of the resurvey. Owing to the measuring-point changes, the accuracy of the historical water-level records became questionable, because the timing of the change in measuring-point elevations is unknown. The original measuring-point elevations could have been wrong initially, they could have changed over time owing to settling or land-surface change, or they could have changed abruptly due to damage, earthquake, or other causes. Because the timing of the measuring-point changes is unknown, water levels measured before 2008 were unadjusted and subsequent water levels were adjusted using the new measuring-point elevations. The exception was at well 5739-03, where the originally reported measuring point was about 4 ft too high and obviously incorrect; therefore all of the water-level measurements from this well were corrected to the updated measuring point.

The magnitude of the horizontal hydraulic gradient varies spatially and ranges from 0.0003 ft/ft (about 1.7 ft/mile) in the north to 0.0005 ft/ft (about 2.5 ft/mi) in the south, where caprock sediments are assumed to impede flow. Water-level information is not available for determining vertical gradients, but it is likely that near inland recharge areas, heads in the aquifer may decrease with depth, whereas near coastal discharge areas heads in the aquifer may increase with depth.

Salinity

Salinity is one of the main factors controlling the availability of fresh groundwater in the study area. Monitoring the salinity profiles in deep open boreholes that fully penetrate the freshwater lens is a standard method in Hawai‘i to understand better the salinity distribution with depth in freshwater-lens systems. Salinity profiles are usually measured in terms of chloride concentration or fluid specific conductance. For this study, seawater was assumed to have a chloride concentration of 19,600 mg/L and a fluid specific conductance of 50,000 µS/cm, values that are near the maximum value measured in deep boreholes (Meyer and Presley, 2001, p. 48). Measured concentration or fluid specific conductance values were divided by 19,600 mg/L or 50,000 µS/cm as appropriate and multiplied by 100 to obtain salinity in terms of percent of seawater salinity.

In general, the salinity of water withdrawn from wells in the study area increases with depth, proximity to the coast, and withdrawal rate, although exceptions to this generalization exist. Public supply wells in the Lahaina Aquifer Sector mostly produce water with chloride concentrations less than 250 mg/l, or about 1.3 percent or less of seawater salinity, but occasionally as high as 900 mg/l, or 4.6 percent of seawater salinity (fig. 11). Many of the older, high-capacity irrigation wells and shafts operated by the plantations produced water exceeding 3 percent of seawater salinity; some reported values are as high as 20 percent of seawater salinity (Yamanaga and Huxel, 1969). Saltwater intrusion is a problem at these wells because of the high withdrawal rates and relatively large drawdowns.

Measured salinity profiles provide an indication of the freshwater volume in the aquifer, and collection of

salinity profiles over time provides an indication of the changes in freshwater volume. In the Lahaina District, salinity profiles are available from three deep wells (fig. 13). The Māhinahina Deep Monitor Well (5739-03) was monitored for fluid specific conductance by the CWRM during 2002–06 (State of Hawai‘i, 2008). Salinity profiles collected from this well indicate no apparent change in the position of the transition zone over time (Rotzoll and others, 2010). The middle of the transition zone (depth of 50-percent seawater salinity) ranged from -140 to -130 ft altitude during 2002–06.

Transition-zone information near the coast is limited to a few measurements from three wells indicating that the freshwater lens is relatively thin in this area. Data from a well (Pioneer Well K-1 near well 5240-01) in Lahaina collected during September 1954 show that the middle of the transition zone was about 43 ft below sea level (fig. 13) (Yamanaga and Huxel, 1969, table 3). Data from a single profile of a deep well (well 5641*01) near the injection site at the Lahaina Sewage Treatment Plant indicated that the middle of the transition zone was at about -90 ft altitude prior to the start of injection in 1980 (U.S. Geological Survey, 2010).

Salinity profiles from deep open boreholes may be affected by flow within the borehole (Paillet and others, 2002; Rotzoll, 2010). Borehole flow can be caused by natural and withdrawal-induced vertical-head differences in the aquifer. Head may increase with depth in the aquifer near coastal discharge areas and near partially penetrating pumped wells, and increasing head in

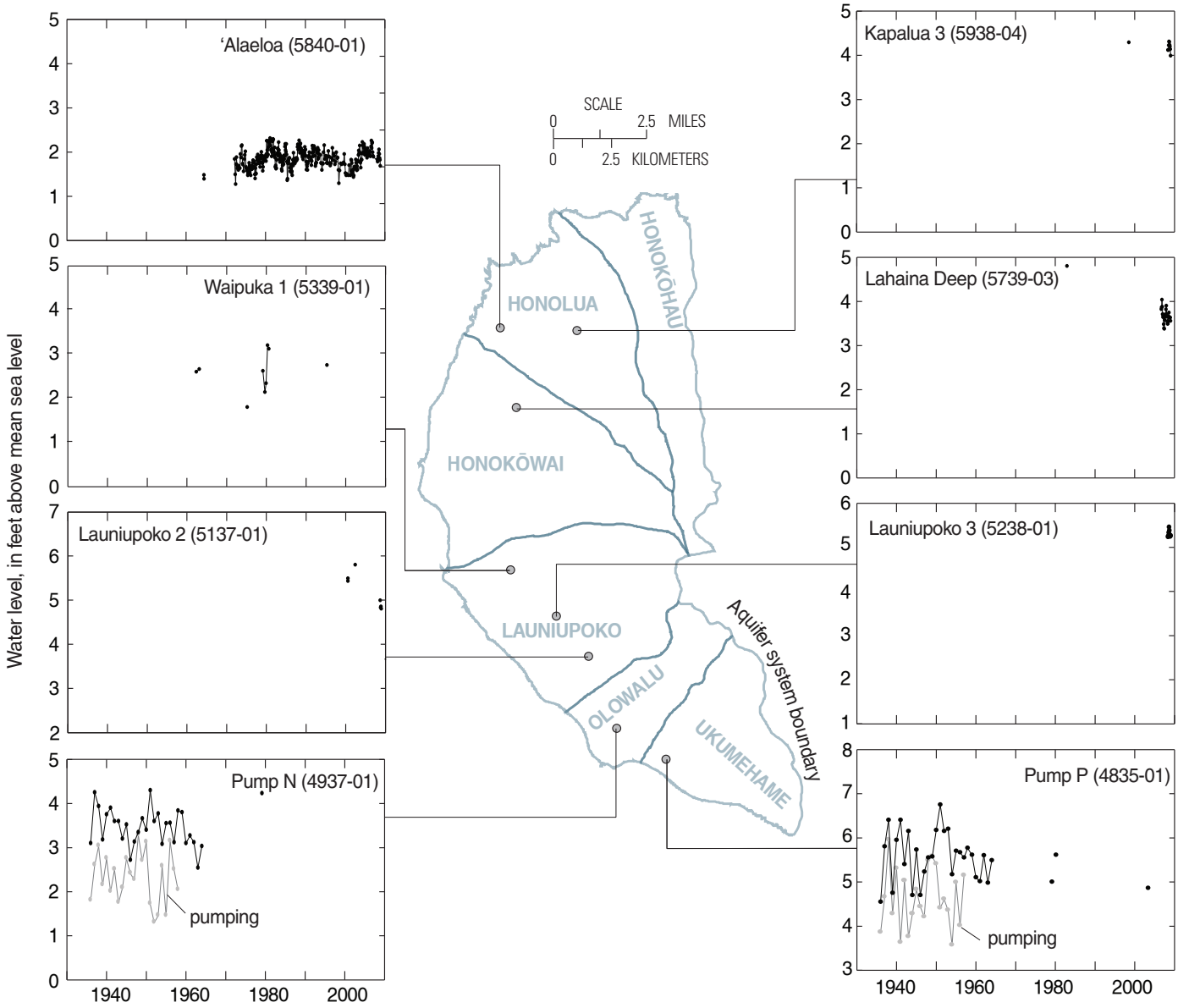

Figure 10. Measured water levels and chloride concentrations in selected wells in the Lahaina District, west Maui, Hawai‘i. Water level and chloride data from Pioneer Mill Co., Maui Department of Water Supply, Hawaii Water Service Company, and U.S. Geological Survey NWIS database.

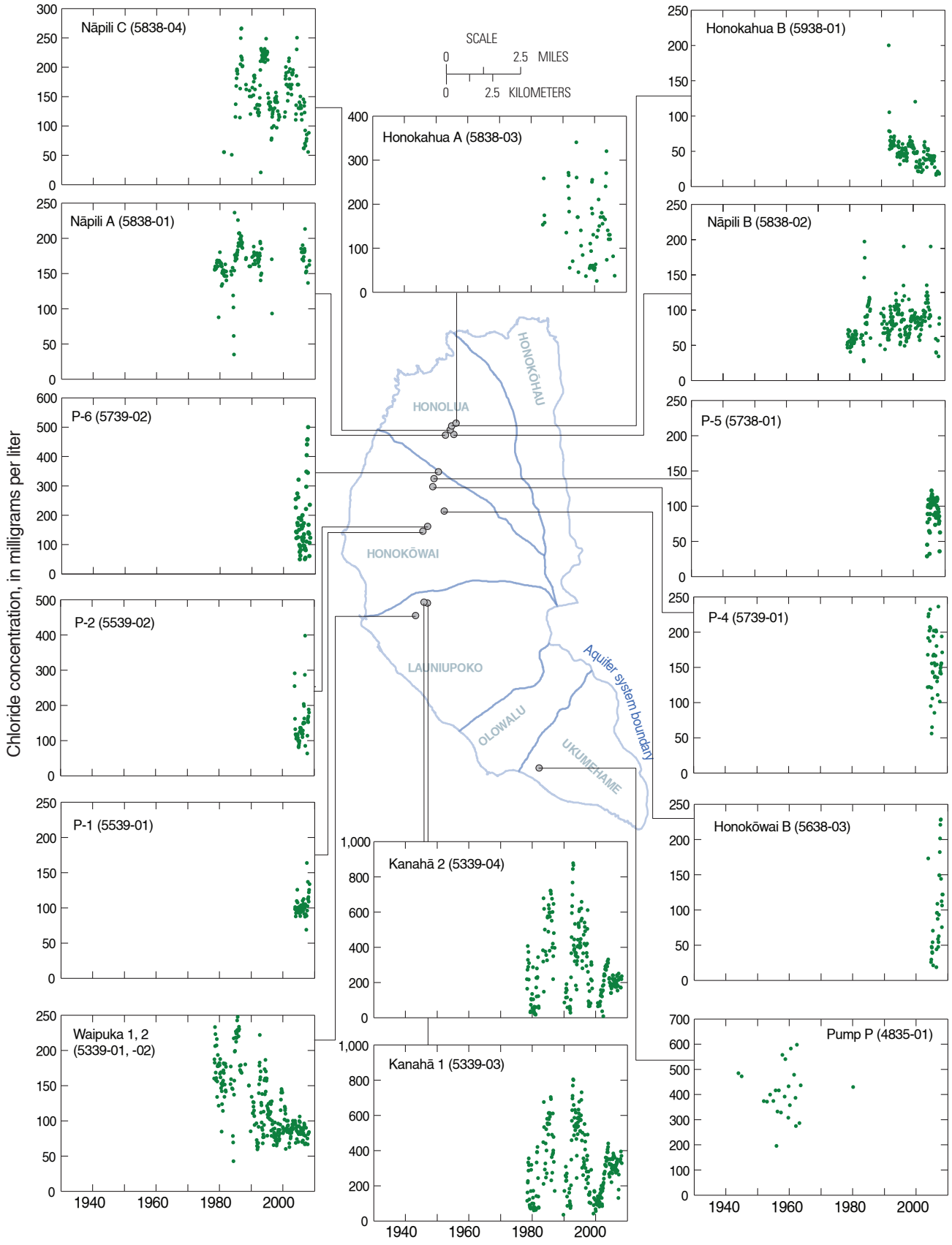

Figure 10. Measured water levels and chloride concentrations in selected wells in the Lahaina District, west Maui, Hawai'i. Water level and chloride data from Pioneer Mill Co., Maui Department of Water Supply, Hawaii Water Service Company, and U.S. Geological Survey NWIS database—continued.

the aquifer with depth may lead to upward flow within an open borehole. Upward borehole flow may cause saltwater to flow upward in the borehole, which in turn may lead to an underestimate of the freshwater-lens thickness based on the recorded salinity profile. In areas where head decreases with depth, however, downward borehole flow may lead to an overestimate of the freshwater-lens thickness based on the recorded salinity profile.

Simulation of Groundwater Flow

The groundwater flow model developed for this study is a three-dimensional, numerical model that simulates the transition from freshwater to saltwater and incorporates hydrogeologic features such as the sediments that form the less-permeable caprock, valley-fill deposits, and low-permeability rejuvenated-stage volcanic rocks. The model was constructed with the SUTRA code (version 2.1) (Voss and Provost, 2002, version of June 2, 2008), modified to account for water-table storage (Gingerich and Voss, 2005) by including the aquifer specific yield. SUTRA is a finite-element code that simulates fluid movement and the transport of dissolved substances in a groundwater system. SUTRA (version 2.1) is capable of simulating three-dimensional, variable-density groundwater flow and solute transport in heterogeneous anisotropic aquifers. Model construction was facilitated using a graphical user interface (SutraGUI) (Winston and Voss, 2003) capable of reading geographic information system spatial data and writing files used by SUTRA.

Model Construction

The numerical model of groundwater flow and transport was developed to simulate groundwater levels and salinity movement within the freshwater-lens system in west Maui during 1926–2008, and it incorporates time-varying recharge, withdrawals, and ocean level. Model construction includes designation of spatial and temporal discretization, assignment of boundary conditions and initial conditions, and delineation of fluid and aquifer properties.

Model Mesh

The model finite-element mesh used for this study comprises 373,883 nodes and 361,456 elements, covers the entire freshwater-lens system in the western part of West Maui Volcano, and extends 1–2 miles offshore to include the zone where fresh groundwater discharges to the ocean (fig. 14). The model mesh excludes dike-intruded areas as described by Yamanaga and Huxel (1969, 1970) (with slight modifications based on the new water-level measurement of 5.4 ft in Honokōwai B well [fig. 12]) in the West Maui Volcano interior, although flow from these excluded areas to the freshwater-lens system is included in the model.

The top and bottom of the model domain and the spacing of the nodes in the model mesh are controlled by hydrogeologic features and the availability of data for Maui and similar Hawaiian Islands. The top of the onshore model domain is assumed equal to sea level. Although the top water-table boundary in onshore areas is truncated at sea level, the aquifer transmissivity is underestimated by less than 1 percent using this assumption. The top of the offshore model domain is defined by ocean-bottom bathymetry (Taylor and others, 2008). The modeled domain extends to 5,906 ft below mean sea level, coinciding with an assumed aquifer bottom where rock pore space is expected to be closed by compaction due to the weight of the overlying rocks. In the absence of any data on aquifer properties at depth on Maui, values were chosen from groundwater modeling studies of O‘ahu (where seismic velocity data were available to define the thickness) (Souza and Voss, 1987; Oki, 2005). O‘ahu has a geologic history similar to that of Maui. Node spacing is variable in the vertical and horizontal directions and is finest in the upper part of the aquifer and near areas of increased groundwater withdrawal and discharge. Horizontal spacing is variable but identical at all depths in the aquifer. Onshore, the vertical spacing between nodes varies from 16 ft within the top 200 ft of the aquifer to 550 ft within the bottom 1,640 ft of the modeled domain; offshore, the vertical spacing between nodes is dependent on the bathymetry within the top 1,312 ft of the aquifer, but it is the same as the onshore spacing within the bottom 4,594 ft of the modeled domain (fig. 15).

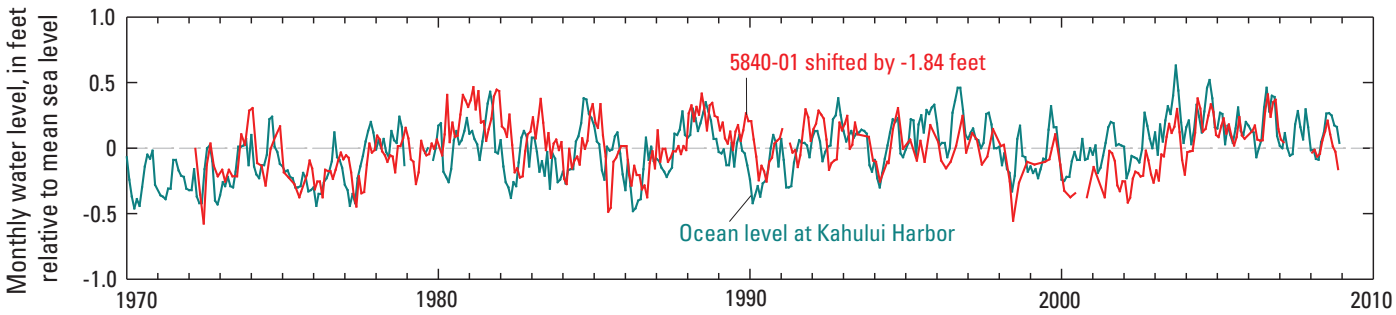

Figure 11. Monthly water level during 1970–2008 at Kahului Harbor (data from National Oceanic and Atmospheric Administration, 2009) and the ‘Alaeloa well (5840-01), Maui, Hawai‘i.

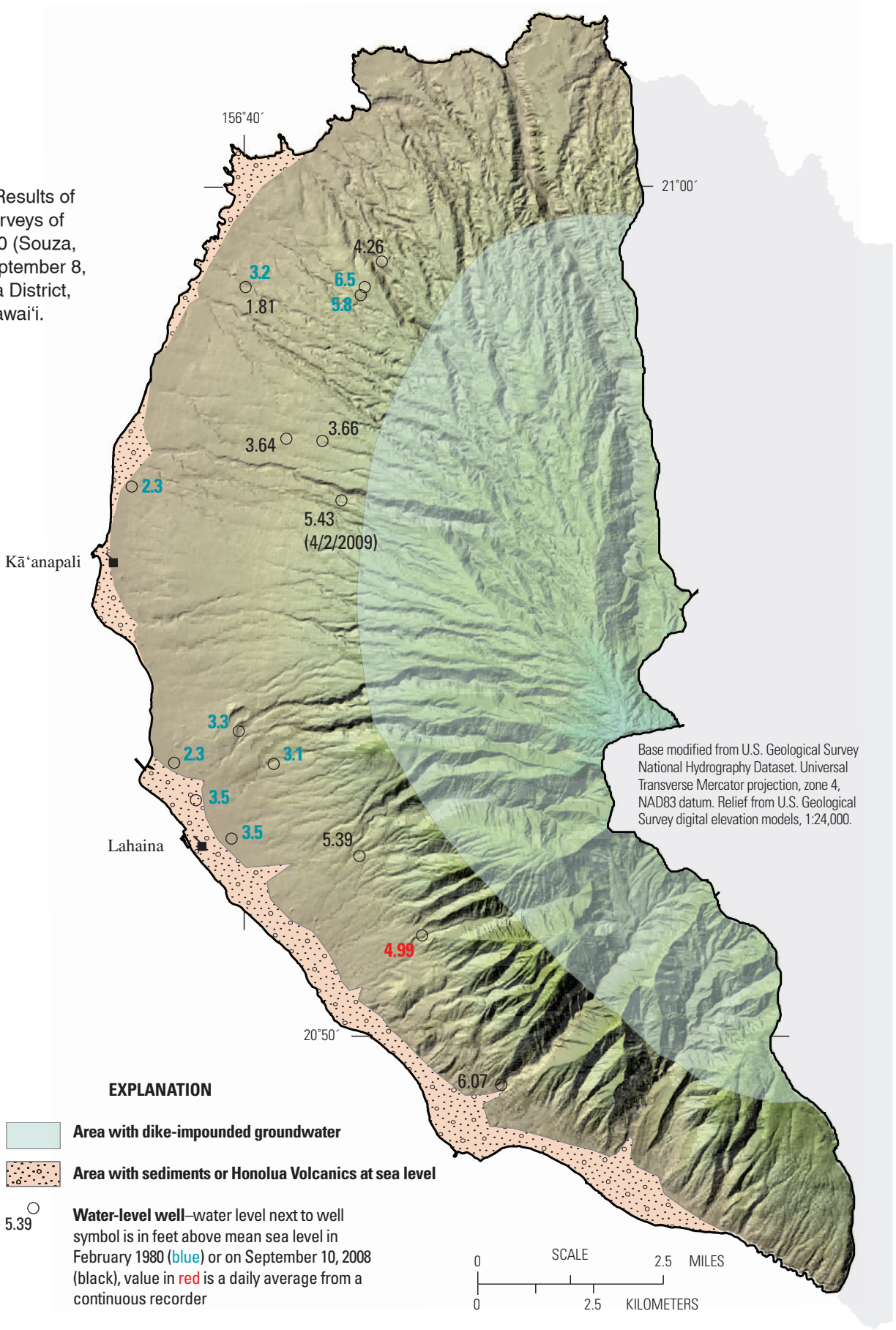

Figure 12. Results of water-level surveys of February 1980 (Souza, 1981) and September 8, 2008, Lahaina District, west Maui, Hawai‘i.

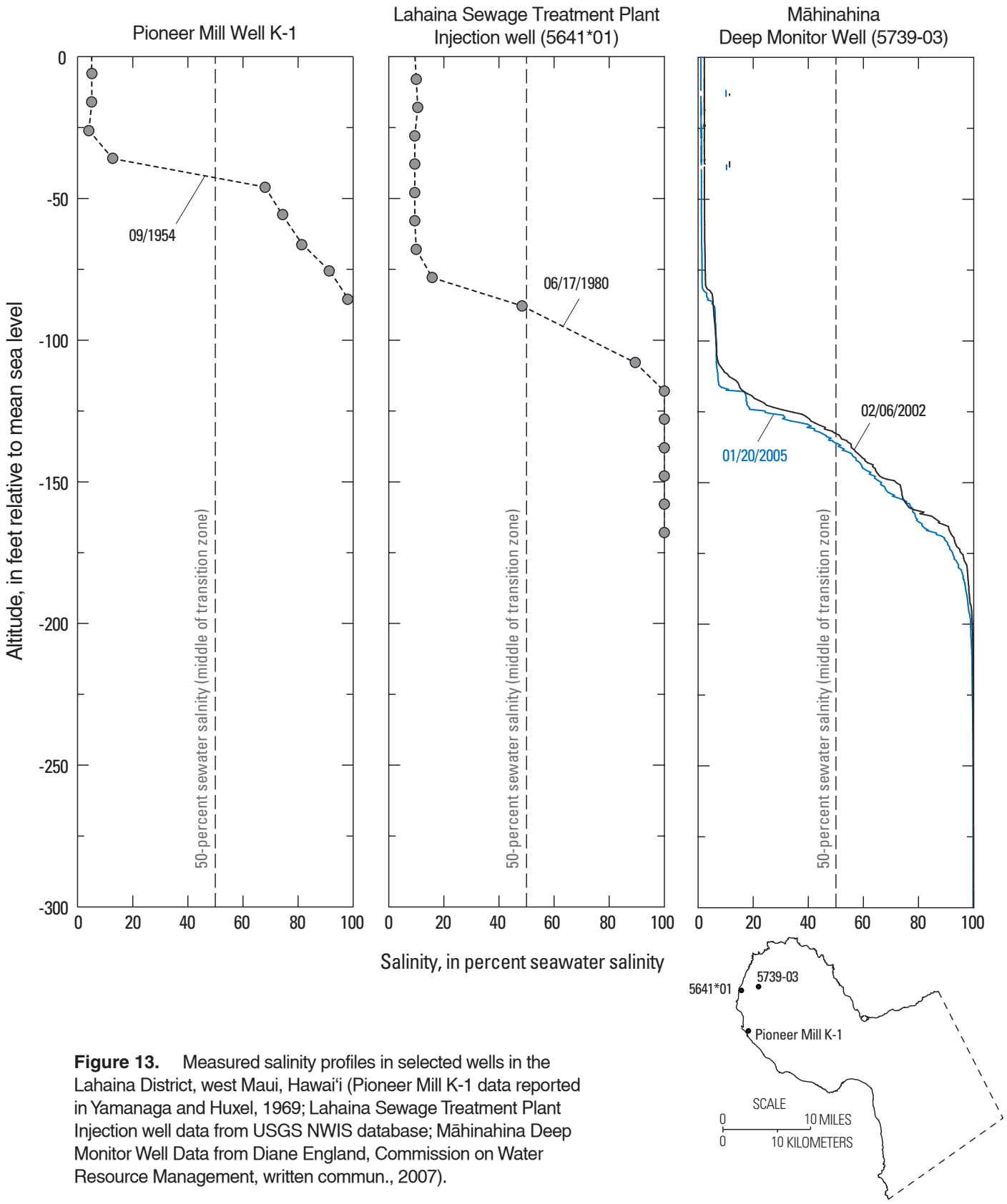

Figure 13. Measured salinity profiles in selected wells in the Lahaina District, west Maui, Hawai'i (Pioneer Mill K-1 data reported in Yamanaga and Huxel, 1969; Lahaina Sewage Treatment Plant Injection well data from USGS NWIS database; Māhinahina Deep Monitor Well Data from Diane England, Commission on Water Resource Management, written commun., 2007).

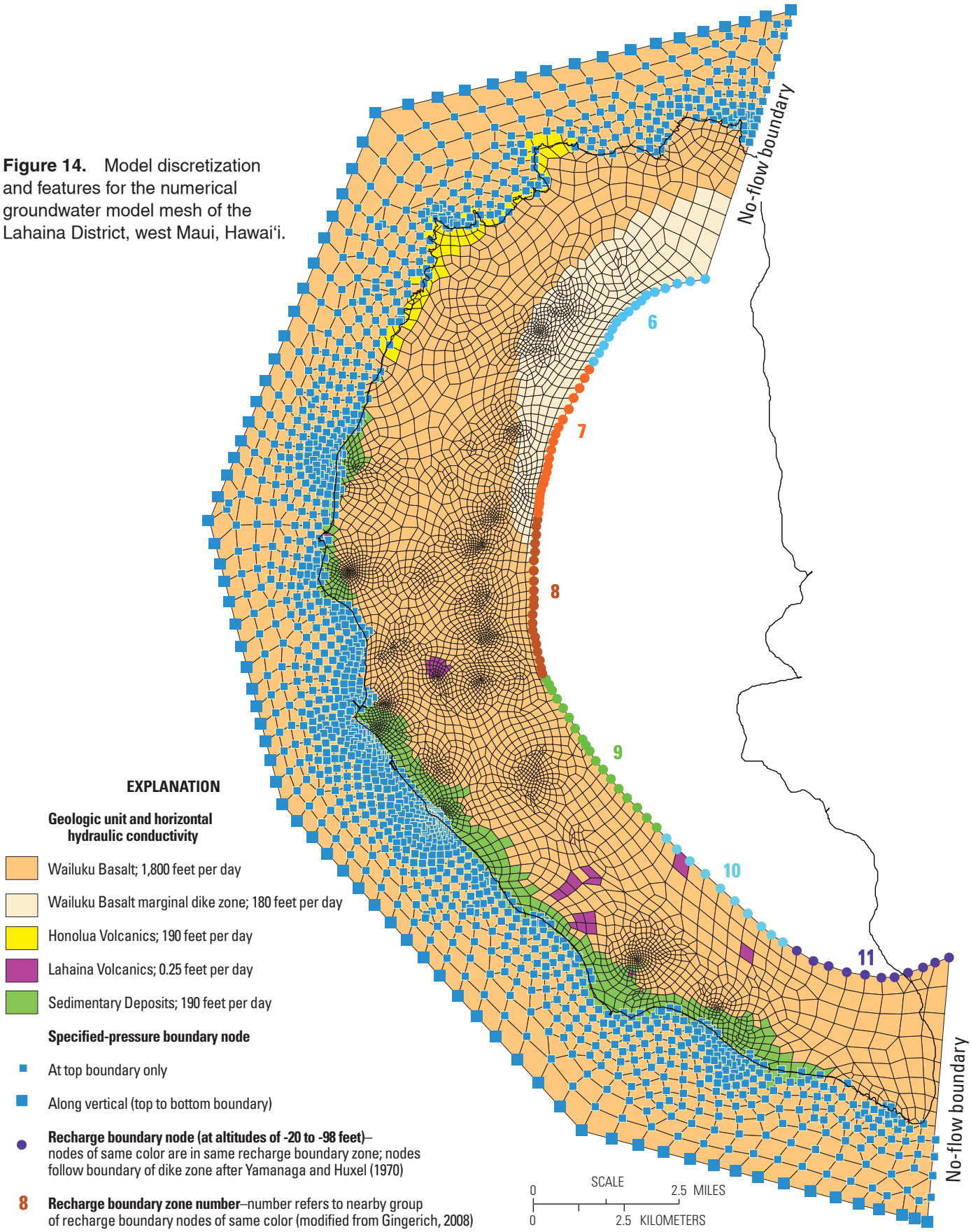

Figure 14. Model discretization and features for the numerical groundwater model mesh of the Lahaina District, west Maui, Hawai‘i.

Boundary Conditions

The model domain extent is defined by vertical boundaries that are either specified-pressure, no-flow, or recharge boundaries. Specified pressure and recharge varied with time and the no-flow boundaries remained constant throughout all simulations.

Specified Pressures and No-Flow Boundaries

The offshore, vertical boundaries of the model domain are a specified-pressure (hydrostatic ocean water) boundary condition. Pressure at each node along the offshore boundary is equal to the pressure of a column of ocean water extending from the node to sea level. In simulations for periods before 1970, when ocean-level data are not available, specified pressures were held constant in time. During 1970–2008, the pressures were varied monthly to match the observed ocean level at the Kahului Harbor (fig. 12). For simulations of future conditions, pressures also were held constant in time. Water may either enter or exit the groundwater-flow system across the offshore vertical boundary of the model. Water entering along this boundary has salinity equal to that of seawater, and water exiting along the boundary has salinity equal to that of water in the adjacent aquifer.

The top of the offshore model domain is defined by the ocean-bottom bathymetry (Taylor and others, 2008) and is a specified-pressure (hydrostatic ocean water) boundary condition. This pressure was also held constant for simulations before 1970, was varied monthly to match observed ocean levels during 1970–2008, and held constant for simulations of future conditions. Seawater may enter the model domain at the top of the boundary in offshore areas and water from the aquifer may exit at the top boundary in offshore areas.

The eastern boundaries are formed by the northern and southern rift zones of West Maui Volcano and are treated as no-flow boundaries in the model. The assumption that the rift zones can be treated as no-flow boundaries is supported by the results of the previous modeling study for central and west Maui in which the rift zones correspond to flow paths that are unaffected by regional pumping (Gingerich, 2008). The interior eastern model boundary represents the contact between the dike-intruded areas and the flank lavas of West Maui Volcano (fig. 14). Flow from the dike-intruded area recharges the model along this boundary and the determination of the amount and distribution of inflow to the model from the dike-intruded area is described below. Below altitudes of -98 ft, this boundary is a no-flow boundary. The model bottom is assumed to be a no-flow boundary due to a lack of any effective porosity as discussed above.

Recharge

Recharge was added to the model for the periods 1926–79, 1980–84, 1985–89, 1990–94, 1995–99, 2000–04 based on the distributions estimated by Engott and Vana (2007), with a modification to the 1926–79 total as described below. Recharge for 2004–08 was assumed to continue at the 2000–04 rate and distribution because land use and rainfall continued similarly. Recharge enters the model at the top, water-table boundary in onshore areas. Because the modeled area did not include the West Maui Volcano interior, recharge along the eastern model boundary (referred to as “lateral inflow”) was distributed with the aid of a simple groundwater-flow model (Gingerich, 2008) constructed using the MODFLOW-2000 code (Harbaugh and others, 2000). Lateral inflow from the interior boundary enters the model between altitudes of -20 ft and -98 ft relative to mean sea level. This interval was chosen because it is below the top layer of nodes, thus avoiding assigning two sets of recharge (lateral and areal) at the same node in SUTRA, and shallow enough to avoid adding freshwater to a node of simulated saltwater. All recharge was assigned a salinity concentration (expressed as a mass fraction) of 0.0000364 kg/kg, about equal to a chloride concentration of 20 mg/L, the average concentration measured in flow from a water-supply tunnel tapping the dike-impounded water body (U.S. Geological Survey, 2006). The water is assumed to be representative of recharge reaching the freshwater-lens system.

The MODFLOW model, described in Gingerich (2008), was constructed to represent the groundwater flow system of West Maui Volcano, including the low-permeability caldera and dike complexes of the volcano interior and the deeply incised stream valleys that drain much of the interior. For this study, the model was updated using parameter estimation techniques (Poeter and others, 2005) to better constrain the estimates of lateral inflow into the freshwater lens system. This model, which simulates only freshwater flow, is applicable because the groundwater flow system in the dike complex is tens to thousands of feet above sea level and is assumed to contain mainly freshwater. Aquifer hydraulic conductivity (assumed homogenous because of the lack of hydraulic-conductivity data) and streambed leakance values were adjusted in the model using parameter estimation techniques until simulated discharge from the aquifer to the stream valleys for the 1926–79 recharge period matched estimated base flow from the volcano’s interior during the same period as determined from the historical records of West Maui’s stream-gaging stations (table 2). For subsequent recharge periods, the best-fit adjusted values of hydraulic conductivity and streambed leakance were used in the MODFLOW model to calculate base flow based on the specified recharge for the period. The program ZONEBUDGET (Harbaugh, 1990) was used to calculate the lateral inflow from six regions (roughly the space between adjacent streams) of the dike-impounded water body (fig. 14) into adjacent parts of the freshwater-lens system in the modeled area. Because no data exist to determine areas of preferential flow to the adjacent freshwater-lens system, the flow was distributed uniformly on the basis of the length of the boundary of each of the regions. The amount of lateral inflow through each of the six regions in the Lahaina study area as a percentage of the total flow from the dike-impounded system to the freshwater-lens system ranges from 6.4 percent in recharge boundary zone 6 to 18.7 percent

Table 2. Estimated base flow and base flow simulated with MODFLOW-2000 model (Gingerich, [2008] updated using parameter estimation) for selected study area streams, west Maui, Hawai‘i.

[Mgal/d, million gallons per day]

Stream name	Estimated average base flow during 1926-79[a] (Mgal/d)	Simulated base flow using 1926–79 recharge (Mgal/d)	Difference between simulated and estimated average base flow	
			Mgal/d	Percent
Waikapū	4.19	4.20	0.01	0
‘Īao	19.09	19.07	-.02	0
Waiehu	2.98	2.15	-.83	-28
Waihe‘e	30.93	30.64	-.29	-1
Kahakuloa	4.45	4.31	-.14	-3
Honokōhau	11.91	11.81	-.10	-1
Honolua	0.93	0.63	-.30	-33
Honokōwai	3.50	4.52	1.02	29
Kahoma	3.31	3.57	0.26	8
Kanahā	2.59	2.69	.10	4
Kaua‘ula	4.01	4.04	.03	1
Launiupoko	0.65	0.67	.02	3
Olowalu	3.50	3.51	.01	0
Ukumehame	3.74	3.75	.01	0
Total	**95.79**	**95.56**	**-.23**	**-.24**

[a]Estimated from daily streamflow records.

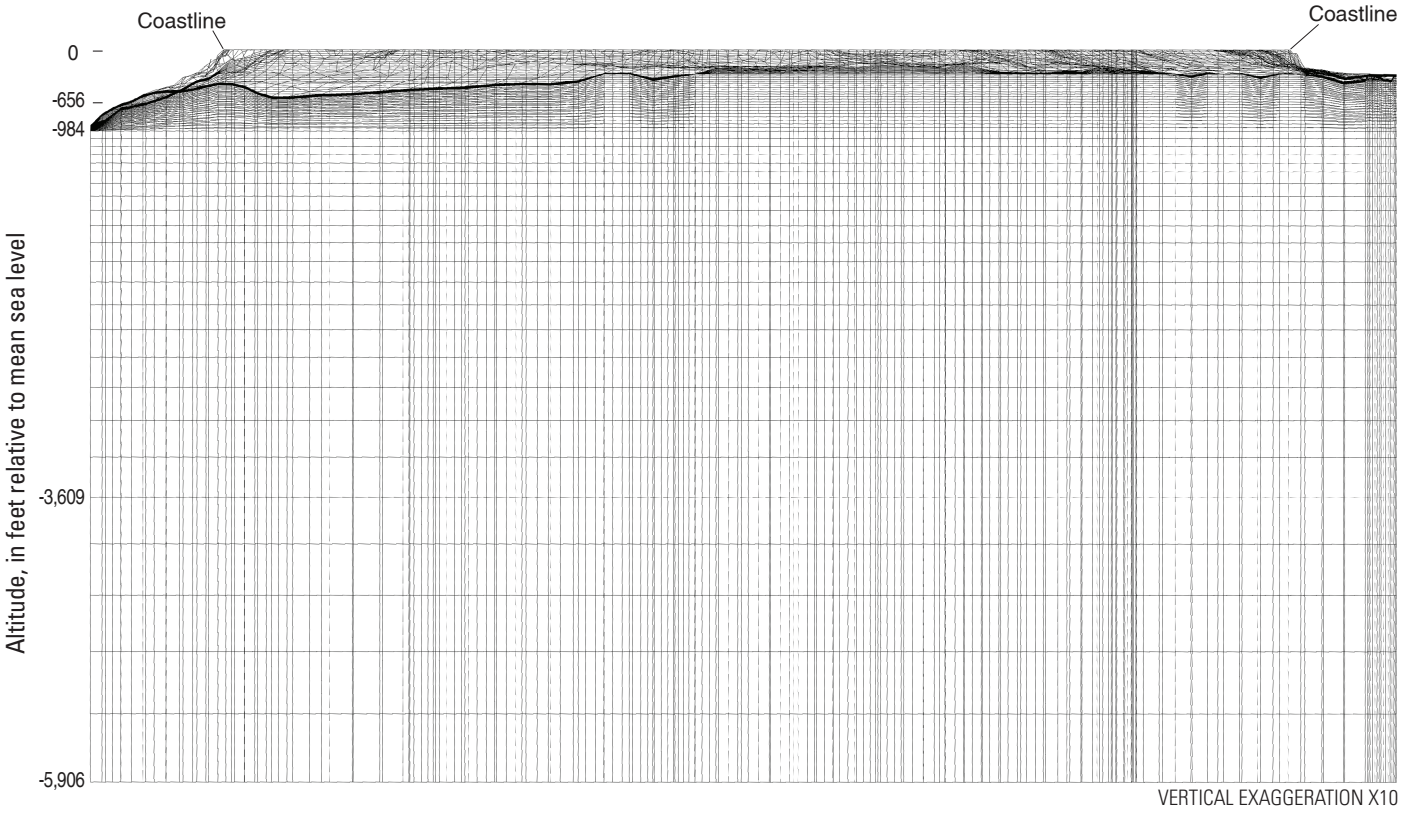

Figure 15. Vertical cross section of model mesh of the Lahaina District, west Maui, Hawai‘i.

Table 3. Recharge for historical simulation, 1926–2008, Lahaina District, Maui, Hawai'i.

[All values in million gallons per day; appendix B describes estimated recharge and recharge scenarios modified from Engott and Vana (2007); total recharge used in simulation is the sum of the estimated recharge to the modeled area and the estimated lateral inflow from the dike complex; estimated base flow to streams estimated using MODFLOW simulations; estimated lateral inflow from dike complex to surrounding aquifers divided into zones shown in Gingerich (2008) based on the following percentages: zone 1–9.9, zone 2–4.7, zone 3–5.8, zone 4–4.9, zone 5–5.6, zone 6–6.4, zone 7–8.9, zone 8–11.3, zone 9–18.7, zone 10–16.2, zone 11–7.6]

Model period	Estimated recharge		Estimated base flow to streams from dike complex	Estimated lateral inflow from dike complex to surrounding aquifers	Total recharge used in SUTRA simulation
	Modeled area	Dike complex (zones 6–11)			
1926–79	101	88	34	54	155
1980–84	65	98	40	58	123
1985–89	72	114	51	63	135
1990–94	60	101	42	59	119
1995–99	51	82	30	52	103
2000–04	31	71	23	48	79
2005–08	31	71	23	48	79
No agriculture (LU3)	34	90	35	55	89
1998–2002 drought (LU3 drght)	18	73	26	47	65
No agriculture (LU3) and restored streamflow	50	90	35	55	105

in recharge boundary zone 9 (table 3). These flow percentages were used for each recharge period to determine the amount of water added to the SUTRA model along the eastern boundary for the entire modeled period. Lateral inflow across the interior eastern boundary ranged from a high of 63 Mgal/d during 1985–89 to a low of 48 Mgal/d during 2000–08 (table 3). Total recharge to the model including lateral inflow from the dike complex was highest during 1926–79 at 155 Mgal/d and lowest during 2000–08 at 79 Mgal/d.

Withdrawal

Reported monthly withdrawals from wells during 1926–2008 were simulated in the numerical model (appendix C). Reported withdrawals were compiled from published records (Stearns and Macdonald, 1942; Yamanaga and Huxel, 1969, 1970), information contained in USGS database files (USGS Pacific Islands Water Science Center, unpub. data), and a CWRM digital database (CWRM, unpub. data, 2009).

Withdrawal wells (fig. 16) were represented in the model by the nearest vertical column of nodes to the withdrawal well. Within that column of nodes, only those nodes corresponding to the interval(s) of the well open to the aquifer (appendix D) were coded to represent withdrawal. Withdrawal from the aquifer was assumed uniform within the well interval open to the aquifer. Withdrawals from shafts with large-capacity infiltration tunnels were represented in the model by several nodes along the tunnel orientation, if known, or perpendicular to the shoreline, if unknown. In several cases where wells are closely spaced, a model node represented more than one well. In the model, withdrawals were not simulated from the top layer of nodes, thus avoiding the assignment of areal recharge and pumpage at the same node in the model.

Initial Conditions

Initial conditions for the historical simulation during 1926–2008 were estimated from a steady-state simulation using average (1926–79) recharge and average withdrawals for 1902–26. Average total recharge of 155 Mgal/d was used in the steady-state model, and simulated withdrawal, mainly from sugarcane irrigation wells, was about 27.6 Mgal/d. A two-step iterative process was used to determine model-adjusted hydrologic properties and initial conditions. Firstly, selected hydrologic properties were adjusted to improve the match between simulated heads and salinities, and historically measured values during the simulation of 1926–2008 conditions; and secondly, the steady-state simulation was repeated with the adjusted properties to compute new initial conditions. This process was repeated until the change in model adjusted hydrologic properties did not further improve the match.

Representation of Hydrologic Features

Several hydrogeologic features of low permeability were represented in the numerical model. The low permeability sedimentary wedges (fig. 14) at the mouths of many of the stream valleys form a confining unit beneath and along the coast as far south as Ukumehame Stream. To the north of Lahaina, the sedimentary units are not continuous and confine water only locally. The vertical extent of low-permeability sediments beneath the stream valleys is unknown. Water-level data are not available to indicate whether the sediments act as valley-fill barriers impeding water flow parallel to the coast. The Honolua Volcanics are also represented as low-permeability confining units where they are below sea level at the coast.

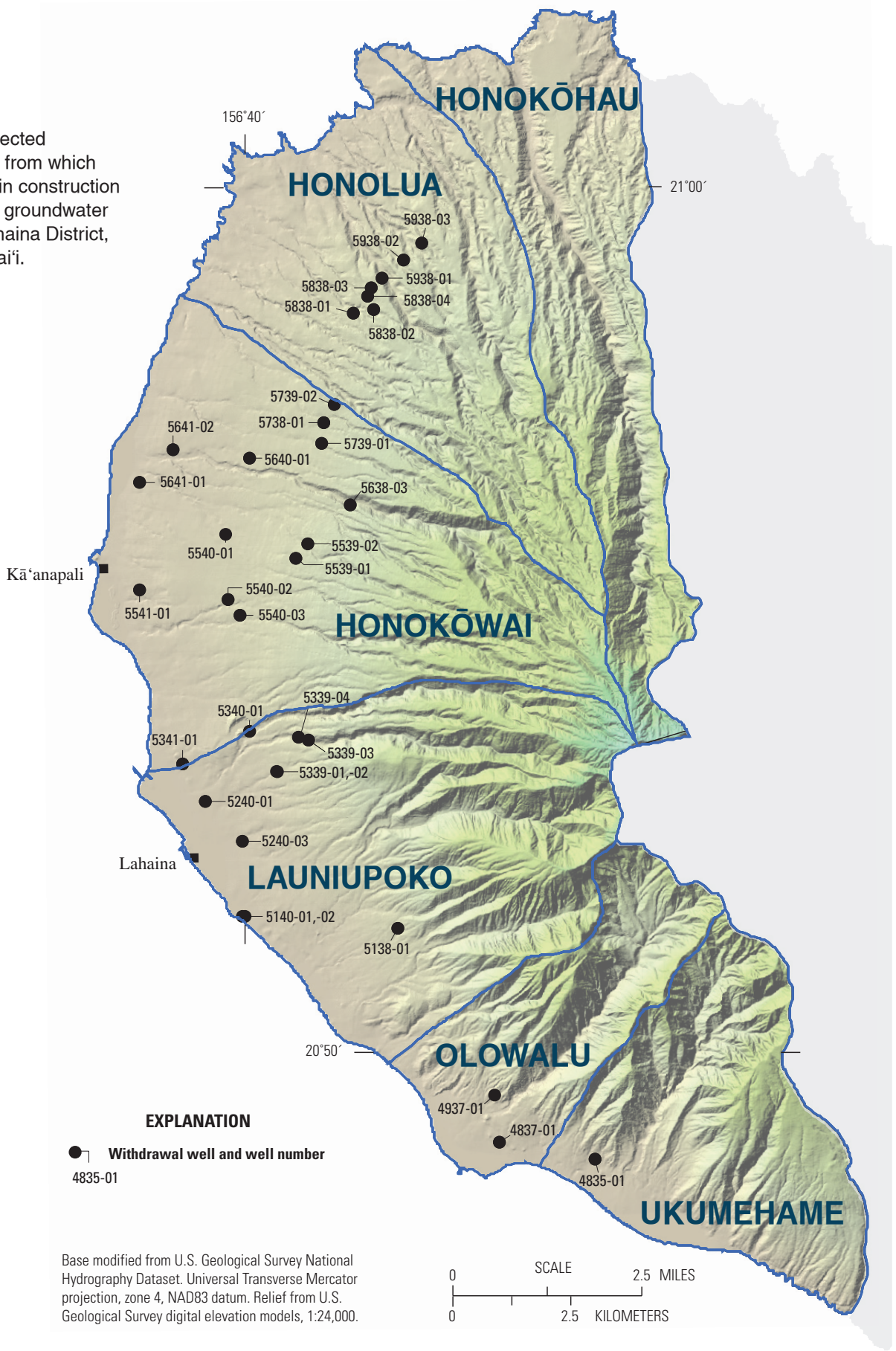

Figure 16. Selected withdrawal wells from which data were used in construction of the numerical groundwater model of the Lahaina District, west Maui, Hawai‘i.

Table 4. Aquifer-property values used in the construction of the numerical groundwater model of the Lahaina District, Maui, Hawai'i.

[ft/d, feet per day; ft, feet; ft^2/lb, feet squared per pound; Values for transverse dispersivity are equal in x, y, and z directions]

Parameter	Estimated value		
Hydraulic conductivity (ft/d)	**Vertical**	**Horizontal, transverse**	**Horizontal, longitudinal**
Wailuku Basalt	17	590	1,800
Wailuku Basalt, marginal dike zone	12	60	180
Honolua Volcanics	3.8	190	190
Sedimentary deposits	3.8	190	190
Lahaina Volcanics	0.25	0.25	0.25
Dispersivity (ft)	**Transverse**	**Longitudinal, minimum**	**Longitudinal, middle and maximum**
All volcanic units	0.18	25	250
Sedimentary and valley-fill deposits	0.18	25	250
Porosity (and specific yield)	0.15		
Solid-matrix compressibility (ft^2/lb)	1.2×10^{-7}		

Water Properties

Water was assigned a fluid compressibility of 2.14×10^{-8} $ft^2\ lb^{-1}$ (4.47×10^{-10} Pa^{-1}) and a dynamic viscosity of 2.1×10^{-5} slug $ft^{-1}\ s^{-1}$ (1.00×10^{-3} kg $m^{-1}\ s^{-1}$). Solute concentrations in the model are expressed as a mass fraction: mass of total dissolved solids (TDS) per unit mass of fluid. Freshest water was assigned a TDS concentration of 3.64×10^{-5} kg/kg and 100 percent seawater was assigned a TDS concentration of 3.57×10^{-2} kg/kg. The density of water was assumed to increase linearly with salinity from 62.42 lb ft^{-3} (1,000 kg m^{-3}) for freshwater to 63.98 lb ft^{-3} (1,024.99 kg m^{-3}) for seawater.

Molecular diffusion (Fickian) of a solute is driven by concentration gradients in the fluid and may take place in the absence of groundwater flow. Molecular diffusion of a solute in a fluid is characterized by the molecular diffusivity, which was assigned a value of 1.1×10^{-8} ft^2/s (1.0×10^{-9} m^2/s) (Voss and Provost, 2002, version of June 2, 2008) in the model.

Aquifer Properties

For the numerical model, initial aquifer properties (table 4) were assigned values based on experience with the previously published model (Gingerich, 2008). For all units, the transverse dispersivity was decreased from the values in Gingerich (2008) (0.66 ft [0.2 m] and 3.3 ft [1 m] for volcanic and sedimentary units, respectively) to a value of 0.18 ft (0.055 m) for both units so the model could reproduce the relatively thin transition zone in the study area (table 4). Longitudinal dispersivity was assigned a value of 250 ft (76 m) in the horizontal direction (corresponding to the major and semi-major axes of the permeability tensor) (Souza and Voss, 1987; Gingerich, 2008) and 25 ft (7.6 m) in the vertical direction (corresponding to the minor axis of the permeability tensor). Because limited data were available, the dispersivity values for all units were assigned the same values for simplicity.

The hydraulic-conductivity values for the different geologic features were adjusted in the numerical model to provide an acceptable match to measured water levels and salinity profiles from selected wells in the study area. Horizontal hydraulic-conductivity values used in the model ranged from 0.25 ft/d for Lahaina Volcanics to 1,800 ft/d for the dike-free Wailuku Basalt (table 4). Horizontal hydraulic-conductivity values for the volcanic-rock aquifers in the model were highest along the assumed longitudinal axis of the surficial lava flows (approximately perpendicular to the existing topographic contours) and one-third as much along the transverse axis. Vertical hydraulic conductivity of the volcanic-rock aquifers in the model was 105 to 15 times lower than the longitudinal hydraulic conductivity. Horizontal hydraulic conductivity of the sedimentary deposits was 190 ft/d and vertical hydraulic conductivity was 3.8 ft/d, a ratio of 50 to 1, which is similar to the ratio used for sedimentary deposits in Gingerich (2008).

Simulated Historical Conditions 1926–2008

Transient historical conditions were simulated using three-day time steps (for numerical stability) during 1926–2008 and initial conditions derived from the steady-state simulation. Withdrawal rates varied monthly, recharge rates were steady for each of the seven recharge periods, and specified pressures representing the ocean varied monthly after 1970. The main hydrologic parameters controlling groundwater flow in the Lahaina District are the hydraulic conductivities of the Wailuku Basalt and the sedimentary deposits. The higher water levels in the south could be simulated only by creating continuous barriers to oceanward groundwater flow.

The final distribution of hydrologic parameters was determined through a trial and error process. The trial-and-error fitting process included matching (1) simulation results to measured values of long-term water level changes throughout the system over tens of years, (2) short-term changes over a few months at individual wells, (3) hydrologic gradients from well to well and from wells to the coast, (4) salinity profile changes over time, and (5) salinities at individual pumped wells. Aquifer properties were adjusted over a wide range of reasonable values until a suitable combination of property values was found that produced a reasonable match between simulated heads, gradients, and salinities to the historical hydrologic data.

Water Levels

Simulated water levels generally are in agreement with measured water levels from representative wells in the modeled area (fig. 17). Greater emphasis was placed on matching measured water levels from wells monitored during this study (5137-01, 5739-01, 5840-01, and 5938-04) because much of the historical water-level data were less certain due to questionable measuring-point altitudes or unknown pumping conditions before the measurements were collected.

The effects of including ocean-level variations in the historical simulation are most apparent at wells near the coast and away from areas of relatively lower permeability sedimentary deposits. Simulated water levels at the ʻAlaeloa well (5840-01) reasonably match short- and long-period observed water-level variations although the modeled long-term water levels trend higher than observed. For example, the increase in ocean level of about 0.5 ft during 2000–04 (figs. 11 and 17) is reflected by the increase in water level in this well during a time when the recharge rate was relatively low and withdrawal near this well was not decreasing.

Within the Lahaina District, simulated water levels generally match the distribution of water levels measured on September 10, 2008 (fig. 18). The best match to measured water levels was obtained in the central and northern part of the study area, where most of the pumping is concentrated. The water level at well 5638-03 (5.43 ft) was measured on April 2, 2009 after the pump was removed from the well for maintenance. Therefore, the water level was probably lower on September 10, 2008 when all of the other wells were measured because well 5638-03 was being pumped regularly. A lower expected water level would better match the simulated water-table distribution from September 2008.

Some of the discrepancy between measured and simulated water levels can be attributed to uncertainties in the estimated distribution of hydraulic properties in the numerical model. Some discrepancy also may be related to other factors, including: (1) no predevelopment water levels are available in the Lahaina District, (2) temporally coarse 5-yr recharge estimates may not reflect conditions antecedent to the day when water levels were measured, (3) reported groundwater-withdrawal information may be inaccurate, (4) model spatial discretization may be too coarse in some areas to accurately simulate local water-level changes.

During 1926–2008, simulated groundwater levels varied the most near pumped wells, but water levels remained relatively steady away from pumped wells throughout the entire period. For example, water levels declined about 2 ft at well 4937-01 during 1926–1980 but recovered to pre-pumping levels by 2008 as pumping at this well decreased and eventually stopped. At well 5840-01, distant from any pumping stress, water levels varied about 0.5 ft year to year but water levels at the end of the simulation were within 0.5 ft of the starting water level (fig. 17). The area of most recent water-level decline is in the northern part of the study area near wells 5838-01, -02, -03, and -04; and 5938-01 where pumping is concentrated. Simulated water levels around these wells are 2-4 ft lower than simulated pre-pumping water levels.

Salinity in Wells

Pumped wells

Simulated salinity values at pumped wells generally are in agreement with measured salinity values of the pumped water (fig. 19) with the exception of the Kanahā wells in the 1980s and 1990s. No reason for this mismatch is readily apparent, but a possible reason could be unaccounted localized variability in recharge or withdrawal near the Kanahā wells. Observed salinity values were converted from reported chloride concentrations by dividing the pumped-water chloride concentration by the assumed seawater chloride concentration (19,600 mg/L) and multiplying the result by 100. Chloride concentration values were obtained from various MDWS, Hawaii Water Service Company, and Pioneer Mill records on file at the USGS Pacific Islands Water Science Center (PIWSC). When matching simulated salinity values to measured values, greater emphasis was placed on matching measured chloride-concentration values within the last ten years than on the older measure-ments from Pioneer Mill because those older measurements were commonly reported as end of the year averages.

Profiles

The shapes of the simulated salinity profiles are consistent with the measured profiles (fig. 20). At Pioneer Mill Well K-1, simulated and measured depths where salinity is 50 percent that of seawater are within about 15 feet of each other at the time the profile was measured. At the Lahaina Sewage Treatment Plant (STP) injection well, the simulated 50-percent depth is within 3 ft of the measured depth, and at the Māhinahina Deep Monitor well, the simulated depth where salinity is 50 percent that of seawater is about 8 ft deeper than the measured depth in 2005. As mentioned previously, because measured salinity

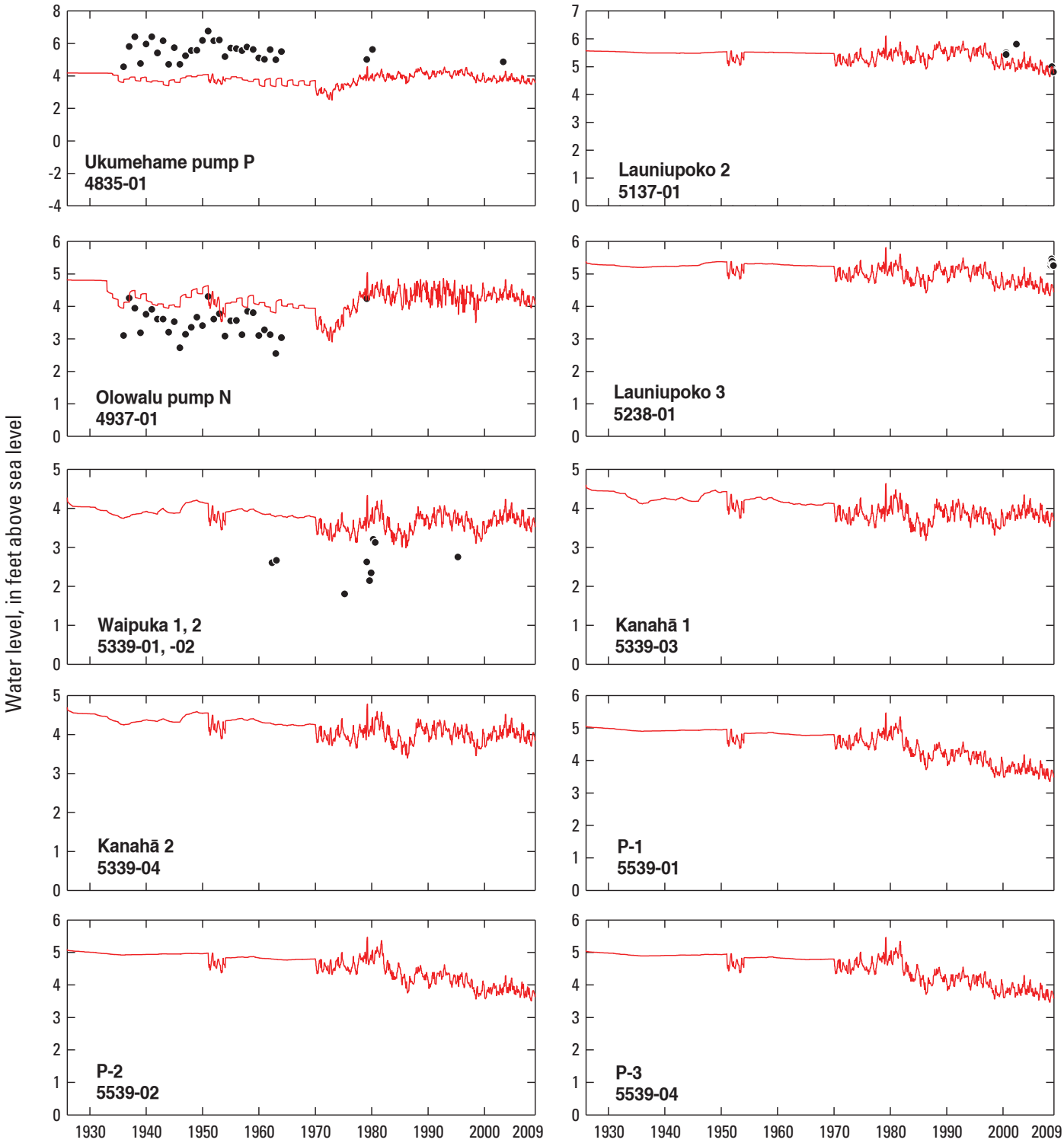

Figure 17. Measured (black circles) and simulated (red lines) water levels in selected wells in the Lahaina District, west Maui, Hawai‘i. Well number shown below well name. Water-level data from Pioneer Mill Co. and U.S. Geological Survey NWIS database.

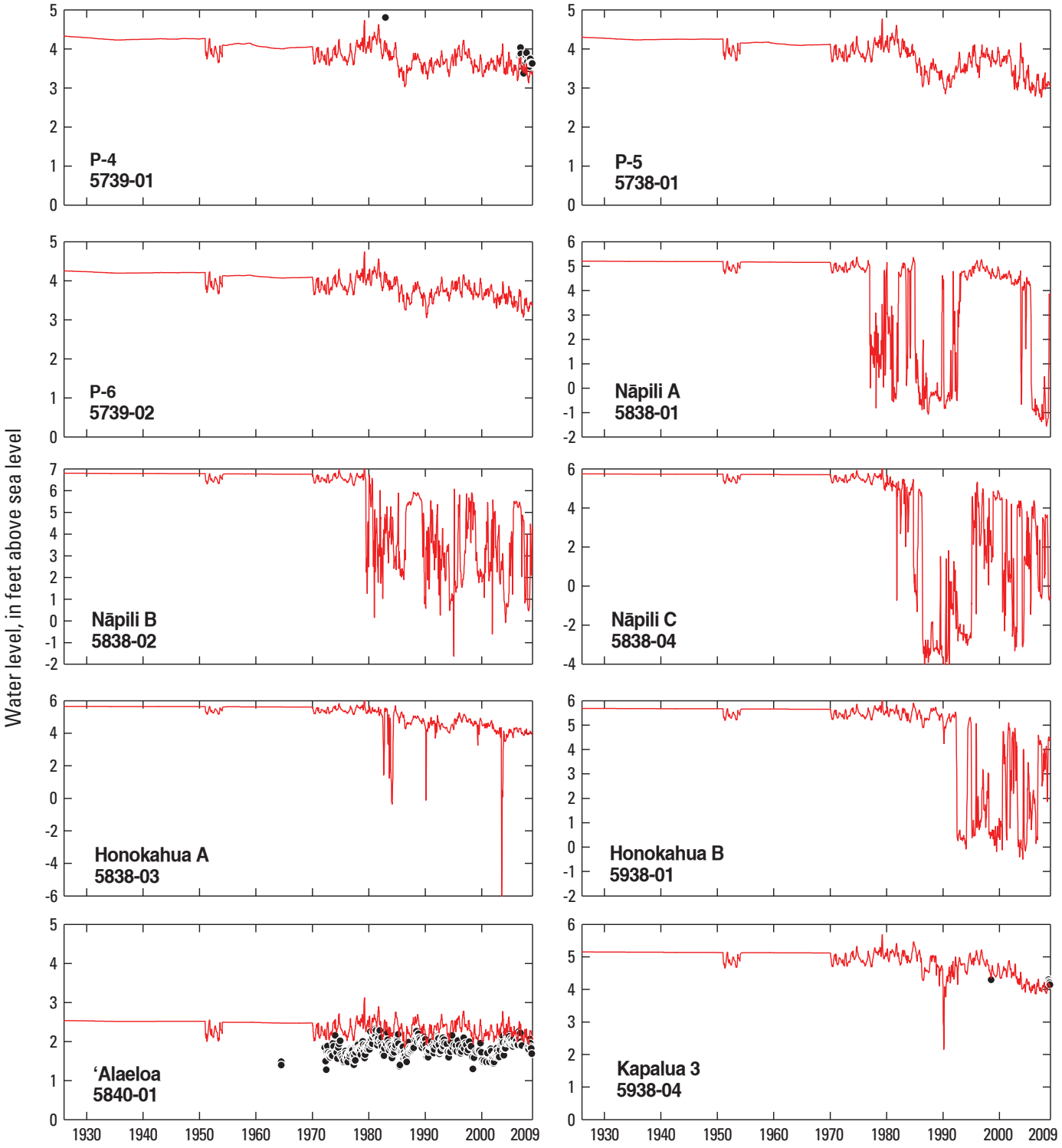

Figure 17. Measured (black circles) and simulated (red lines) water levels in selected wells in the Lahaina District, west Maui, Hawai'i. Well number shown below well name. Water-level data from Pioneer Mill Co. and U.S. Geological Survey NWIS database—continued.

profiles indicate a relatively thin transition zone, the values of transverse dispersivity had to be decreased to 0.18 ft in order for the model to reproduce the measured salinity profiles. The transverse dispersivity values used in this model are about 27 percent of the values used in the previous central Maui model (Gingerich, 2008).

Some of the discrepancy between measured and simulated salinity profiles can be attributed to (1) uncertainties in the estimated distribution of hydraulic properties in the model, (2) possible borehole flow in the deep monitor wells (Paillet and others, 2002), (3) insufficient vertical discretization in the numerical model mesh, and (4) additional factors described above for simulated water levels. The model does not account for borehole flow yet borehole flow in the deep monitor wells can cause shifting of the salinity profile relative to the salinity distribution in the surrounding aquifer (Rotzoll, 2010). Therefore, a lack of agreement between the simulated and measured profiles is possible. Near the coast, the head at depth tends to be greater than at the water table. Hence, the midpoint of the measured salinity profile in the well will tend to be shallower than that in the aquifer.

The simulated depth at which the salinity of water in the aquifer is 2 percent seawater is shallower than 40 ft below sea level over much of the coastal part of the Lahaina Aquifer Sector (fig. 21). The 2-percent salinity contours generally follow the pattern of the simulated water-level map (fig. 18), being deeper inland where water levels are higher.

Simulated Future Scenarios

The numerical model constructed for this study was used to quantify changes in groundwater level and salinity with continued groundwater withdrawal under several hypothetical withdrawal and recharge scenarios (table 5). The simulated initial conditions of water levels and salinities for all scenarios were the final conditions from the 1926–2008 historical simulation. All scenarios had 2000–04 land use (without agricultural irrigation). These scenarios included:

- Scenario 1–groundwater withdrawal at average 2008–09 rates and locations and recharge and 1926–2006 rainfall,
- Scenario 2–withdrawal at projected rates and locations and recharge and 1926–2006 rainfall,
- Scenario 3–withdrawal at maximum-build out projected rates and locations and recharge and 1926–2006 rainfall,
- Scenarios 4 and 5–withdrawal at redistributed rates and locations and recharge and 1926–2006 rainfall,
- Scenario 6–withdrawal at redistributed rates and locations with added recharge from restored streamflow and 1926–2006 rainfall, and
- Scenario 7–recharge during a historic drought.

All scenarios were simulated for the period 2010–2039. For each scenario, recharge was kept at rates used during 2000–08 for two years (accounting for a lag between recent rainfall and the time it takes to recharge the aquifer similar to the lag used in Gingerich (2008)] and then changed to the average (2000–04 land use without agricultural irrigation and 1926–2006 rainfall) recharge during 2012–2039. All future recharge estimates are based on continuation of historical average or, in one case, drought rainfall conditions, and do not include potential effects of climate change on rainfall amounts or distribution. All scenarios reached equilibrated hydrologic conditions within a few years, after which no water-level or salinity changes are apparent.

For each scenario, the simulated salinity at selected pumped wells is classified as: (1) acceptable, salinity less than 1.0 percent seawater; (2) cautionary, salinity between 1.0 and 2.5 percent seawater; and (3) threatened, salinity greater than 2.5 percent seawater. Wells with simulated salinity in the cautionary class have the potential to produce water with salinity higher than is acceptable for drinking. Wells with simulated salinity in the threatened class are likely to produce water unacceptable for drinking. This classification was developed cooperatively with the MDWS (Gingerich, 2008) to provide a basis for comparing the various scenarios investigated in this study.

Scenario 1—2008–09 Withdrawal Rates and Locations using 2000–04 Land Use without Plantation-Scale Agriculture and 1926–2004 Rainfall

In Scenario 1, the most likely future average recharge without plantation-scale agriculture and most recent withdrawal estimates were used to simulate the effects of continuing the current conditions over the next 30 years. Assigned total recharge over the model domain was 89 Mgal/d, based on 2000–04 land use without agricultural irrigation and 1926–2004 rainfall (table 5). Total withdrawal was simulated using average annual reported 2008–09 withdrawal (table 6). Gingerich (2008) demonstrated that using average annual rates, which provide faster and slightly more stable model solutions rather than using monthly rates, was acceptable. Total withdrawal averaged 6.29 Mgal/d throughout the Lahaina Aquifer Sector. Injection of treated wastewater effluent was 2.0 Mgal/d.

Simulated salinity for the period 2010–39 is shown for select wells in figure 22. For each well shown, the simulated salinity is for the deepest node representing the well. The largest long-term simulated salinity increases are at P-4 (5739-01) and P-6 (5739-02) wells, where the salinity increases by about 2-percent seawater salinity over 30 years. These are the only two pumped wells at which the simulated salinity increases into the threatened class. The simulated salinity at the Puamana wells (5140-01,-02), which are used for irrigation,

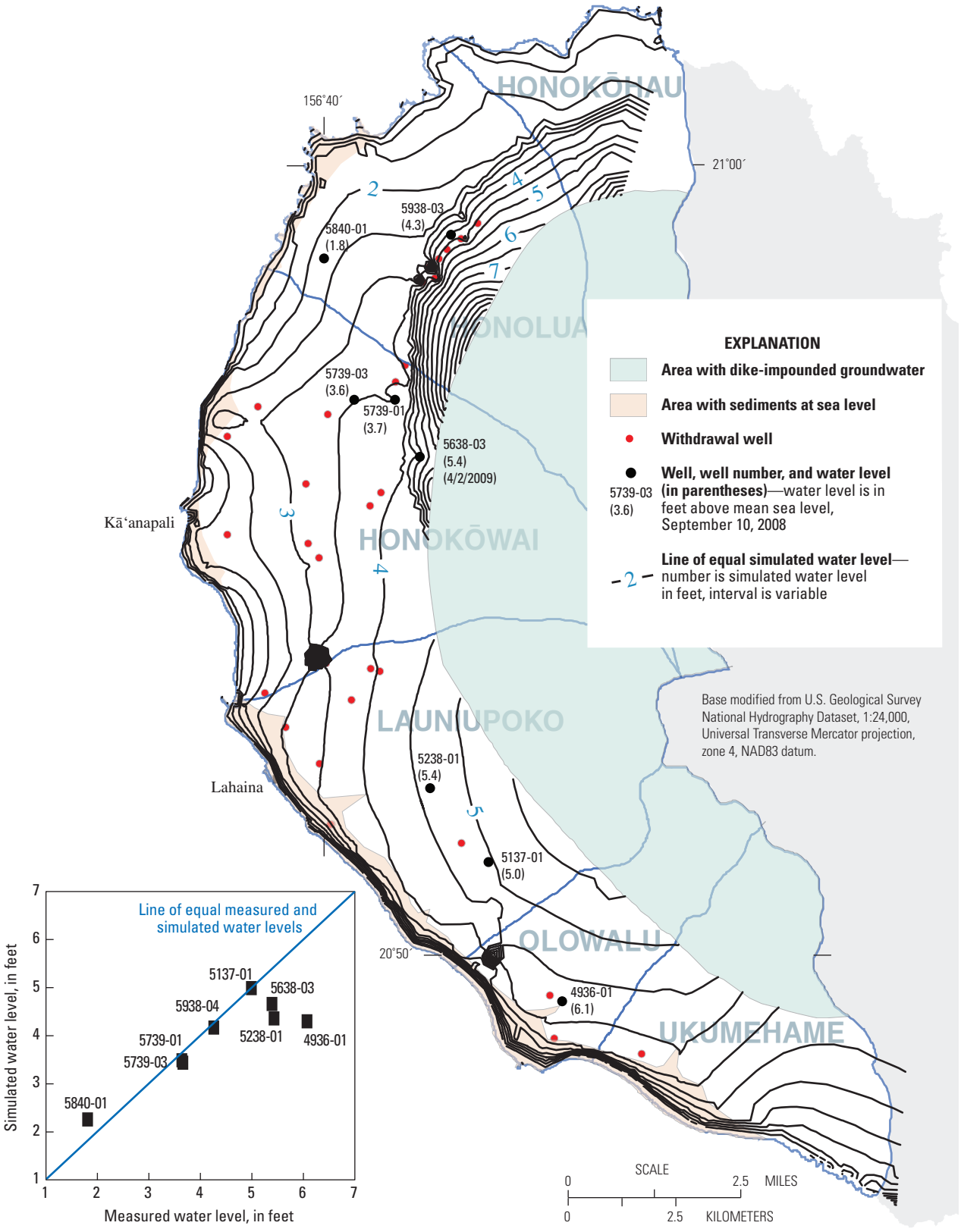

Figure 18. Measured water levels on September 10, 2008 compared with simulated water levels in the Lahaina District, west Maui, Hawai‘i. (The datum for all water levels is mean sea level.)

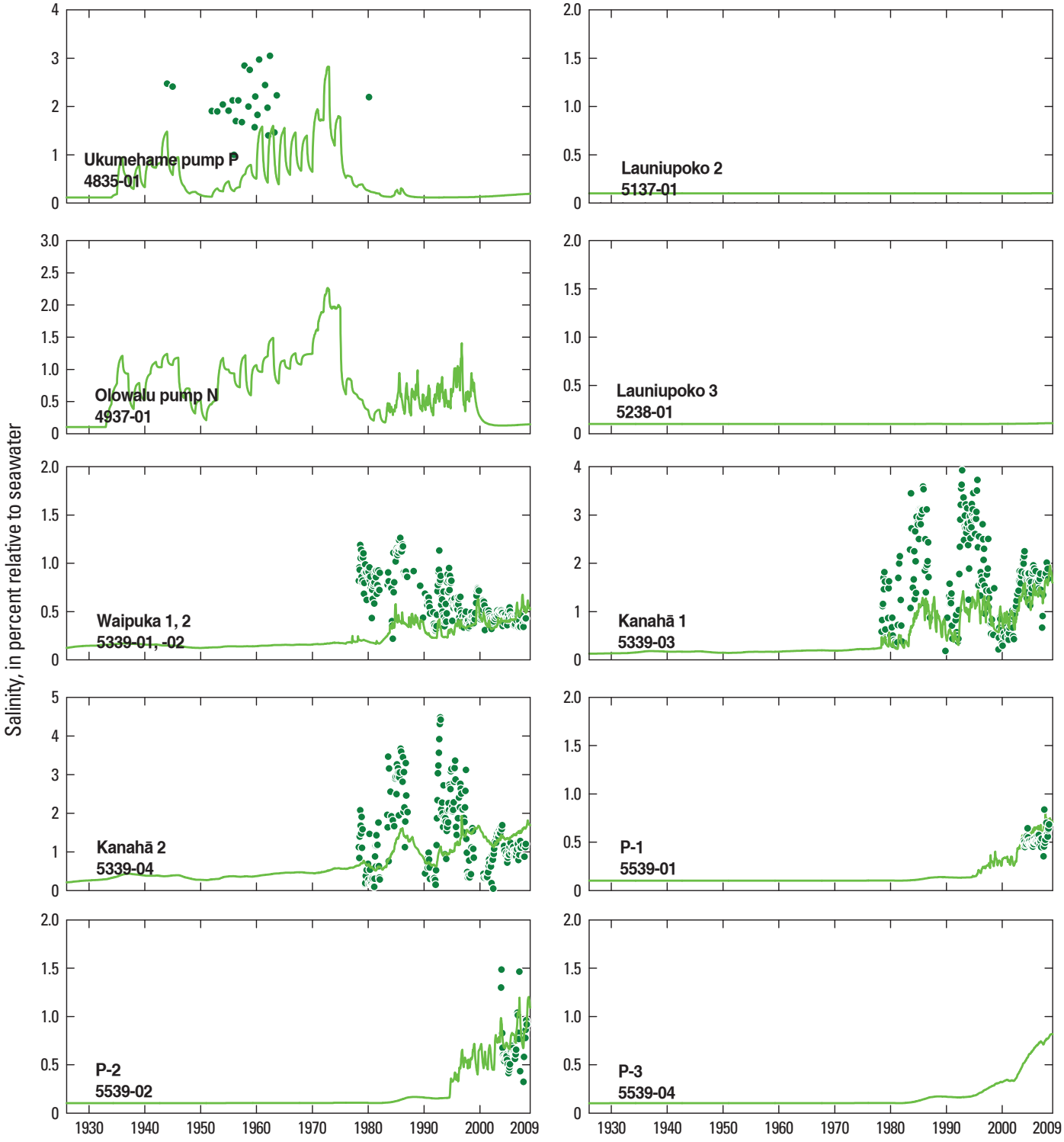

Figure 19. Measured (green circles) and simulated (green lines) salinity in selected wells in the Lahaina District, west Maui, Hawai‘i. Well number shown below well name. Chloride data provided by Pioneer Mill Co., Maui Department of Water Supply, Hawaii Water Service Company, and Maui Land & Pineapple Co., Inc.

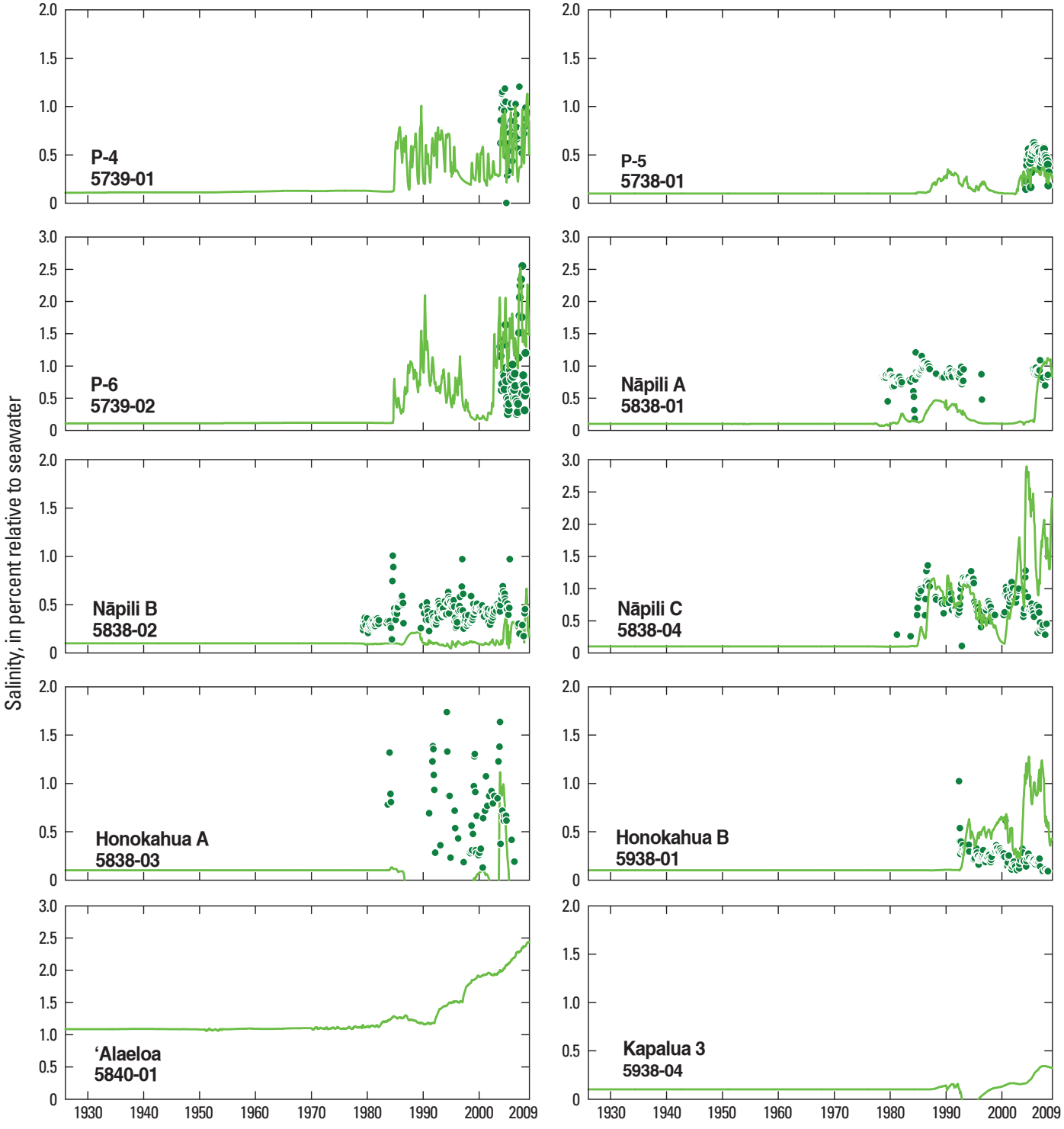

Figure 19. Measured (green circles) and simulated (green lines) salinity in selected wells in the Lahaina District, west Maui, Hawai‘i. Well number shown below well name. Chloride data provided by Pioneer Mill Co., Maui Department of Water Supply, Hawaii Water Service Company, and Maui Land & Pineapple Co., Inc—continued.

Table 5. Withdrawal and recharge used in various simulation scenarios, Lahaina District, west Maui, Hawai‘i.

[All simulations are from 2010–2039; Mgal/d, million gallons per day; yr, year]

Scenario	Recharge condition	Pumping condition
1	89 Mgal/d: 2000–04 land use without plantation-scale agriculture; 1926–2004 rainfall	6.3 Mgal/d: 2008–09 withdrawal rates; 2.0 Mgal/d injection
2	89 Mgal/d: 2000–04 land use without plantation-scale agriculture; 1926–2004 rainfall	11.2 Mgal/d: 30-yr projected withdrawal rates; 7.0 Mgal/d injection
3	89 Mgal/d: 2000–04 land use without plantation-scale agriculture; 1926–2004 rainfall	11.2 Mgal/d: 30-yr projected withdrawal rates; no injection
4	89 Mgal/d: 2000–04 land use without plantation-scale agriculture; 1926–2004 rainfall	17.1 Mgal/d: 30-yr projected withdrawal rates with full Hawaii Water Service Company projection; 7.0 Mgal/d injection
5	89 Mgal/d: 2000–04 land use without plantation-scale agriculture; 1926–2004 rainfall	20.7 Mgal/d: Redistributed withdrawal; 7.0 Mgal/d injection
6	105 Mgal/d: 2000–04 land use without plantation-scale agriculture; 1926–2004 rainfall; added 16 Mgal/d from streambed recharge	11.2 Mgal/d: 30-yr projected withdrawal rates; 7.0 Mgal/d injection
7	89 Mgal/d: 2000–04 land use without plantation-scale agriculture; 1926–2004 rainfall	11.2 Mgal/d: 30-yr projected withdrawal rates; 7.0 Mgal/d injection with worst historic drought (65 Mgal/d; 1998–2002 rainfall) during 2025–29

is in the threatened class for all withdrawal rates in all scenarios because the wells are so close to the coast (fig. 16). Simulated salinity remains in the cautionary class during the entire 30-year simulation at Kanahā 1 and 2 wells (5339-03 and -04), P-2 well (5539-02), and Nāpili C well (5838-04). The amount of withdrawn water in which salinities are either threatened or cautionary after 30 years, expressed as a percentage of total withdrawal, for each of the four most-utilized aquifer systems is as follows: Honolua, 29 percent; Honokōwai, 48 percent; Launiupoko, 60 percent; Olowalu, 0 percent.

Regional changes of average water levels in the aquifer after 30 years, presented relative to conditions at the end of the 1926–2008 historical simulation, are greatest in the Honokōwai Aquifer System, where average water-level differences are more than 0.5 ft lower (fig. 23*A*). The freshwater body thinned slightly in this area as the depths of the bottom of the freshwater and the middle of the transition zone are shallower by more than 30 ft and 20 ft, respectively (figs. 23*B-C*).

Regional changes of coastal groundwater discharge after 30 years are presented in arbitrarily assigned one-mile segments of the coastline relative to conditions at the end of the 1926–2008 historical simulation (fig. 24). Coastal groundwater discharge is calculated from the SUTRA model output by summing the freshwater flux (total water flux multiplied by percent freshwater fluid concentration) leaving each specified pressure node along the coast. Coastal groundwater discharge is higher after 30 years along segments of the coast in the Honokōwai and Honolua Aquifer Systems due mainly to the increased recharge for average conditions relative to the recharge at the end of 2008 (fig. 24*A*). Coastal groundwater discharge is lower in the Launiupoko, Olowalu, and Ukumehame Aquifer Systems.

As the freshwater body becomes thinner, the simulated salinity at the P-4 (5739-01) and P-6 (5739-02) wells moves into the cautionary salinity class (1.0–2.5 percent seawater) after 30 years (fig. 25*A*). Wells in the northern part of the Lahaina Aquifer Sector are more vulnerable to increased salinities because they are in the area with no continuous sedimentary caprock, so the freshwater lens is thinner and less isolated from the ocean.

For this scenario, withdrawal of 6.29 Mgal/d from Lahaina Aquifer Sector results in 1.67 Mgal/d of cautionary yield[1] and 0.98 Mgal/d of threatened yield[2] after 30 years (table 7). The Honokōwai Aquifer System has the highest amount of combined cautionary (0.6 Mgal/d) and threatened (0.93 Mgal/d) yield.

Scenario 2—Projected Withdrawal Rates and Locations using 2000–04 Land Use without Plantation-Scale Agriculture and 1926–2004 Rainfall

In Scenario 2, the most likely future average recharge and projected withdrawal estimates were used to simulate the effects of planned groundwater development in the Lahaina District during the next 30 years. Assigned total recharge over the model domain was 89 Mgal/d, based on 2000–04 land

[1] Cautionary yield – The volume of withdrawn water that has a salinity from 1 to 2 percent that of seawater

[2] Threatened yield – The volume of withdrawn water that has a salinity greater than 2 percent that of seawater

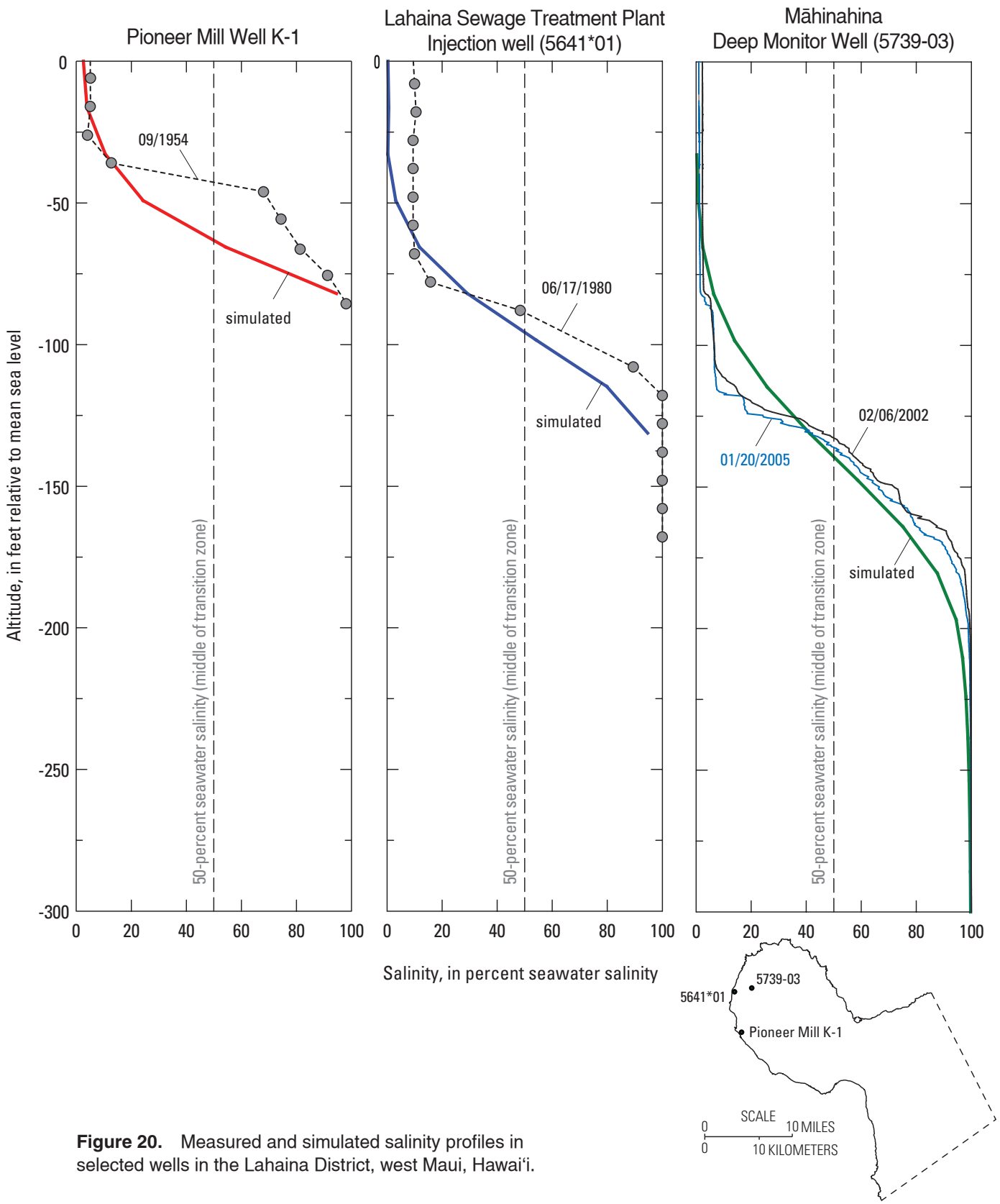

Figure 20. Measured and simulated salinity profiles in selected wells in the Lahaina District, west Maui, Hawai‘i.

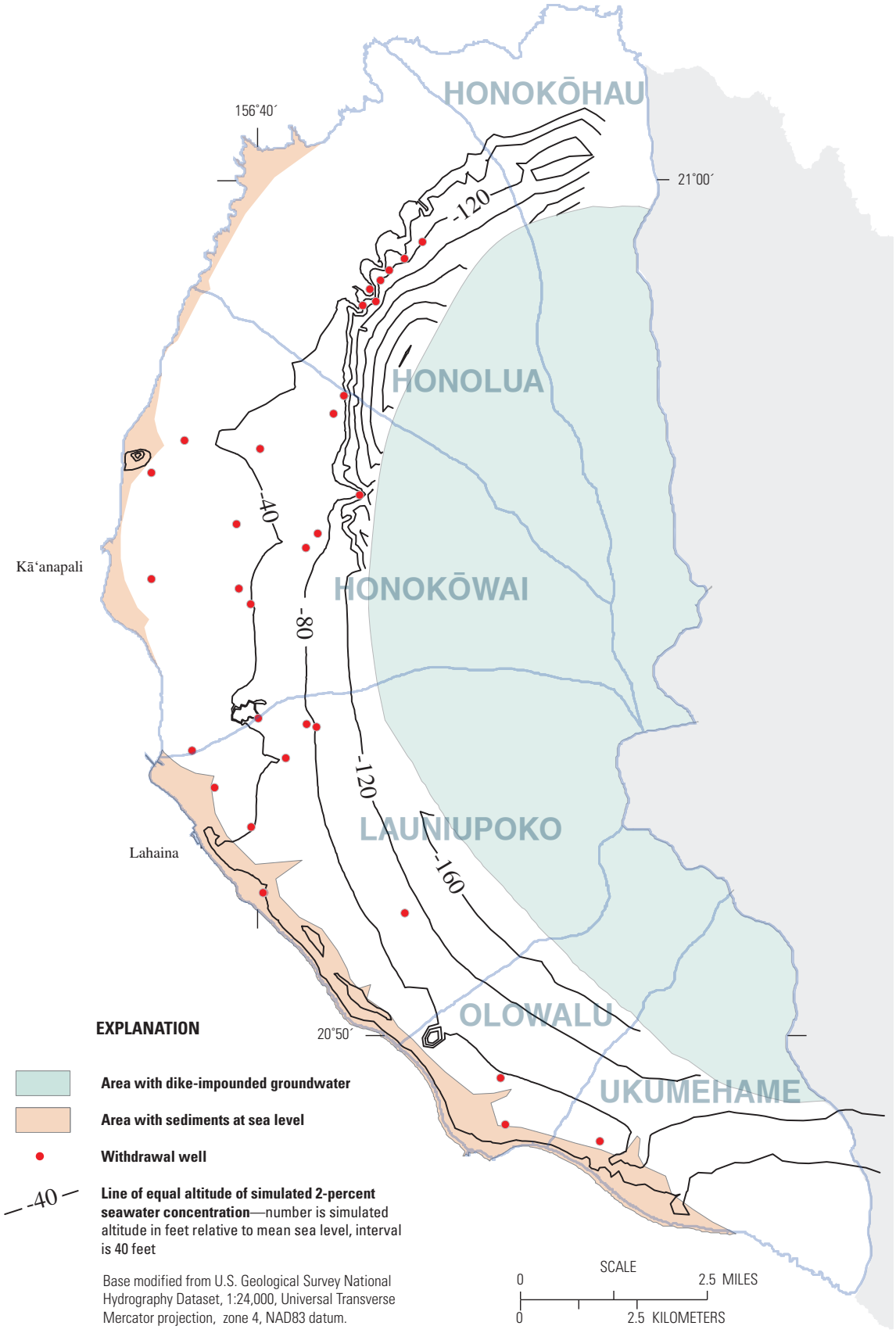

Figure 21. Simulated depth of 2-percent seawater salinity at the end of the historical simulation (2008), Lahaina District, west Maui, Hawai‘i.

Table 6. Selected wells and withdrawal rates used in Scenarios 1 and 5, west Maui, Hawai‘i.

[Values in pink or red represent wells with salinity in the cautionary or threatened range; cautionary yield is the volume of withdrawn water that has a salinity from 1 to 2 percent that of seawater; threatened yield is the volume of withdrawn water that has a salinity greater than 2 percent that of seawater; --, not applicable; *italics* text indicates injection]

Well name	Well number	Withdrawal rate (million gallons per day)	
		Scenario 1	Scenario 5
Honolua Aquifer System			
Nāpili A	5838-01	0.34	0.55
Nāpili B	5838-02	.75	.27
Nāpili C	5838-04	.65	.08
Honokahua A	5838-03	.0	.14
Honokahua B	5938-01	.09	.45
Kapalua 1	5938-02	.17	.27
Kapalua 2	5938-03	.27	.2
Nāpili (proposed)	--	.0	1.2
Total		**2.27**	**3.16**
Honokōwai Aquifer System			
P-1	5539-01	0.54	0.4
P-2	5539-02	.27	.0
P-3	5539-04	.0	.35
P-4	5739-01	.63	.0
P-5	5738-01	.89	1.1
P-5A	5739-04	.0	0.0
P-6	5739-02	.3	.0
Honokōwai B	5638-03	.23	.6
Hāhākea	5540-03	.31	.0
Pu‘ukoli‘i	5540-01	.02	.0
Māhinahina (proposed)	--	.0	.42
DHHL (proposed)	--	.0	.15
Honokōwai (proposed)	--	.0	.32
Wahikuli 5 (proposed)	--	.0	.6
Wahikuli 4 (proposed)	--	.0	.34
Wahikuli 3 (proposed)	--	.0	.29
Wahikuli 2	5439-02	.0	.16
Wahikuli 1	5439-01	.0	.34
Lahaina Injection	*5641*01, *02, *03, *04*	*- 1.96*	*- 1.96*
Total		**3.19**	**5.07**
Launiupoko Aquifer System			
Waipuka 1, 2	5339-01, -02	0.17	0.0
Kanahā 1	5339-03	.26	.0
Kanahā 2	5339-04	.16	.0
Launiupoko 1	5138-01	.11	1.4
Launiupoko 2	5137-01	.01	4.0
Launiupoko 3	5238-01	.02	3.4
Puamana 1, 2	5140-01, -02	.05	0.0
Kanahā (proposed)	--	.0	1.25
Waipuka (proposed)	--	.0	0.8
Total		**.78**	**10.85**
Olowalu Aquifer System			
Olowalu Elua	4936-01	0.05	1.6
Total		**.05**	**1.6**
Ukumehame Aquifer System			
Sugar Way 1, 2	4835-02, -03	not available	not available
Total		**not available**	**not available**
Total Lahaina Aquifer Sector management area		**6.29**	**20.68**

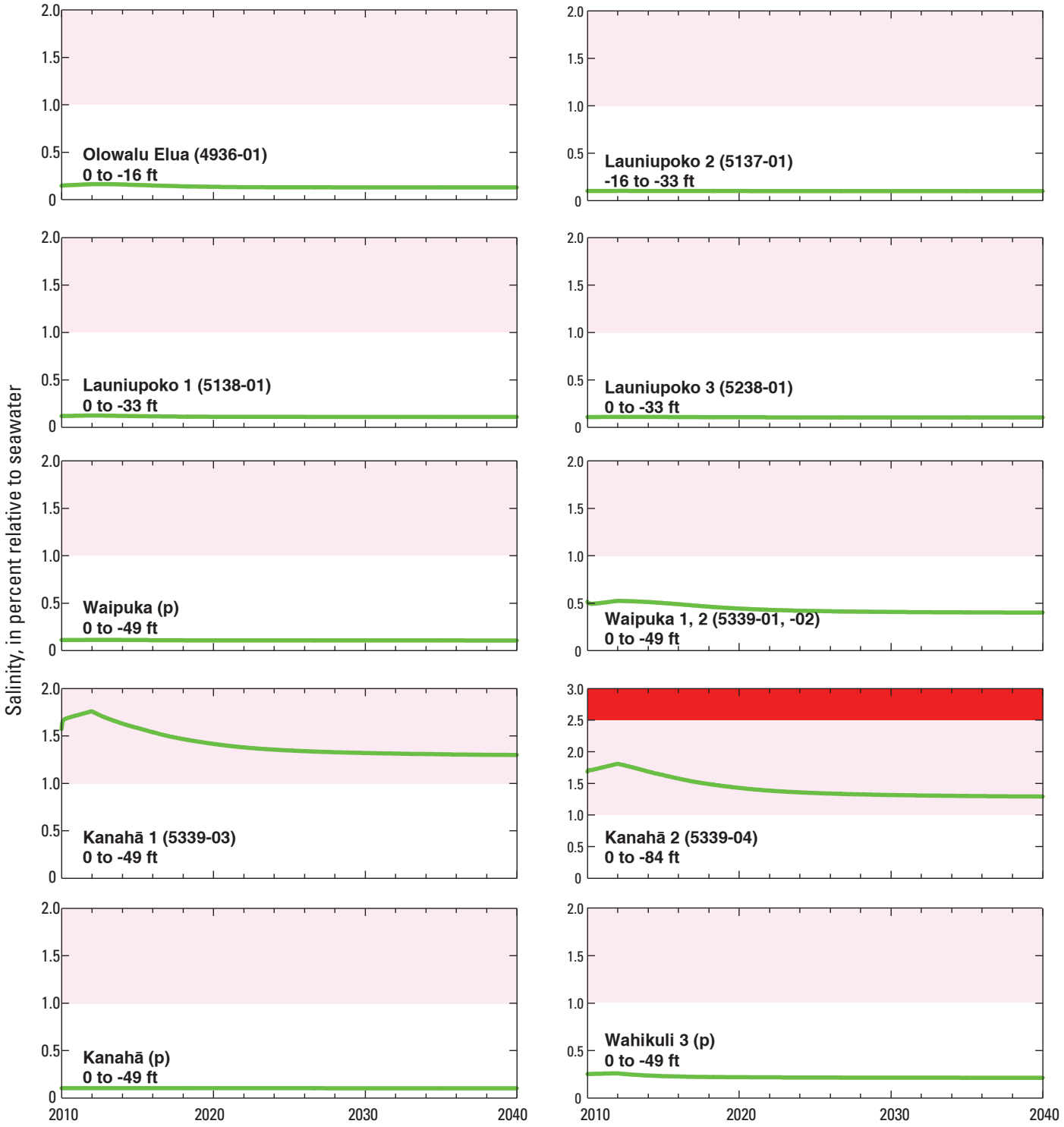

Figure 22. Simulated salinity data (green lines) for the period 2010–39 for Scenario 1, assuming average 2008–09 pumping rates at selected wells in the Lahaina Aquifer Sector, West Maui, Hawai‘i. For each well shown, the simulated salinity is for the deepest node representing the well. The depths of the nodes used are shown under each well name and number. Well names followed by (p) are proposed wells. The pink area represents a cautionary salinity class and the red area represents a threatened salinity class.

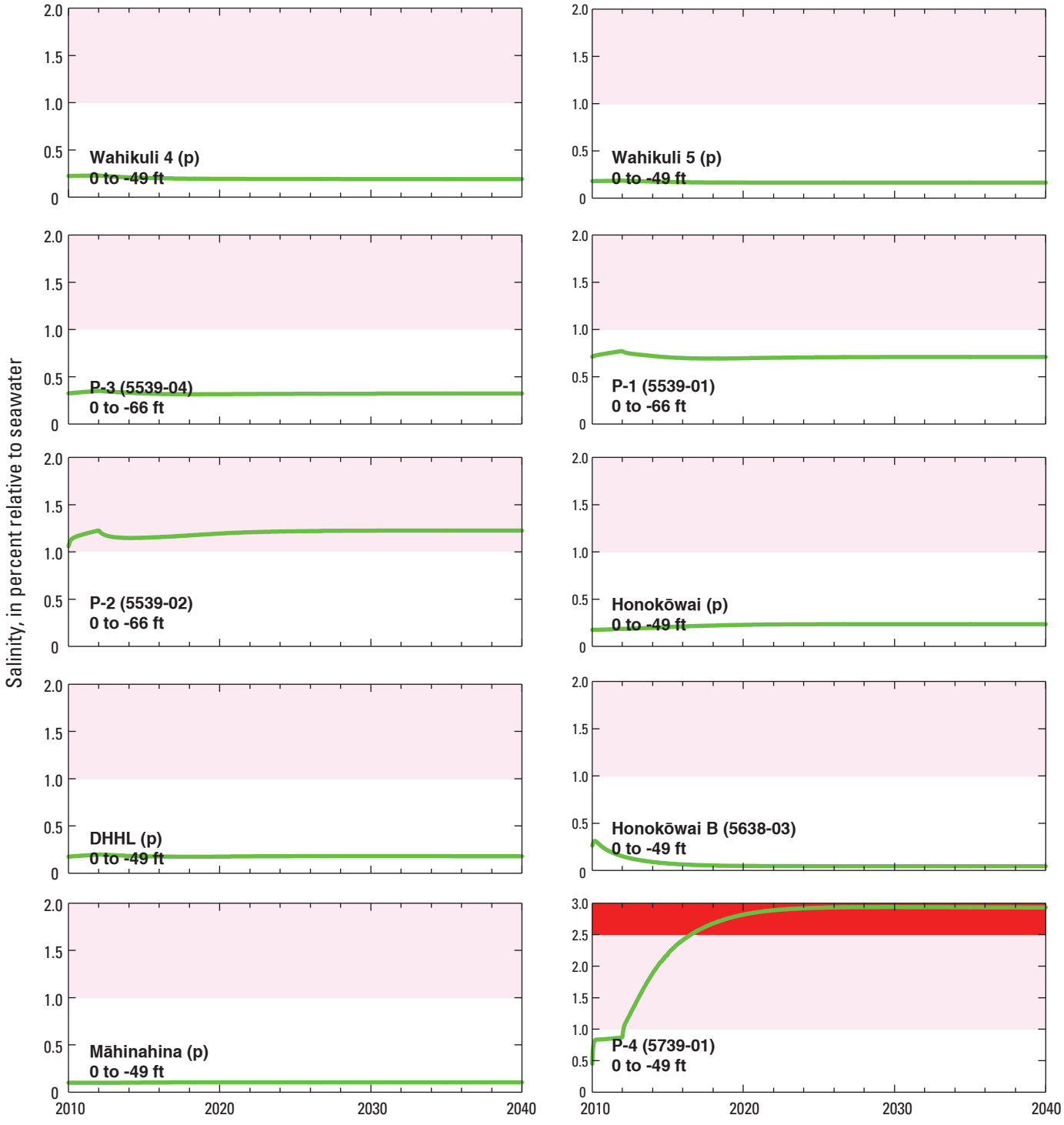

Figure 22. Simulated salinity data (green lines) for the period 2010–39 for Scenario 1, assuming average 2008–09 pumping rates at selected wells in the Lahaina Aquifer Sector, West Maui, Hawai'i. For each well shown, the simulated salinity is for the deepest node representing the well. The depths of the nodes used are shown under each well name and number. Well names followed by (p) are proposed wells. The pink area represents a cautionary salinity class and the red area represents a threatened salinity class—continued.

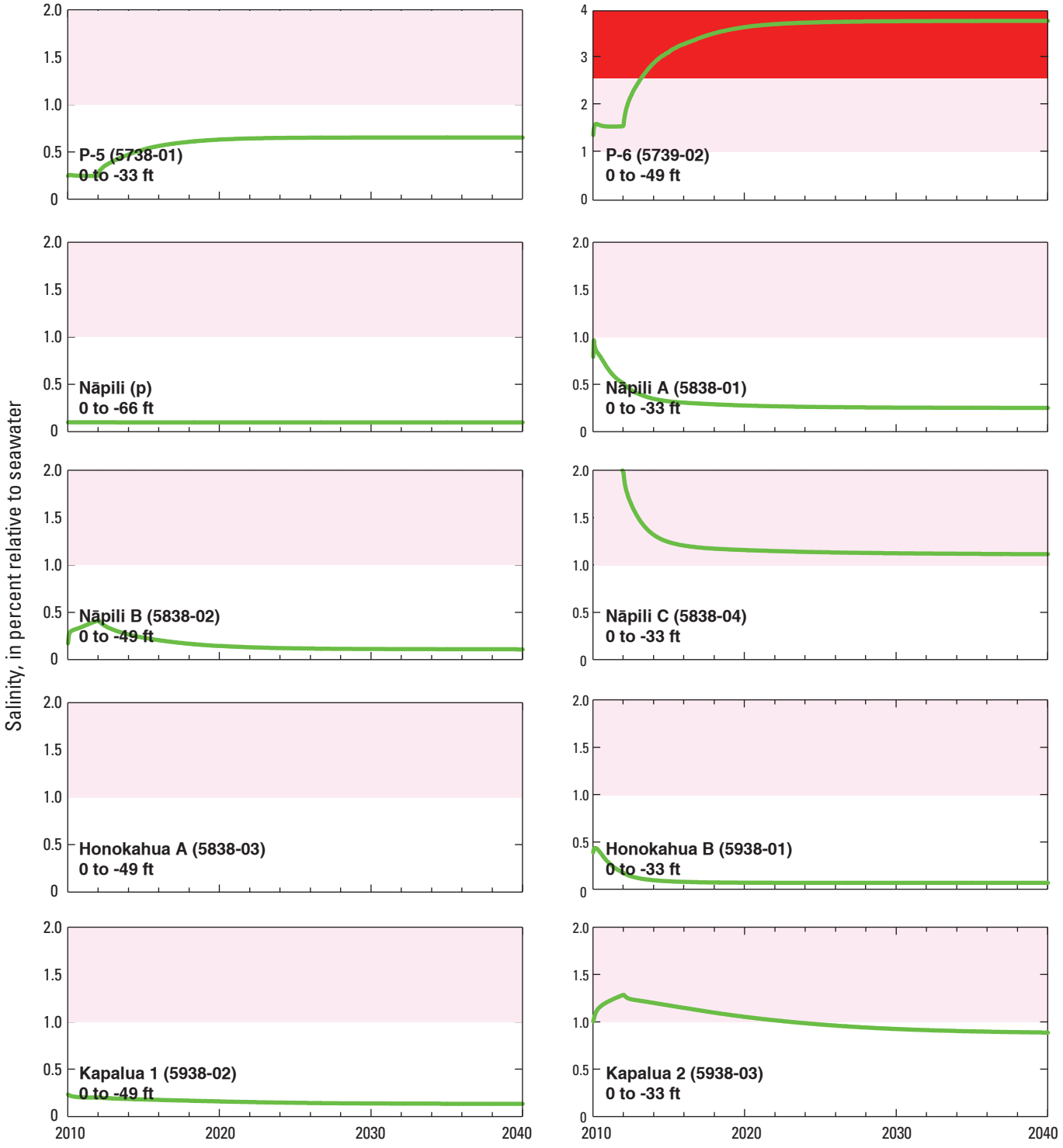

Figure 22. Simulated salinity data (green lines) for the period 2010–39 for Scenario 1, assuming average 2008–09 pumping rates at selected wells in the Lahaina Aquifer Sector, West Maui, Hawai‘i. For each well shown, the simulated salinity is for the deepest node representing the well. The depths of the nodes used are shown under each well name and number. Well names followed by (p) are proposed wells. The pink area represents a cautionary salinity class and the red area represents a threatened salinity class—continued.

use without agricultural irrigation and 1926–2004 rainfall (table 5). Withdrawal rates (table 8) were estimated on the basis of projected demands determined by a MDWS planning consultant from various Maui county planning scenarios (Carl Freedman, written commun., 2010). Projected demands for the different water purveyors and distribution areas were provided to the USGS. These projected demands for each water purveyor were distributed over the existing and proposed wells for that purveyor. Withdrawal at existing wells with higher salinities was reduced or terminated where needed to lower pumped-water salinities and withdrawal at proposed wells was added to provide enough water to meet the demand for each period. New demand in this scenario was met with the fewest number of wells, each pumping at its full rate rather than more wells with each well pumping at reduced rates. This method of adding additional wells was determined by the MDWS as the most realistic representation of future well development. In this scenario, total average withdrawal started at 6.0 Mgal/d and increased after 30 years to 11.2 Mgal/d throughout the Lahaina Aquifer Sector. Injection of treated wastewater effluent was 7.0 Mgal/d after 30 years.

The largest long-term simulated salinity increases are at Kapalua 1 and 2 wells in the Honolua Aquifer System and at P-4 and P-6 wells in the Honokōwai Aquifer System, where the salinity increases by as much as 3-percent seawater salinity over 30 years (fig. 26). At four wells (Kapalua 2, Kanahā 2, P-5A, and P-6), the simulated salinity increases into the threatened class for a total threatened yield of all wells of 1.22 Mgal/d (table 8). Simulated salinity is in the cautionary class after 30 years at five wells for a total yield of 3.9 Mgal/d. The amount of withdrawn water in which salinities are either threatened or cautionary after 30 years, expressed as a percentage of total withdrawal, for each of the four most-utilized aquifer systems is as follows: Honolua, 45 percent; Honokōwai, 62 percent; Launiupoko, 4 percent; Olowalu, 0 percent.

Regional changes of average water levels in the aquifer after 30 years at the projected withdrawal rates, presented relative to conditions at the end of the 1926–2008 historical simulation, are greatest in the Honokōwai Aquifer System, where average water-level differences are more than 0.5 ft lower (fig. 27). Water levels are also lower around several wells in the Honolua Aquifer System. The freshwater body thinned the most in the Honokōwai Aquifer System as the depths of the bottom of the freshwater and the middle of the transition zone are shallower by more than 30 ft and 20 ft, respectively. However, the freshwater lens became slightly thicker in the area of the Lahaina STP injection well because of the injection of about 7.0 Mgal/d of freshwater, and downgradient of the Nāpili wells in the Honolua Aquifer System where withdrawal was decreased.

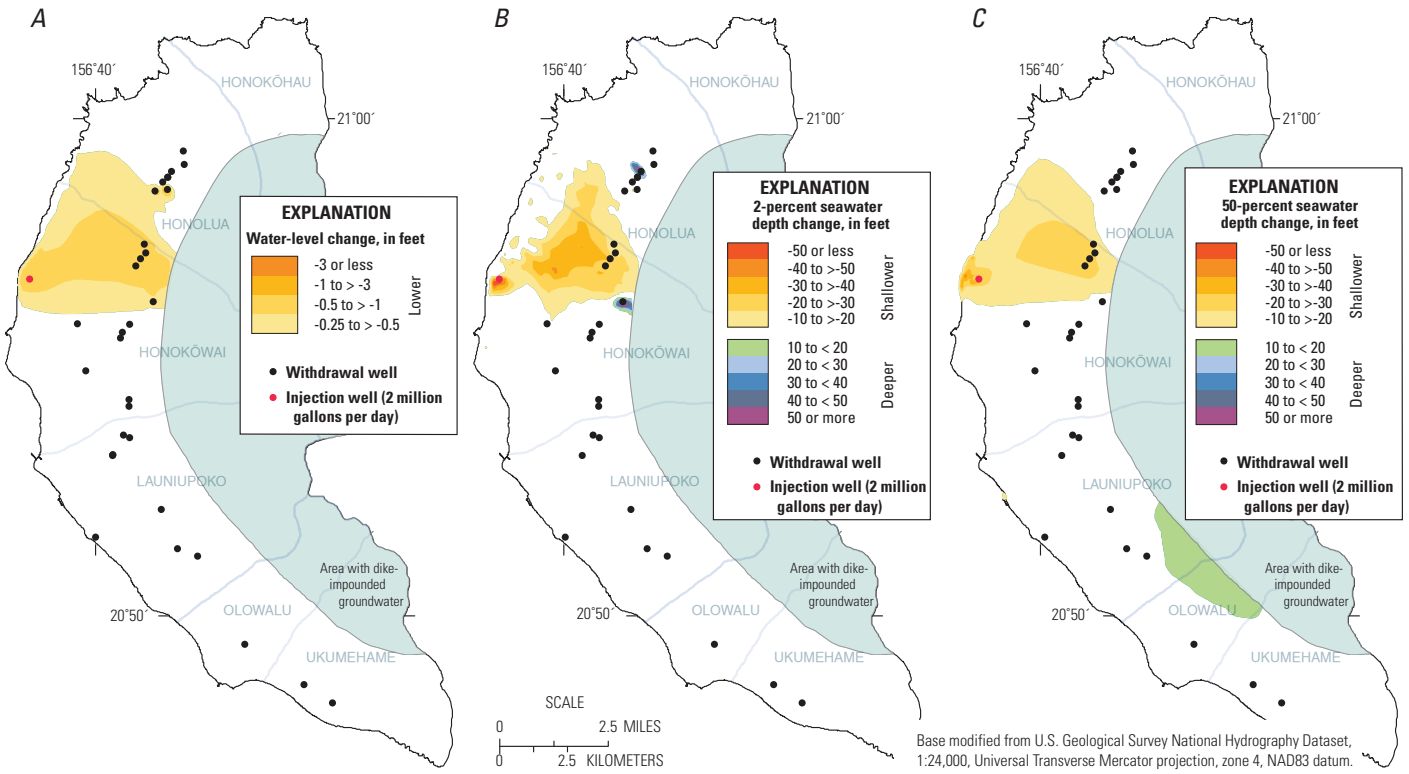

Figure 23. Simulated change (relative to end of historical simulation) in (*A*) water level, (*B*) 2-percent seawater salinity depth, and (*C*) 50-percent seawater salinity depth after 30 years of withdrawal at 2008–09 rates with long-term projected recharge of 89 Mgal/d (Scenario 1), Lahaina District, west Maui, Hawai'i. Well names shown on figure 16.

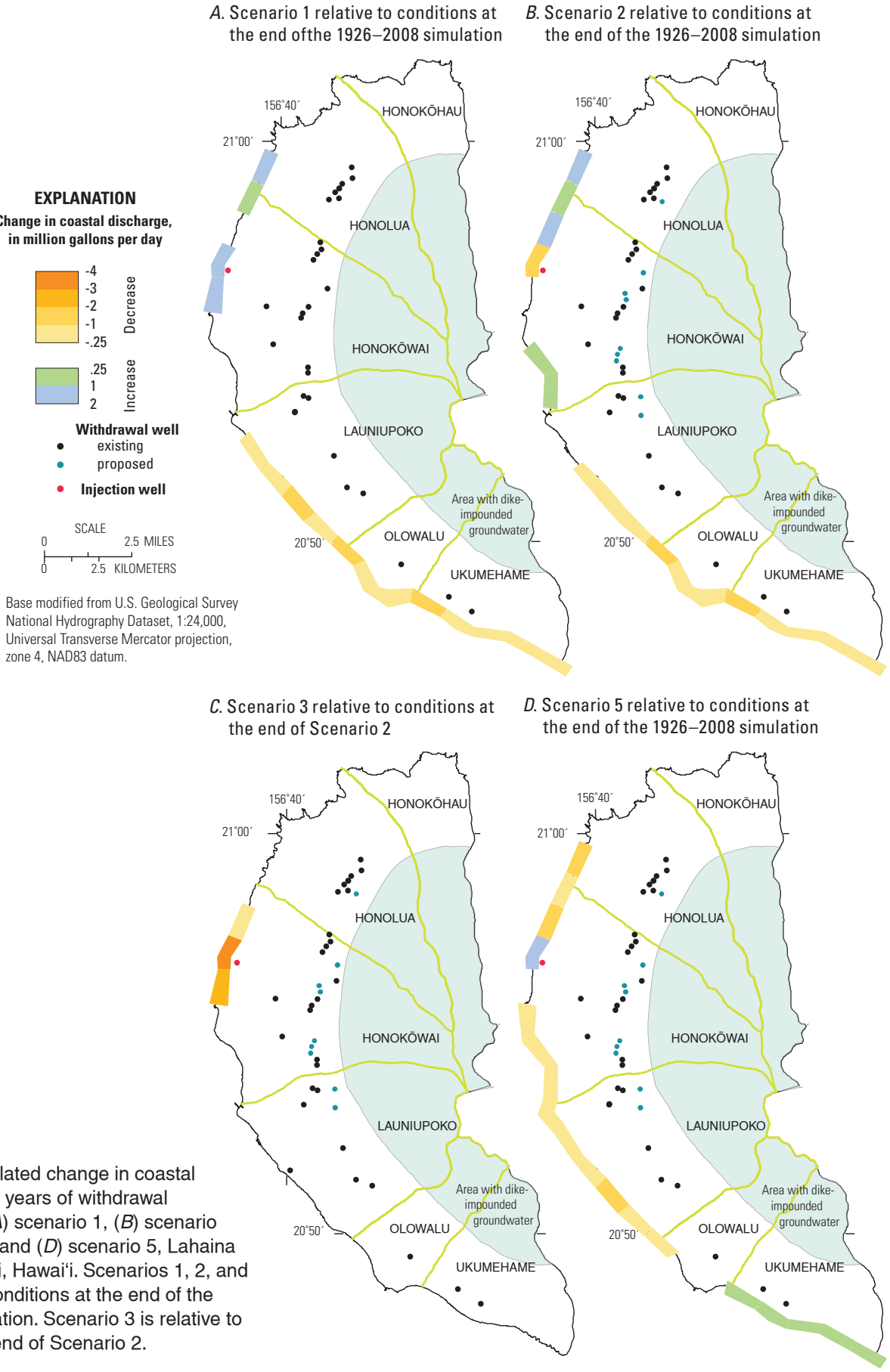

Figure 24. Simulated change in coastal discharge after 30 years of withdrawal (2010-2039) for (*A*) scenario 1, (*B*) scenario 2, (*C*) scenario 3, and (*D*) scenario 5, Lahaina District, west Maui, Hawai‘i. Scenarios 1, 2, and 5 are relative to conditions at the end of the 1926–2008 simulation. Scenario 3 is relative to conditions at the end of Scenario 2.

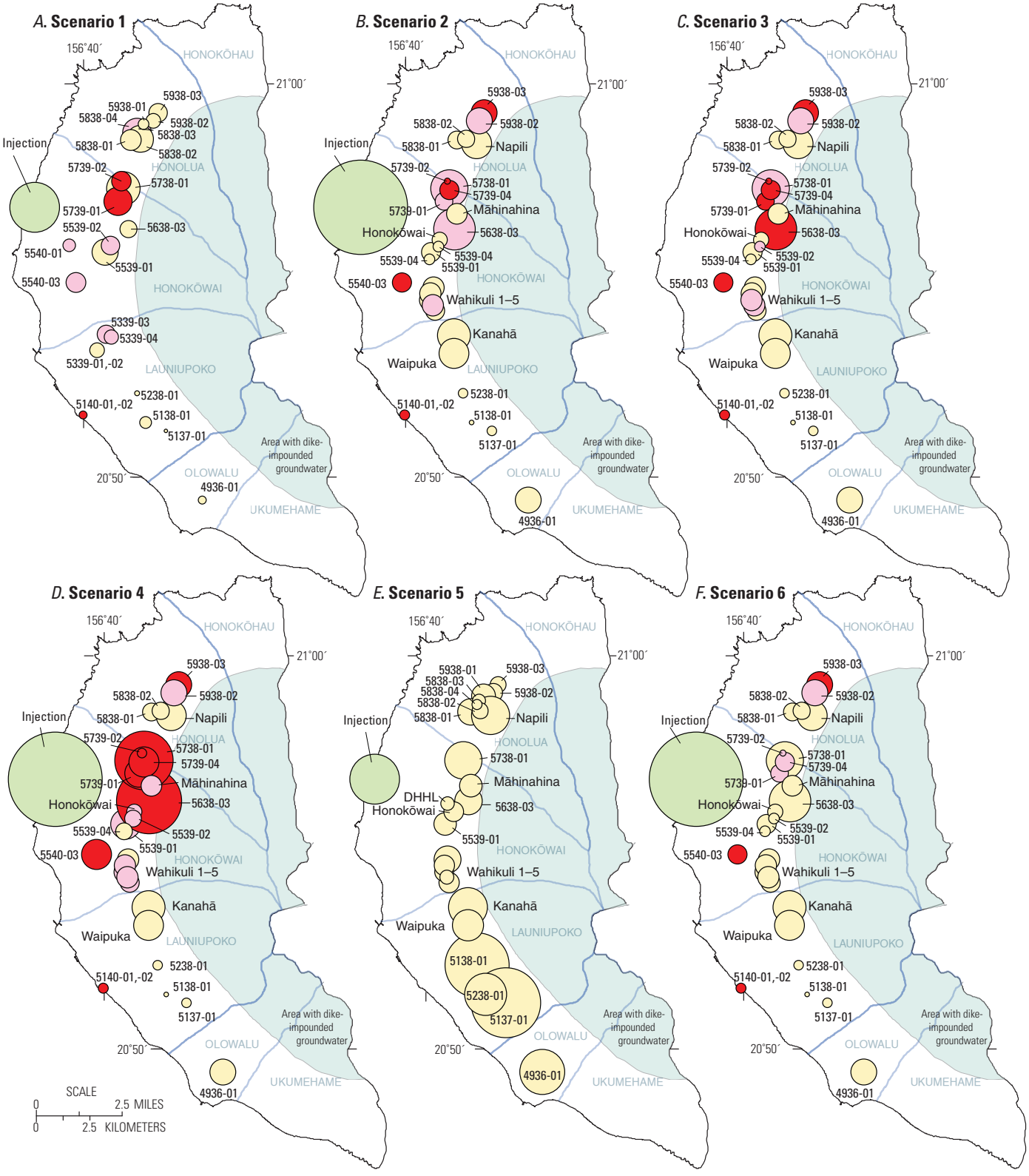

Figure 25. Predicted salinities in wells included in scenarios 1–6, Lahaina District, west Maui, Hawai‘i. Injection refers to Lahaina Sewage Treatment Plant treated effluent disposal.

Regional changes of coastal groundwater discharge after 30 years are presented relative to conditions at the end of the 1926–2008 historical simulation (fig. 24*B*). Coastal groundwater discharge is higher after 30 years along segments of the coast in the Honokōwai and Honolua Aquifer Systems due mainly to the increased amount of injection of treated sewage effluent. Coastal groundwater discharge is lower in the Launiupoko, Olowalu, and Ukumehame Aquifer Systems.

For this scenario, the Honokōwai Aquifer System has the highest amount of cautionary (3.37 Mgal/d) and threatened (0.61 Mgal/d) yield (fig. 25*B*). The Honolua Aquifer System has 0.53 Mgal/d of cautionary yield and 0.53 Mgal/d of threatened yield, all from the Kapalua wells. In the Launiupoko Aquifer System, redistributing the pumpage to the proposed Waipuka and Kanahā wells allows the projected withdrawal to remain in the acceptable class.

Scenario 3—Projected Withdrawal Rates and Locations using 2000–04 Land Use Without Plantation-Scale Agriculture and 1926–2004 Rainfall assuming no injection

In Scenario 3, the same recharge and withdrawal as Scenario 2 was used, however all injection at the Lahaina STP was stopped. Occasionally, strong interest is expressed in stopping the injection of treated sewage effluent into the coastal aquifer (for example *[Mayor] Tavares on 18 injection wells: Get rid of all of them,* The Maui News, August 23, 2009). This scenario was simulated to investigate the potential effects of this alternative on the hydrologic system.

The removal of 7 Mgal/d of injected water has a notable effect on salinity nearest the injection site. The injected freshwater acts as a hydrologic barrier and reduces the amount of saltwater that encroaches into the aquifer due to withdrawal farther inland. When this barrier is removed, salinities increase in pumped wells upgradient of the injection site. The largest long-term simulated salinity increases relative to Scenario 2 are at the P-1 through P-6 wells and the Honokōwai B well in the Honokōwai Aquifer System, where the salinity increases by as much as 1-percent seawater salinity after 30 years (fig. 28). The Honokōwai and DHHL proposed wells have similar increases in salinity but those salinities remain below the cautionary limit. Salinity increases from the cautionary to threatened class at P-4 and Honokōwai B wells and from acceptable to cautionary in the Wahikuli 3 well. After 30 years, the total threatened rate is 2.74 Mgal/d and the total cautionary rate is 2.84 Mgal/d (table 7). The Honokōwai Aquifer System has the highest amount of cautionary (2.21 Mgal/d) and threatened (2.23 Mgal/d) yield (fig. 25*C*). This is an increase of combined cautionary and threatened yield of 0.46 Mgal/d because injection was stopped. The Honolua Aquifer System has 0.53 Mgal/d of cautionary yield and 0.53 Mgal/d of threatened yield, the same as in Scenario 2. The amount of withdrawn water in which salinities are either threatened or cautionary after 30 years, expressed as a percentage of total

Table 7. Classification of withdrawal for simulated scenarios, Lahaina Aquifer Sector, Maui, Hawai'i.

[All results in million gallons per day; CWRM, State of Hawai'i Commission on Water Resource Management; Withdrawal rates for Scenarios 2,3,4,6, and 7 start at lower rates and increase to listed rates by the end of the 30-year simulation; cautionary yield is the volume of withdrawn water that has a salinity from 1 to 2 percent that of seawater; threatened yield is the volume of withdrawn water that has a salinity greater than 2 percent that of seawater]

Aquifer system	CWRM sustainable yield	Total simulated withdrawal after 30 years	After 30 years	
			Cautionary withdrawal	Threatened withdrawal
Scenario 1—2008–09 withdrawal				
Honokōhau	9	0.0	0.0	0.0
Honolua	8	2.27	.65	0.0
Honokōwai	6	3.19	.6	.93
Launiupoko	7	0.78	.42	.05
Olowalu	2	.05	0.0	0.0
Ukumehame	2	0.0	0.0	0.0
Scenario 2—projected withdrawal				
Honokōhau	9	0.0	0.0	0.0
Honolua	8	2.38	.53	.53
Honokōwai	6	6.41	3.37	.61
Launiupoko	7	1.88	0.0	.08
Olowalu	2	0.53	0.0	0.0
Ukumehame	2	0.0	0.0	0.0
Scenario 3—projected withdrawal, no injection				
Honokōhau	9	0.0	0.0	0.0
Honolua	8	2.38	.53	.53
Honokōwai	6	6.41	2.21	2.23
Launiupoko	7	1.88	0.0	0.08
Olowalu	2	0.53	0.0	0.0
Ukumehame	2	0.0	0.0	0.0
Scenario 4—full-build projected withdrawal				
Honokōhau	9	0.0	0.0	0.0
Honolua	8	2.38	.53	.53
Honokōwai	6	12.34	2.9	8.85
Launiupoko	7	1.88	0.0	0.08
Olowalu	2	0.53	0.0	0.0
Ukumehame	2	0.0	0.0	0.0
Scenario 5—redistributed withdrawal				
Honokōhau	9	0.0	0.0	0.0
Honolua	8	3.16	0.0	0.0
Honokōwai	6	5.07	0.0	0.0
Launiupoko	7	10.85	0.0	0.0
Olowalu	2	1.6	0.0	0.0
Ukumehame	2	0.0	0.0	0.0
Scenario 6—restored streamflow				
Honokōhau	9	0.0	0.0	0.0
Honolua	8	2.38	.53	.53
Honokōwai	6	6.41	.81	0.0
Launiupoko	7	1.88	0.0	.08
Olowalu	2	0.53	0.0	0.0
Ukumehame	2	0.0	0.0	0.0
Scenario 7—5-year drought				
Honokōhau	9	0.0	0.0	0.0
Honolua	8	2.38	.53	.53
Honokōwai	6	6.41	3.37	.61
Launiupoko	7	1.88	0.0	.08
Olowalu	2	0.53	0.0	0.0
Ukumehame	2	0.0	0.0	0.0

Table 8. Selected wells and withdrawal rates used in Scenario 2, west Maui, Hawai'i.

[Values in pink or red represent wells with salinity in the cautionary or threatened range; NA, not available; cautionary yield is the volume of withdrawn water that has a salinity from 1 to 2 percent that of seawater; threatened yield is the volume of withdrawn water that has a salinity greater than 2 percent that of seawater; --, not applicable; *italics* text indicates injection]

Well name	Well number	Withdrawal rate (million gallons per day)								
		2010	2011	2012	2013	2014	2015	2020	2025	2030
Honolua Aquifer System										
Nāpili A	5838-01	0.373	0.36	0.25	0.25	0.25	0.25	0.25	0.25	0.25
Nāpili B	5838-02	0.48	0.	0.2	0.24	0.28	0.31	0.31	0.31	0.31
Nāpili C	5838-04	0.085	0.	0.	0.	0.	0.	0.	0.	0.
Honokahua A	5838-03	0.	0.	0.	0.	0.	0.	0.	0.	0.
Honokahua B	5938-01	0.19	0.02	0.	0.	0.	0.01	0.17	0.	0.
Kapalua 1	5938-02	0.228	0.244	0.26	0.276	0.292	0.307	0.378	0.455	0.534
Kapalua 2	5938-03	0.228	0.244	0.26	0.276	0.292	0.307	0.378	0.455	0.534
Nāpili (proposed)	--	0.	0.75	0.75	0.75	0.75	0.75	0.75	0.75	0.75
Total		**1.583**	**1.618**	**1.719**	1.791	**1.863**	**1.935**	**2.237**	**2.221**	**2.378**
Honokōwai Aquifer System										
P-1	5539-01	0.29	0.29	0.29	0.29	0.29	0.29	0.29	0.29	0.29
P-2	5539-02	0.09	0.09	0.09	0.09	0.09	0.09	0.09	0.09	0.09
P-3	5539-04	0.	0.09	0.09	0.09	0.09	0.09	0.09	0.09	0.09
P-4	5739-01	0.247	0.247	0.247	0.247	0.247	0.247	0.247	0.247	0.247
P-5	5738-01	1.103	0.937	0.961	0.985	1.009	1.033	1.139	1.255	1.372
P-5A	5739-04	0.	0.29	0.29	0.29	0.29	0.29	0.29	0.29	0.29
P-6	5739-02	0.029	0.029	0.029	0.029	0.029	0.029	0.029	0.029	0.029
Honokōwai B	5638-03	1.103	0.937	0.961	0.985	1.009	1.033	1.139	1.255	1.372
Hāhākea	5540-03	0.29	0.29	0.29	0.29	0.29	0.29	0.29	0.29	0.29
Pu'ukoli'i	5540-01	0.	0.	0.	0.	0.	0.	0.	0.	0.
Māhinahina (proposed)	--	0.	0.	0.	0.	0.	0.	0.	0.35	0.35
DHHL (proposed)	--	0.	0.	0.	0.	0.	0.	0.	0.	0.
Honokōwai (proposed)	--	0.	0.	0.	0.	0.	0.	0.	0.	0.19
Wahikuli 5 (proposed)	--	0.	0.	0.	0.	0.375	0.375	0.375	0.375	0.375
Wahikuli 4 (proposed)	--	0.	0.	0.	0.	0.375	0.375	0.375	0.375	0.375
Wahikuli 3 (proposed)	--	0.	0.	0.36	0.36	0.375	0.375	0.375	0.375	0.375
Wahikuli 2	5439-02	0.	0.	0.36	0.36	0.375	0.375	0.375	0.375	0.375
Wahikuli 1	5439-01	0.	0.	0.27	0.27	0.3	0.3	0.3	0.3	0.3
Lahaina Injection	*5641*01, *02, *03, *04*	*- 3.901*	*- 4.057*	*- 4.212*	*- 4.368*	*- 4.523*	*- 4.679*	*- 5.457*	*- 6.235*	*- 7.*
Total		**3.152**	**3.2**	**4.238**	**4.285**	**5.143**	**5.191**	**5.403**	**5.985**	**6.41**
Launiupoko Aquifer System										
Waipuka 1, 2	5339-01, -02	0.	0.	0.	0.	0.	0.	0.	0.	0.
Kanahā 1	5339-03	0.	0.	0.	0.	0.	0.	0.	0.	0.
Kanahā 2	5339-04	0.	0.	0.	0.	0.	0.	0.	0.	0.
Launiupoko 1	5138-01	0.012	0.013	0.013	0.013	0.013	0.014	0.015	0.016	0.017
Launiupoko 2	5137-01	0.054	0.055	0.056	0.058	0.059	0.06	0.065	0.07	0.075
Launiupoko 3	5238-01	0.054	0.055	0.056	0.058	0.059	0.06	0.065	0.07	0.075
Puamana 1, 2	5140-01, -02	0.08	0.08	0.08	0.08	0.08	0.08	0.08	0.08	0.08
Kanahā (proposed)	--	0.557	0.574	0.592	0.61	0.628	0.646	0.725	0.811	0.899
Waipuka (proposed)	--	0.455	0.47	0.484	0.499	0.514	0.528	0.593	0.664	0.735
Total		**1.213**	**1.248**	**1.283**	**1.317**	**1.352**	**1.387**	**1.542**	**1.71**	**1.882**
Olowalu Aquifer System										
Olowalu Elua	4936-01	0.07	0.09	0.11	0.14	0.16	0.19	0.3	0.41	0.53
Total		**.07**	**.09**	**.11**	**.14**	**.16**	**.19**	**.3**	**.41**	**.53**
Ukumehame Aquifer System										
Sugar Way 1, 2	4835-02, -03	NA	NA	NA	NA	NA	NA	NA	NA	NA
Total		**NA**	**NA**	**NA**	**NA**	**NA**	**NA**	**NA**	**NA**	**NA**
Total Lahaina Aquifer Sector management area		**6.01**	**6.16**	**7.35**	**7.53**	**8.52**	**8.7**	**9.48**	**10.33**	**11.2**

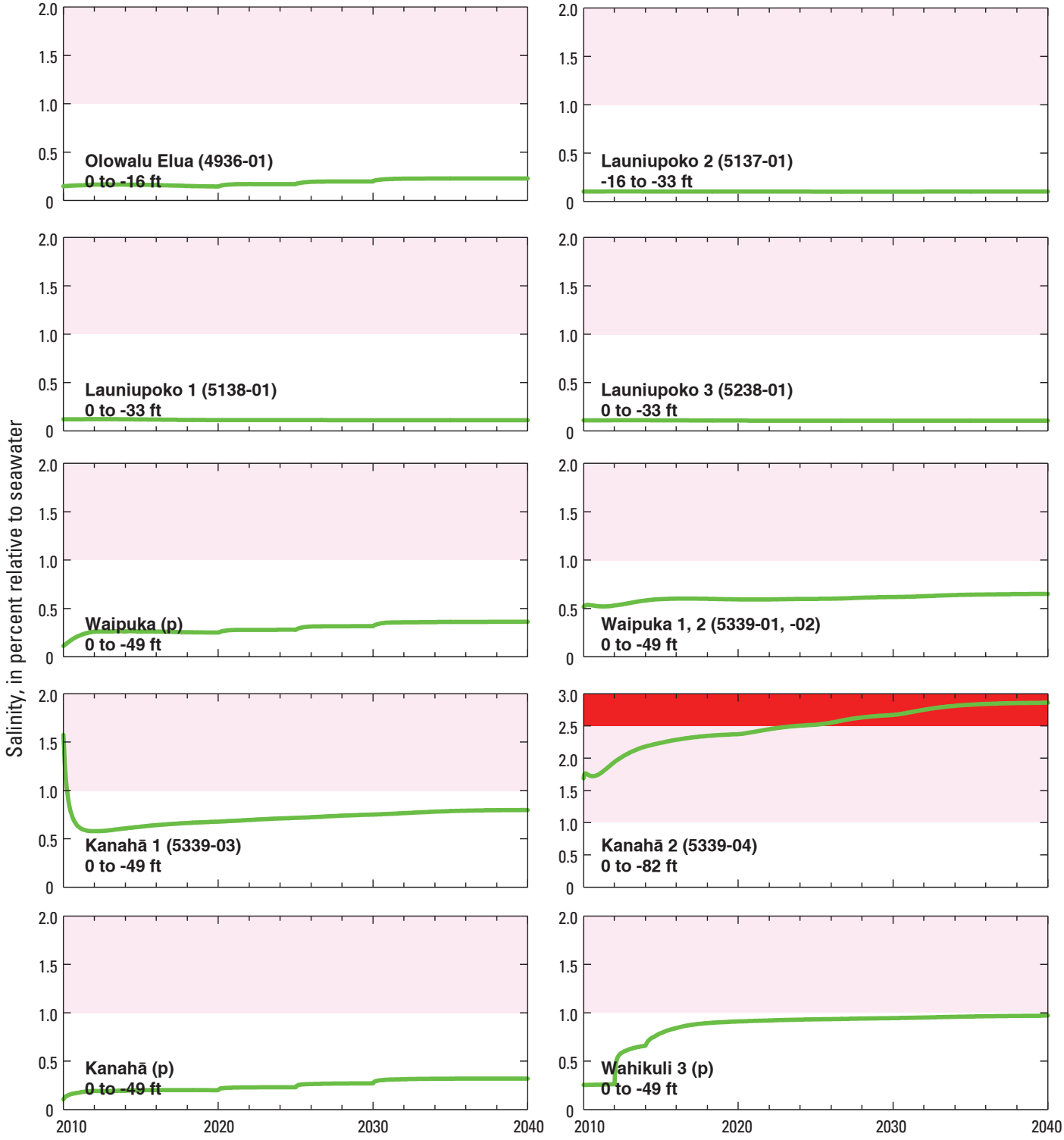

Figure 26. Simulated salinity data (green lines) for the period 2010–2039 for Scenario 2 assuming projected pumping rates at selected wells in the Lahaina Aquifer Sector, west Maui, Hawai‘i. For each well shown, the simulated salinity is for the deepest node representing the well. The depths of the nodes used are shown under each well name and number. Well names followed by (p) are proposed wells. The pink area represents a cautionary salinity class and the red area represents a threatened salinity class.

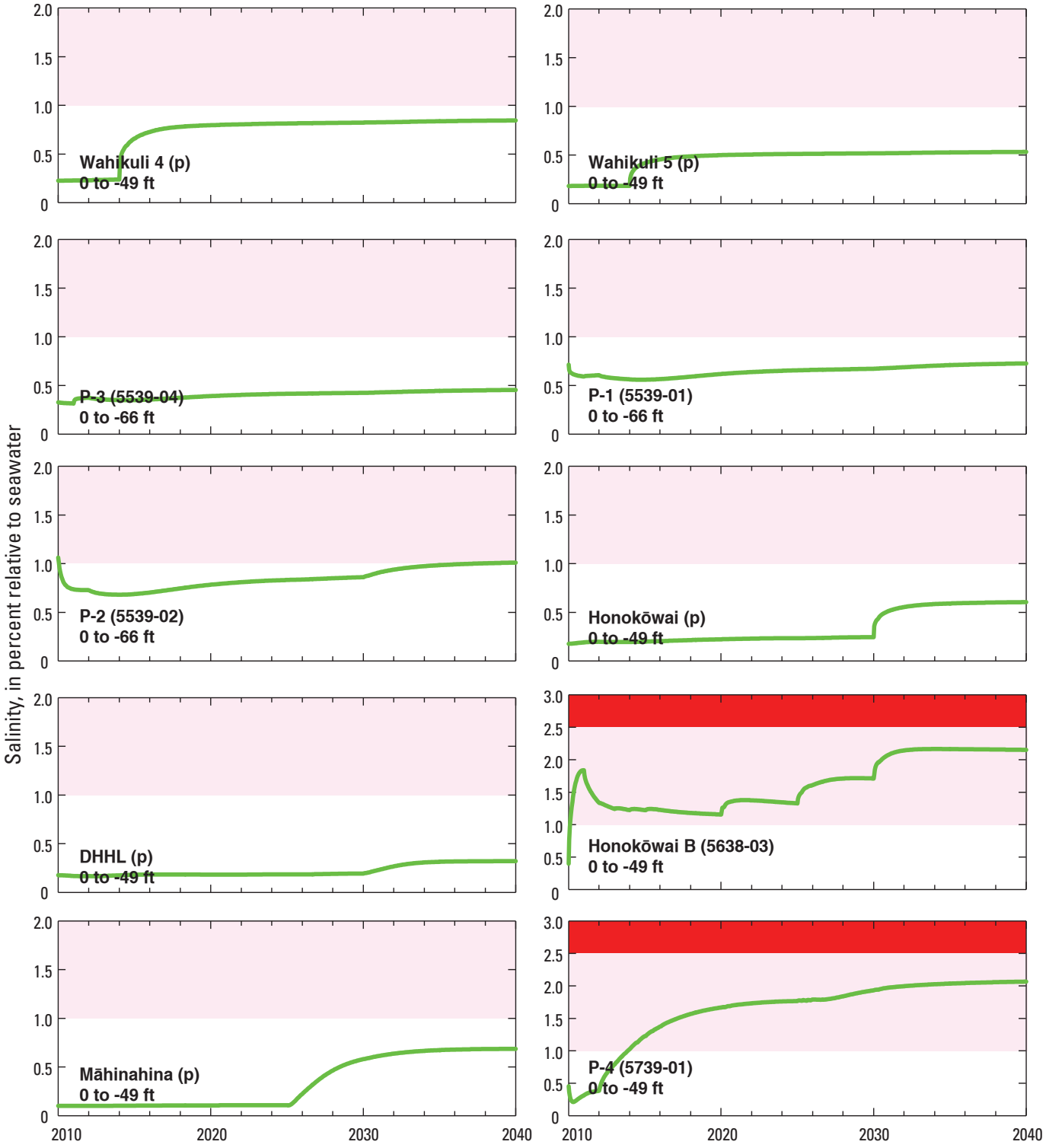

Figure 26. Simulated salinity data (green lines) for the period 2010–2039 for Scenario 2 assuming projected pumping rates at selected wells in the Lahaina Aquifer Sector, west Maui, Hawai‘i. For each well shown, the simulated salinity is for the deepest node representing the well. The depths of the nodes used are shown under each well name and number. Well names followed by (p) are proposed wells. The pink area represents a cautionary salinity class and the red area represents a threatened salinity class—continued.

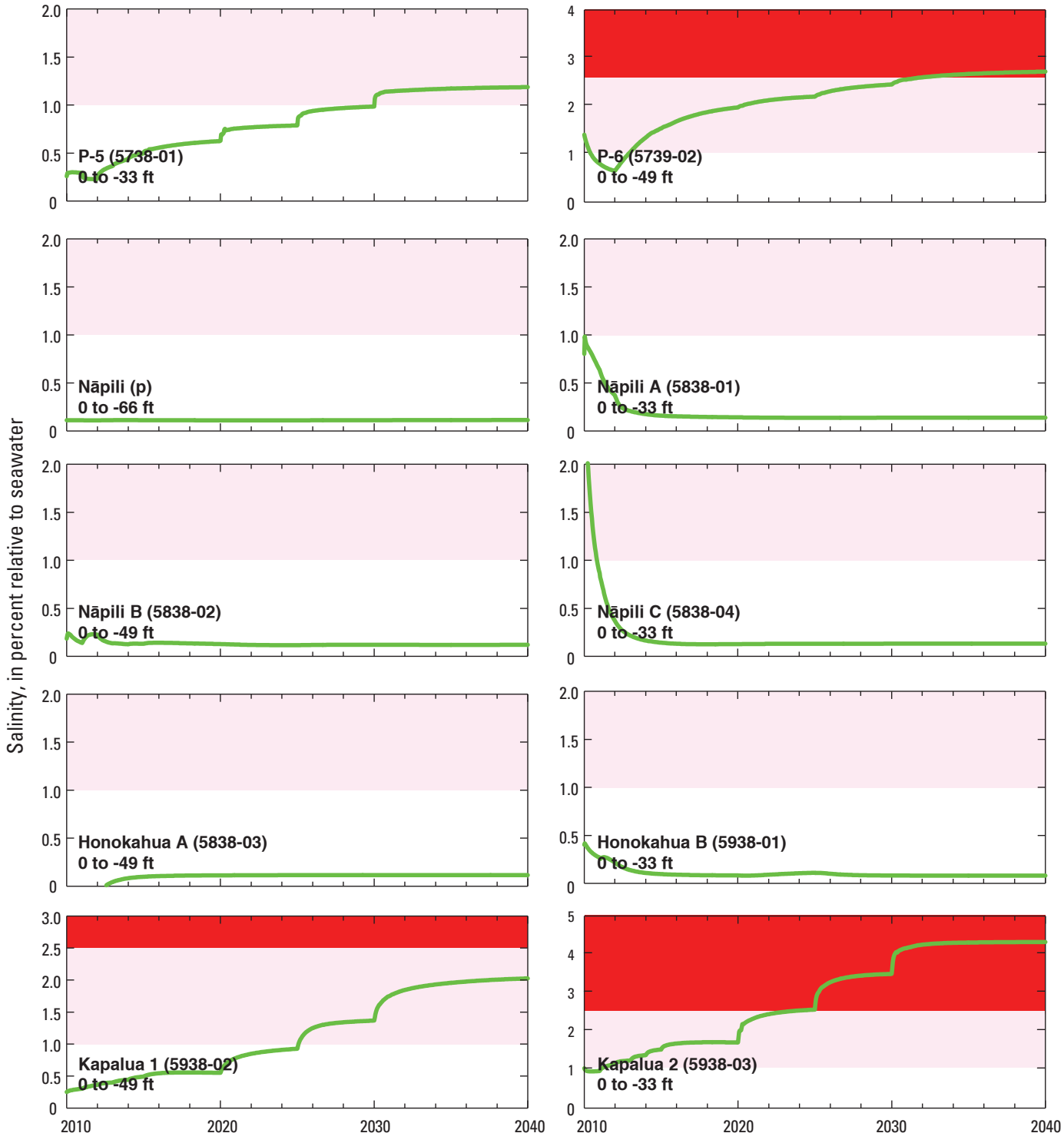

Figure 26. Simulated salinity data (green lines) for the period 2010–2039 for Scenario 2 assuming projected pumping rates at selected wells in the Lahaina Aquifer Sector, west Maui, Hawai‘i. For each well shown, the simulated salinity is for the deepest node representing the well. The depths of the nodes used are shown under each well name and number. Well names followed by (p) are proposed wells. The pink area represents a cautionary salinity class and the red area represents a threatened salinity class—continued.

withdrawal, for each of the four most-utilized aquifer systems is as follows: Honolua, 45 percent; Honokōwai, 69 percent; Launiupoko, 4 percent; Olowalu, 0 percent.

Regional changes of average water levels in the aquifer after 30 years without injection, presented relative to conditions at the end of Scenario 2, are greatest near the injection wells, where average water-level differences are more than 1 ft lower (fig. 29*A*). Without injection, the freshwater body is thinner in this area as the depths of the bottom of the freshwater (fig. 29*B*) and the middle (fig. 29*C*) of the transition zone are shallower by more than 50 ft.

Regional changes of coastal groundwater discharge after 30 years are presented relative to conditions at the end of Scenario 2 (fig. 24*C*). Coastal groundwater discharge is lower after 30 years along a 3-mile section of the coast in the Honokōwai Aquifer Systems due to the cessation of injection of treated sewage effluent.

Scenario 4—Projected Full-Build Withdrawal Rates and Locations using 2000–04 Land Use without Plantation-Scale Agriculture and 1926–2004 Rainfall

In Scenario 4, the most likely future average recharge and projected full-build withdrawal estimates were used to simulate the effects of planned development in the Lahaina District during the next 30 years. Assigned total recharge over the model domain was 89 Mgal/d, based on 2000–04 land use without agricultural irrigation and 1926–2004 rainfall (table 5). Withdrawal rates (table 9) were the same as for Scenario 2 for all wells except the P-1 through P-6 wells, the Honokōwai B well, and the Hāhākea well. These rates were increased evenly over time to an added 5.93 Mgal/d to represent a scenario of higher expected demand totaling 10.00 Mgal/d (table 7 of the Draft Kaanapali Water

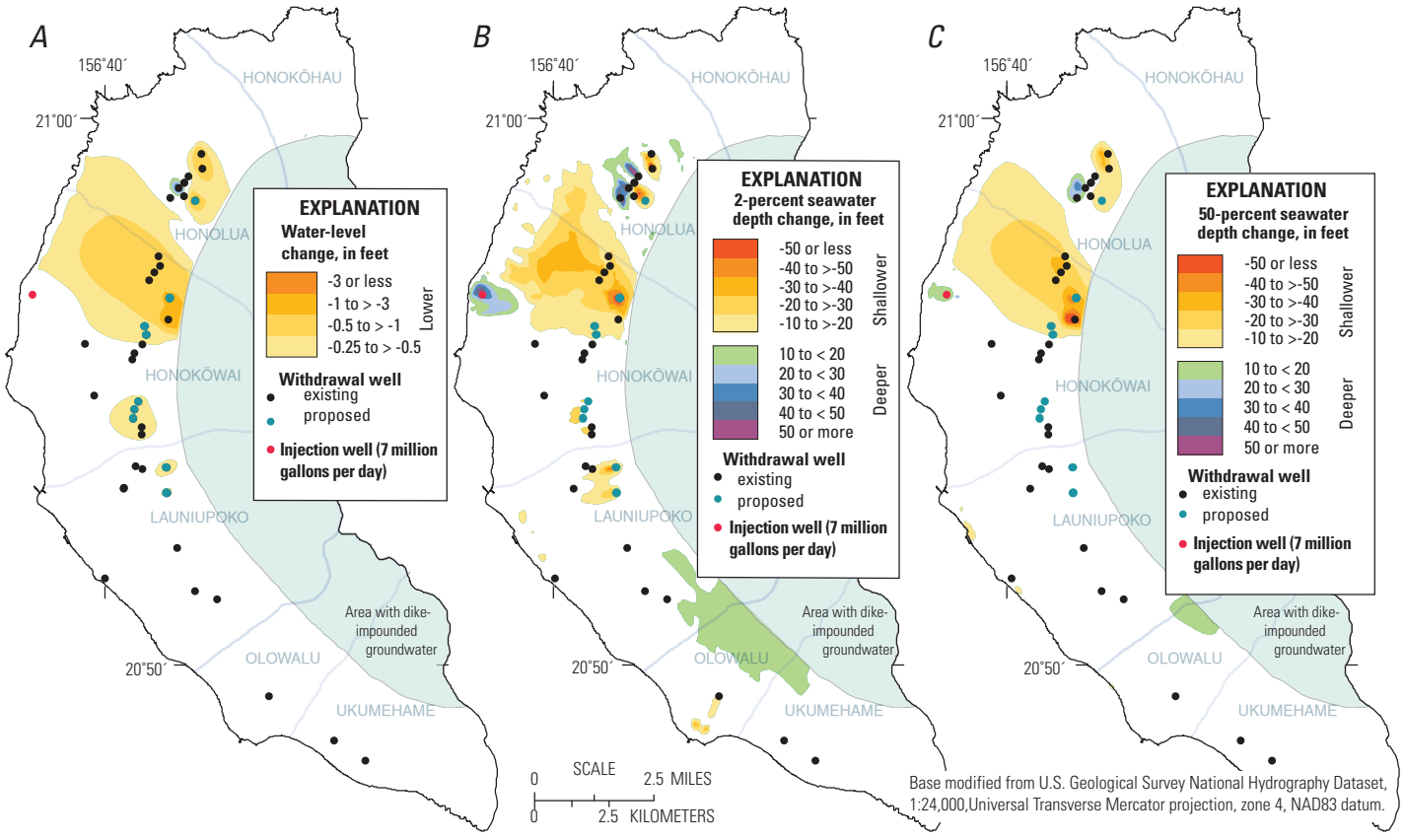

Figure 27. Simulated change (relative to end of historical simulation) in (*A*) water level, (*B*) 2-percent seawater salinity depth, and (*C*) 50-percent seawater salinity depth after 30 years of withdrawal at projected rates with long-term projected recharge of 89 Mgal/d (Scenario 2), Lahaina District, west Maui, Hawai‘i. Well names shown on figure 25.

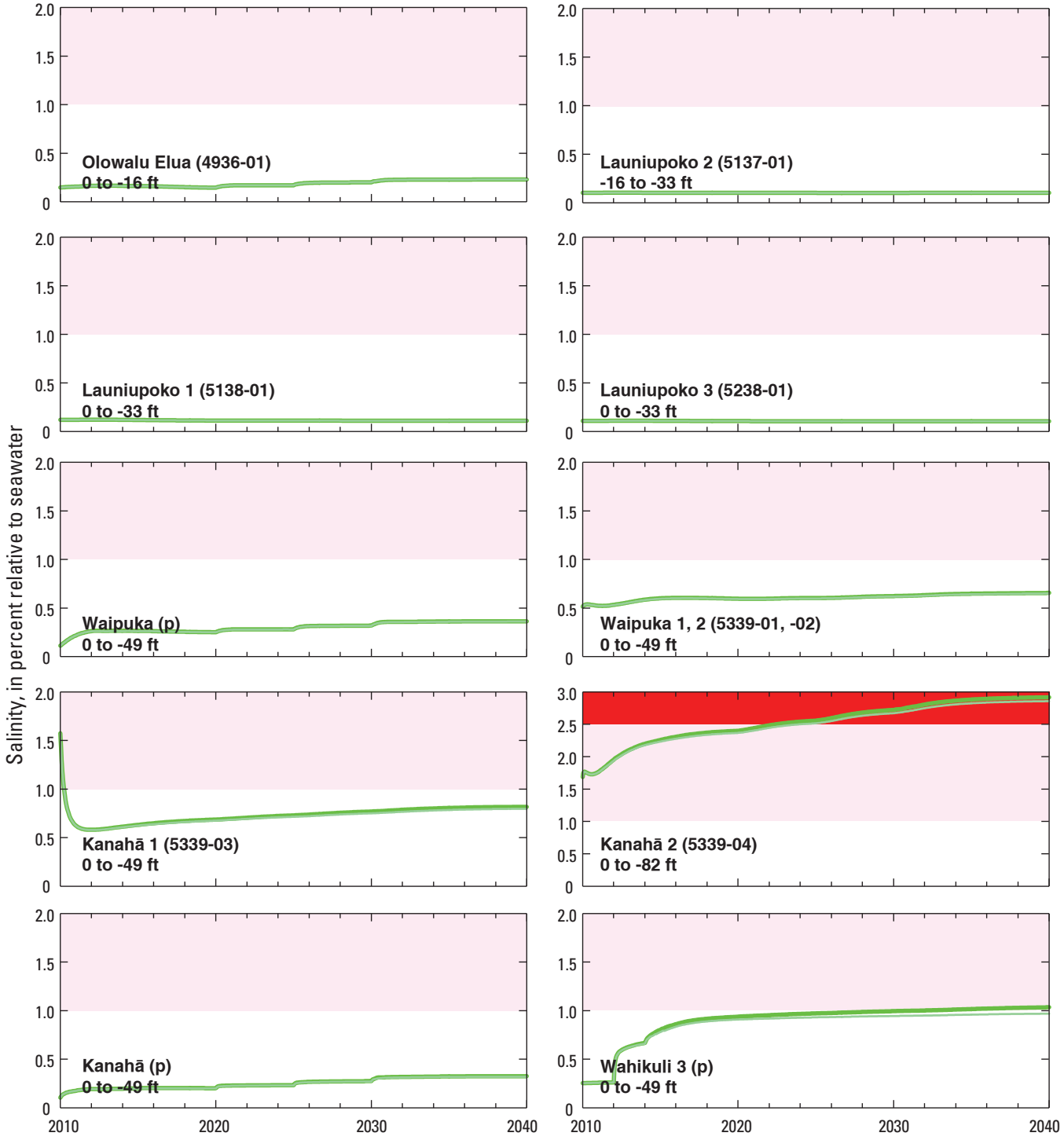

Figure 28. Simulated salinity data for Scenario 3 (dark green lines) for the period 2010–2039 assuming projected pumping rates at selected wells in the Lahaina Aquifer Sector with no injection compared to Scenario 2 (light green lines), west Maui, Hawai‘i. For each well shown, the simulated salinity is for the deepest node representing the well. The depths of the nodes used are shown under each well name and number. Well names followed by (p) are proposed wells. The pink area represents a cautionary salinity class and the red area represents a threatened salinity class.

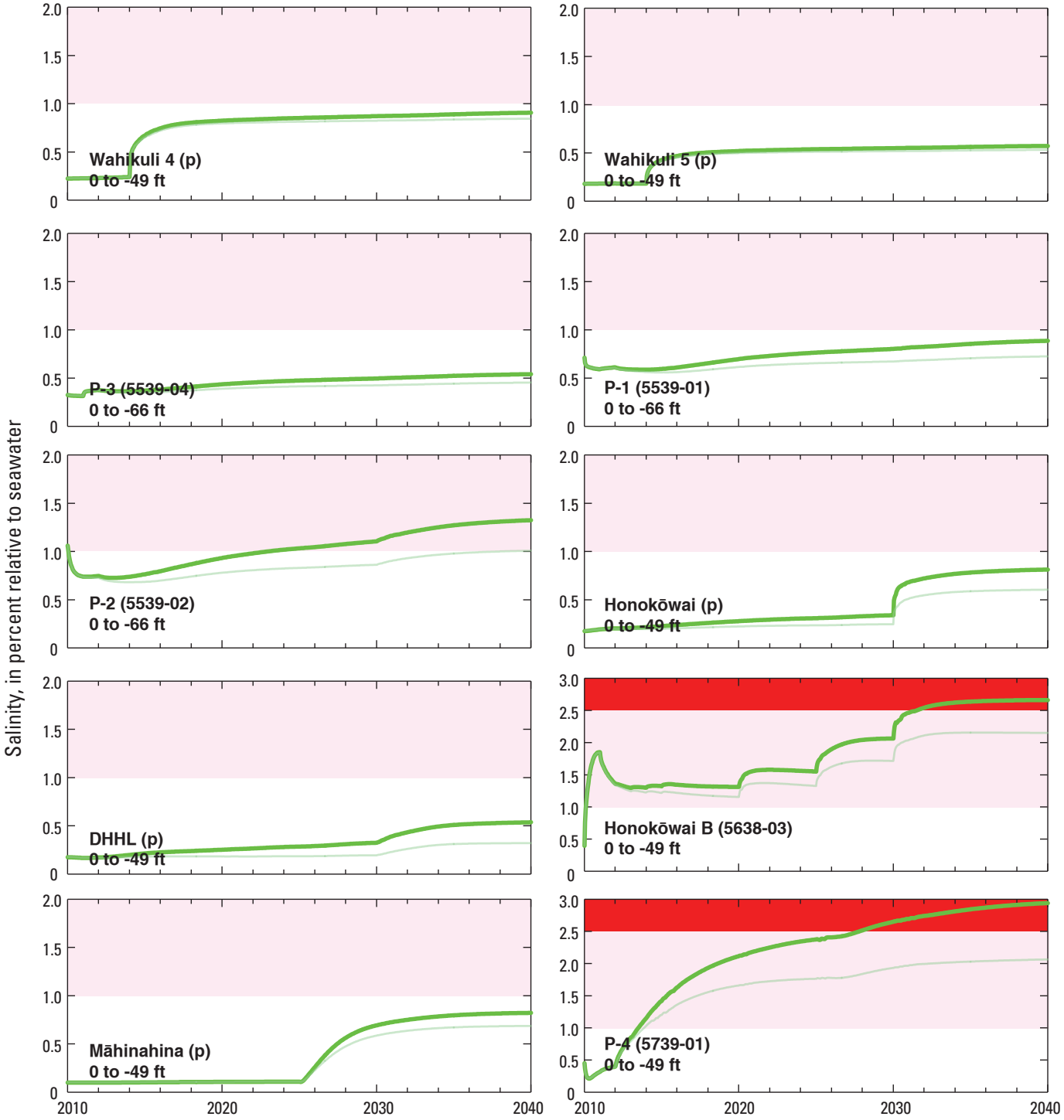

Figure 28. Simulated salinity data for Scenario 3 (dark green lines) for the period 2010–2039 assuming projected pumping rates at selected wells in the Lahaina Aquifer Sector with no injection compared to Scenario 2 (light green lines), west Maui, Hawai'i. For each well shown, the simulated salinity is for the deepest node representing the well. The depths of the nodes used are shown under each well name and number. Well names followed by (p) are proposed wells. The pink area represents a cautionary salinity class and the red area represents a threatened salinity class—continued.

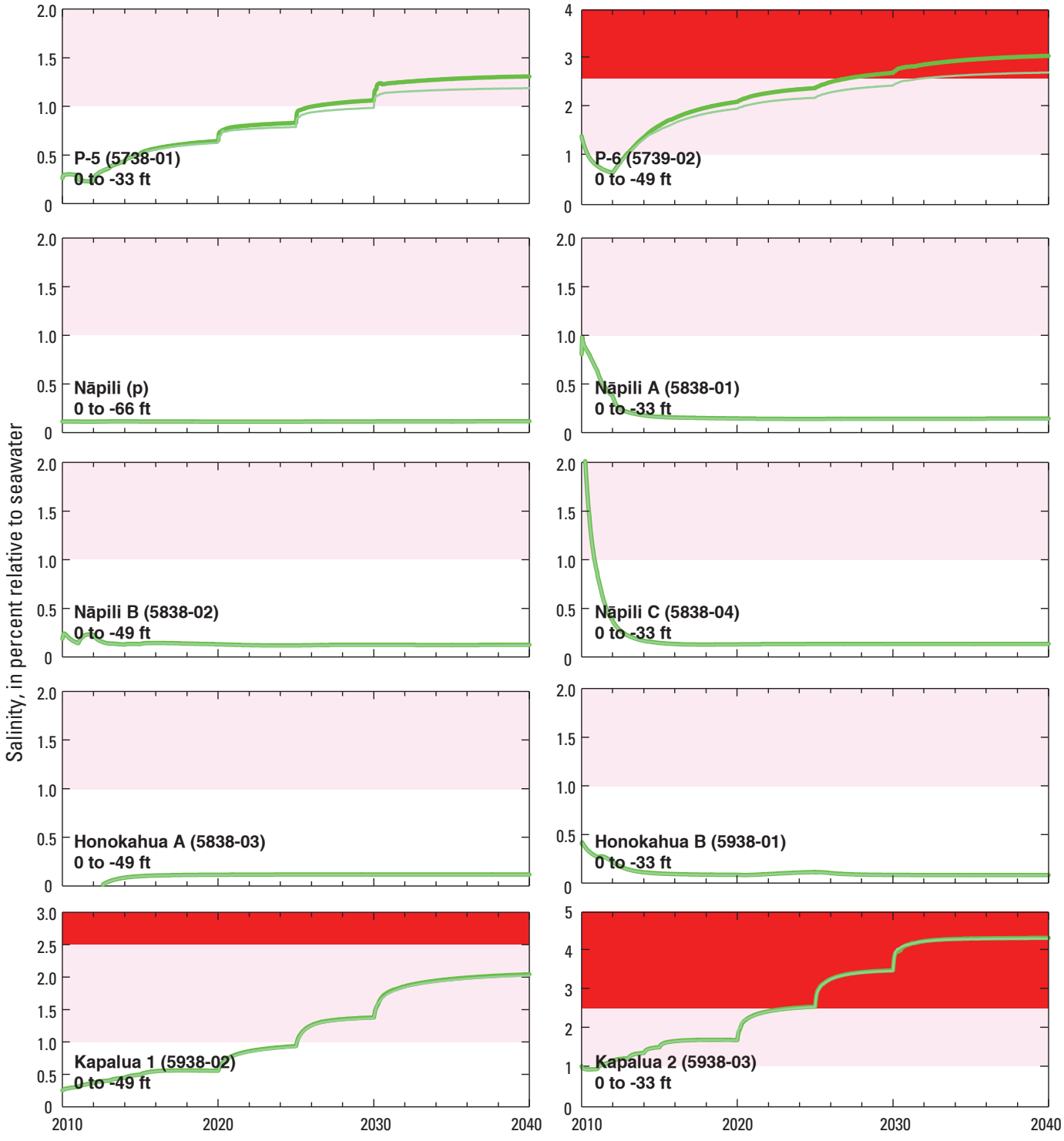

Figure 28. Simulated salinity data for Scenario 3 (dark green lines) for the period 2010–2039 assuming projected pumping rates at selected wells in the Lahaina Aquifer Sector with no injection compared to Scenario 2 (light green lines), west Maui, Hawai‘i. For each well shown, the simulated salinity is for the deepest node representing the well. The depths of the nodes used are shown under each well name and number. Well names followed by (p) are proposed wells. The pink area represents a cautionary salinity class and the red area represents a threatened salinity class—continued.

Supply Assessment [Art Oughton, Hawaii Water Service Company, written commun., June 29, 2010]). In this scenario, total withdrawal started at 6.36 Mgal/d and increased after 30 years to 17.13 Mgal/d throughout the Lahaina Aquifer Sector. This scenario represents one of maximum water demands if all future development considered in the Draft Kaanapali Water Supply Assessment is completed. Injection of treated wastewater effluent was 7.0 Mgal/d after 30 years.

The largest long-term simulated salinity increases relative to Scenario 2 are at Honokōwai B and P-4, P-5, and P-6 wells in the Honokōwai Aquifer System, where the salinity increases by as much as 14-percent seawater salinity after 30 years (fig. 30). The simulated salinity is in the threatened class at eight wells for a total threatened rate of 9.46 Mgal/d at all wells (table 7). Simulated salinity is in the cautionary class after 30 years at nine wells for a total rate of 3.43 Mgal/d. The Honokōwai Aquifer System has the highest amount of cautionary (2.90 Mgal/d) and threatened (8.85 Mgal/d) yield (fig. 25*D*). This is an increase of combined cautionary and threatened yield of 7.8 Mgal/d because of the additional demand. The Honolua Aquifer System has 0.53 Mgal/d of cautionary yield and 0.53 Mgal/d of threatened yield, the same as in Scenario 2. The amount of withdrawn water in which salinities are either threatened or cautionary after 30 years, expressed as a percentage of total withdrawal, for each of the four most-utilized aquifer systems is as follows: Honolua, 45 percent; Honokōwai, 95 percent; Launiupoko, 4 percent; Olowalu, 0 percent.

Regional changes of average water levels in the aquifer after 30 years at the full-build withdrawal rates, presented relative to conditions at the end of Scenario 2, are greatest in the Honokōwai Aquifer System, where average water-level differences are nearly 3 ft lower around the Honokōwai B well (fig. 31*A*). The freshwater body became thinner in much of the Honokōwai and the southern part of the Honolua Aquifer Systems, as the depths of the bottom of the freshwater (fig. 31*B*) and the middle of the transition zone (fig. 31*C*) are shallower by more than 50 ft around the wells with the most increased withdrawal.

Scenario 5—Maximized Withdrawal with Acceptable Salinity using 2000–04 Land Use without Plantation-Scale Agriculture and 1926–2004 Rainfall

In Scenario 5, pumping was redistributed to the existing and proposed wells in an attempt to maximize withdrawal while keeping salinity within the acceptable class at each well. The scenario represents a case in which the withdrawal at each well is established at a rate to maintain salinity values of pumped water within the acceptable class whether or not the well owner has the demand for that water. Withdrawal at existing wells with higher salinities was reduced or terminated where needed and withdrawal at proposed wells was increased to produce water with salinities just below the cautionary class of 1-percent seawater salinity. Withdrawal (table 6) totals 20.68 Mgal/d throughout the Lahaina Aquifer Sector with no cautionary or threatened yield (fig. 25*E*). The highest total rates (10.85 Mgal/d) are available from the existing and proposed wells in the Launiupoko Aquifer System. Assigned total recharge over the model domain was 89 Mgal/d, based on 2000–04 land use without agricultural irrigation and 1926–2004 rainfall (table 5). Injection of treated wastewater effluent was 7.0 Mgal/d after 30 years.

Regional changes of average water levels in the aquifer after 30 years at the redistributed withdrawal rates, presented relative to conditions at the end of the 1926–2008 historical simulation, are greatest in the Launiupoko Aquifer System, where average water-level differences are more than 0.5 ft lower in a broad area and more than 1 ft lower near the withdrawal wells (fig. 32*A*). The freshwater body thinned slightly in this area as the depths of the bottom of the freshwater (fig. 32*B*) and the middle of the transition zone (fig. 32*C*) are shallower in a broad area by more than 20 ft and more than 50 ft near the withdrawal wells. The bottom of the freshwater became shallower by more than 50 ft in a small area of the Honolua Aquifer System.

Regional changes of coastal groundwater discharge after 30 years are presented relative to conditions at the end of the 1926–2008 historical simulation (fig. 24*D*). Coastal groundwater discharge is lower after 30 years along most of the coast. Coastal groundwater discharge is higher in the Ukumehame Aquifer System, however, and also near the injection well.

Scenario 6—Effects of Restoring Streamflow on Projected Withdrawals

In Scenario 6, the projected withdrawal distribution from Scenario 2 (table 8) was used to simulate the effects of additional recharge that would result from restoring flow to losing stream sections in the study area. Partial streamflow restoration has recently been implemented in east and central Maui by reducing the amount of flow diverted for offstream uses such as agriculture (State of Hawai‘i, 2010). This scenario represents one in which total streamflow restoration is implemented. Scenario 6 represents a possible future condition but is not posed here as a recommendation or suggestion for future stream management. Assigned total recharge over the model domain was 105 Mgal/d, based on the no-plantation-scale-agriculture recharge estimate of 89 Mgal/d (table 1) and 16 Mgal/d of streambed recharge distributed evenly along losing stream reaches, assuming that much of the water

returned to the streams infiltrates and becomes groundwater recharge. Injection of treated wastewater effluent was 7.0 Mgal/d after 30 years.

The additional recharge results in salinity decreases relative to Scenario 2 in many of the wells in the study area due to thickening of the freshwater body. The largest long-term simulated salinity decreases relative to Scenario 2 are at Kanahā 2 well in the Launiupoko Aquifer System and at Honokōwai B and P-4, and P-6 wells in the Honokōwai Aquifer System, where the salinity decreases relative to Scenario 2 by as much as 1.7-percent seawater salinity over 30 years (fig. 33). Because the Kanahā 2 and Honokōwai B wells are in stream valleys along losing stream reaches, restored streamflow is likely to affect salinity in these wells the most. The simulated salinity increases into the threatened class at one well for a total threatened rate of 0.61 Mgal/d for all wells (fig. 25*F* and table 7). Simulated salinity is in the cautionary class after 30 years at four wells for a total rate of 1.34 Mgal/d. The amount of withdrawn water in which salinities are either threatened or cautionary after 30 years, expressed as a percentage of total withdrawal, for each of the four most-utilized aquifer systems is as follows: Honolua, 45 percent; Honokōwai, 13 percent; Launiupoko, 4 percent; Olowalu, 0 percent.

Regional changes of average water levels in the aquifer after 30 years of stream restoration at the redistributed withdrawal rates, presented relative to conditions at the end of Scenario 2, are greatest along many of the streams, where average water-level differences are 0.25–0.5 ft higher (fig. 34*A*). Water levels are 0.5 to more than 1 ft higher in the north where the extra recharge is added to the lower-permeability transitional dike zone beneath Honokōhau and Kapalua Streams. The freshwater body thickened most in this area as the depth of the bottom of the freshwater is deeper by more than 50 ft (fig. 34*B*). The bottom of the freshwater becomes at least 20–30 ft deeper beneath many of the other streams.

Scenario 7—Effects of Drought on Projected Withdrawals

The effects of drought and the projected withdrawals were investigated in Scenario 7. Assigned total recharge

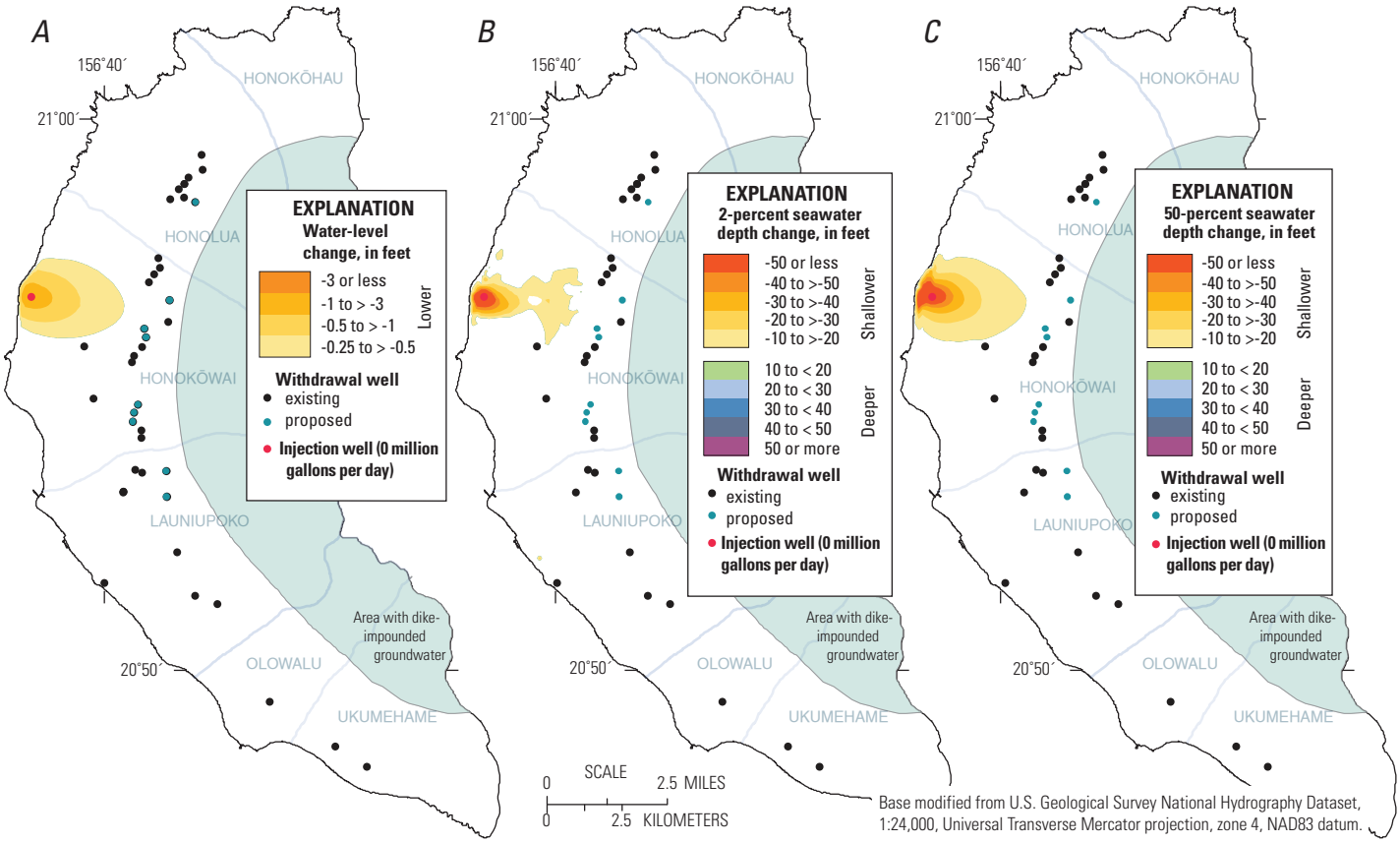

Figure 29. Simulated change (relative to end of Scenario 2) in (*A*) water level, (*B*) 2-percent seawater salinity depth, and (*C*) 50-percent seawater salinity depth after 30 years of withdrawal at projected rates with long-term projected recharge of 89 Mgal/d but no injection (Scenario 3), Lahaina District, west Maui, Hawai‘i. Well names shown on figure 25*C*.

Table 9. Selected wells and withdrawal rates used in Scenario 4, west Maui, Hawai'i.

[Values in pink or red represent wells with salinity in the cautionary or threatened range; NA, not available; cautionary yield is the volume of withdrawn water that has a salinity from 1 to 2 percent that of seawater; threatened yield is the volume of withdrawn water that has a salinity greater than 2 percent that of seawater; --, not applicable; *italics* text indicates injection]

Well name	Well number	Withdrawal rate (millions of gallons per day)								
		2010	2011	2012	2013	2014	2015	2020	2025	2030
Honolua Aquifer System										
Nāpili A	5838-01	0.373	0.36	0.25	0.25	0.25	0.25	0.25	0.25	0.25
Nāpili B	5838-02	0.48	0.	0.2	0.24	0.28	0.31	0.31	0.31	0.31
Nāpili C	5838-04	0.085	0.	0.	0.	0.	0.	0.	0.	0.
Honokahua A	5838-03	0.	0.	0.	0.	0.	0.	0.	0.	0.
Honokahua B	5938-01	0.19	0.02	0.	0.	0.	0.01	0.17	0.	0.
Kapalua 1	5938-02	0.228	0.244	0.26	0.276	0.292	0.307	0.378	0.455	0.534
Kapalua 2	5938-03	0.228	0.244	0.26	0.276	0.292	0.307	0.378	0.455	0.534
Nāpili (proposed)	--	0.	0.75	0.75	0.75	0.75	0.75	0.75	0.75	0.75
Total		**1.583**	**1.618**	**1.719**	**1.791**	**1.863**	**1.935**	**2.237**	**2.221**	**2.378**
Honokōwai Aquifer System										
P-1	5539-01	0.322	0.326	0.375	0.387	0.39	0.393	0.547	0.673	0.713
P-2	5539-02	0.1	0.101	0.116	0.12	0.121	0.122	0.17	0.209	0.221
P-3	5539-04	0.	0.101	0.116	0.12	0.121	0.122	0.17	0.209	0.221
P-4	5739-01	0.274	0.277	0.319	0.329	0.332	0.334	0.465	0.572	0.606
P-5	5738-01	1.225	1.054	1.243	1.315	1.358	1.401	2.149	2.912	3.372
P-5A	5739-04	0.	0.326	0.375	0.387	0.39	0.393	0.547	0.673	0.713
P-6	5739-02	0.032	0.033	0.038	0.039	0.039	0.039	0.055	0.067	0.071
Honokōwai B	5638-03	1.225	1.054	1.243	1.315	1.358	1.401	2.149	2.912	3.372
Hāhākea	5540-03	0.322	0.326	0.375	0.387	0.39	0.393	0.547	0.673	0.713
Pu'ukoli'i	5540-01	0.	0.	0.	0.	0.	0.	0.	0.	0.
Māhinahina (proposed)	--	0.	0.	0.	0.	0.	0.	0.	0.35	0.35
DHHL (proposed)	--	0.	0.	0.	0.	0.	0.	0.	0.	0.
Honokōwai (proposed)	--	0.	0.	0.	0.	0.	0.	0.	0.	0.19
Wahikuli 5 (proposed)	--	0.	0.	0.	0.	0.375	0.375	0.375	0.375	0.375
Wahikuli 4 (proposed)	--	0.	0.	0.	0.	0.375	0.375	0.375	0.375	0.375
Wahikuli 3 (proposed)	--	0.	0.	0.36	0.36	0.375	0.375	0.375	0.375	0.375
Wahikuli 2	5439-02	0.	0.	0.36	0.36	0.375	0.375	0.375	0.375	0.375
Wahikuli 1	5439-01	0.	0.	0.27	0.27	0.3	0.3	0.3	0.3	0.3
Lahaina Injection	*5641*01, *02, *03, *04*	*- 3.901*	*- 4.057*	*- 4.212*	*- 4.368*	*- 4.523*	*- 4.679*	*- 5.457*	*- 6.235*	*- 7.*
Total		**3.5**	**3.6**	**5.19**	**5.39**	**6.3**	**6.4**	**8.6**	**11.05**	**12.34**
Launiupoko Aquifer System										
Waipuka 1, 2	5339-01, -02	0.	0.	0.	0.	0.	0.	0.	0.	0.
Kanahā 1	5339-03	0.	0.	0.	0.	0.	0.	0.	0.	0.
Kanahā 2	5339-04	0.	0.	0.	0.	0.	0.	0.	0.	0.
Launiupoko 1	5138-01	0.012	0.013	0.013	0.013	0.013	0.014	0.015	0.016	0.017
Launiupoko 2	5137-01	0.054	0.055	0.056	0.058	0.059	0.06	0.065	0.07	0.075
Launiupoko 3	5238-01	0.054	0.055	0.056	0.058	0.059	0.06	0.065	0.07	0.075
Puamana 1, 2	5140-01, -02	0.08	0.08	0.08	0.08	0.08	0.08	0.08	0.08	0.08
Kanahā (proposed)	--	0.557	0.574	0.592	0.61	0.628	0.646	0.725	0.811	0.899
Waipuka (proposed)	--	0.455	0.47	0.484	0.499	0.514	0.528	0.593	0.664	0.735
Total		**1.213**	**1.248**	**1.283**	**1.317**	**1.352**	**1.387**	**1.542**	**1.71**	**1.882**
Olowalu Aquifer System										
Olowalu Elua	4936-01	0.07	0.09	0.11	0.14	0.16	0.19	0.3	0.41	0.53
Total		**.07**	**.09**	**.11**	**.14**	**.16**	**.19**	**.3**	**.41**	**.53**
Ukumehame Aquifer System										
Sugar Way 1, 2	4835-02, -03	NA	NA	NA	NA	NA	NA	NA	NA	NA
Total		**NA**	**NA**	**NA**	**NA**	**NA**	**NA**	**NA**	**NA**	**NA**
Total Lahaina Aquifer Sector management area		**6.36**	**6.56**	**8.31**	**8.64**	**9.68**	**9.91**	**12.67**	**15.39**	**17.13**

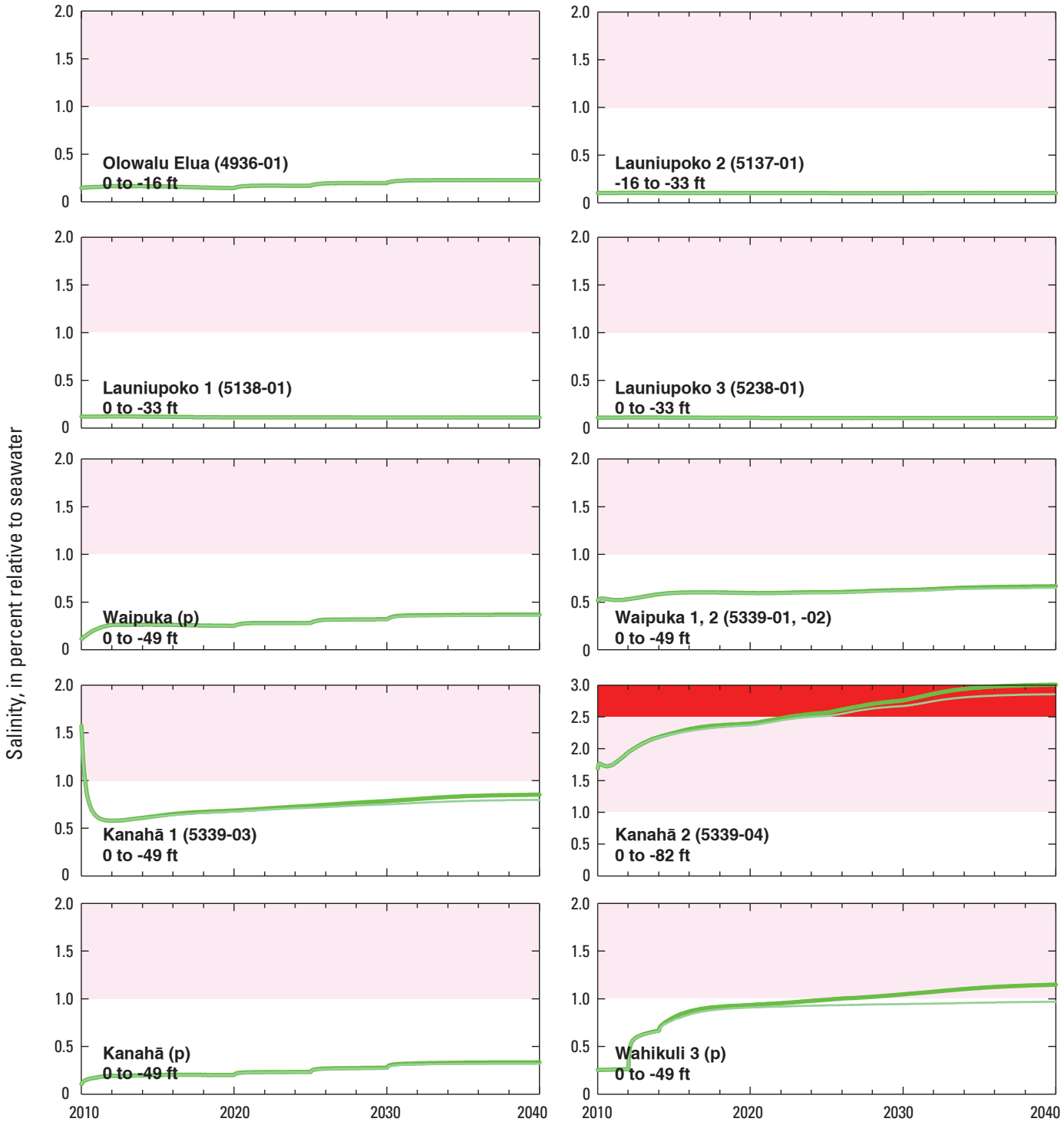

Figure 30. Simulated salinity data for Scenario 4 (dark green lines) for the period 2010–2039 assuming projected full-build pumping rates at selected wells in the Lahaina Aquifer Sector compared to Scenario 2 (light green lines), west Maui, Hawai‘i. For each well shown, the simulated salinity is for the deepest node representing the well. The depths of the nodes used are shown under each well name and number. Well names followed by (p) are proposed wells. The pink area represents a cautionary salinity class and the red area represents a threatened salinity class.

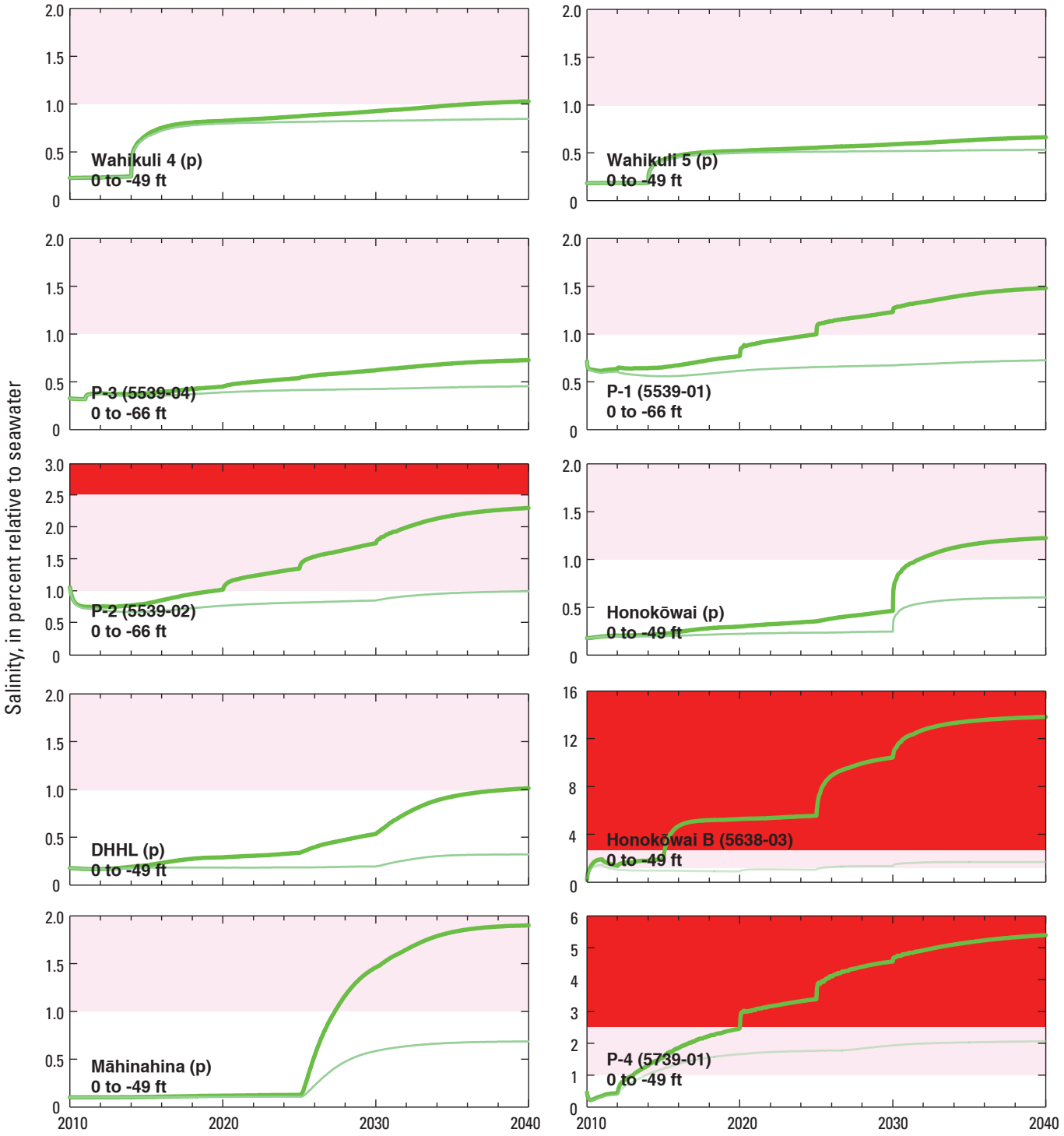

Figure 30. Simulated salinity data for Scenario 4 (dark green lines) for the period 2010–2039 assuming projected full-build pumping rates at selected wells in the Lahaina Aquifer Sector compared to Scenario 2 (light green lines), west Maui, Hawai‘i. For each well shown, the simulated salinity is for the deepest node representing the well. The depths of the nodes used are shown under each well name and number. Well names followed by (p) are proposed wells. The pink area represents a cautionary salinity class and the red area represents a threatened salinity class—continued.

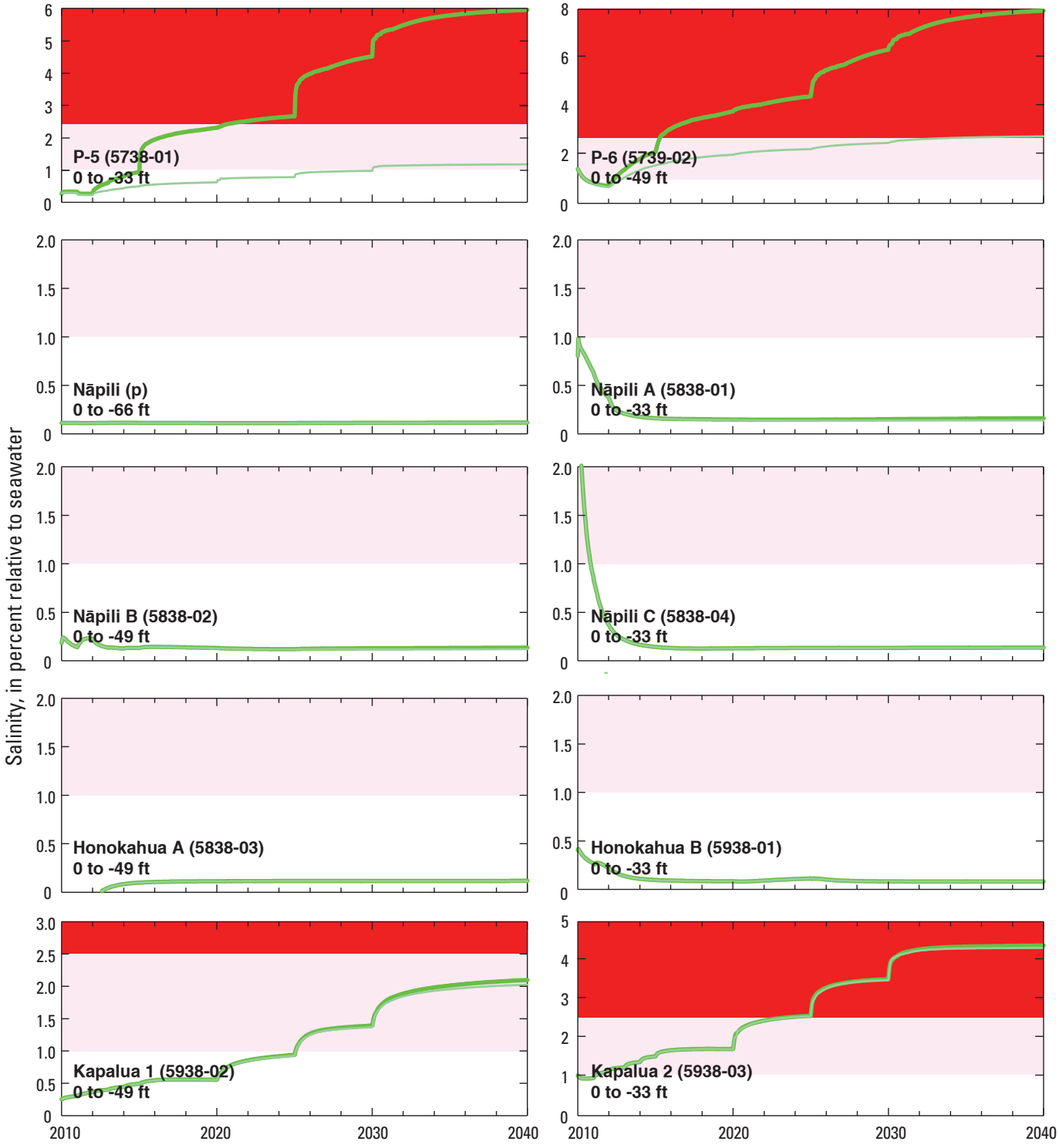

Figure 30. Simulated salinity data for Scenario 4 (dark green lines) for the period 2010–2039 assuming projected full-build pumping rates at selected wells in the Lahaina Aquifer Sector compared to Scenario 2 (light green lines), west Maui, Hawai‘i. For each well shown, the simulated salinity is for the deepest node representing the well. The depths of the nodes used are shown under each well name and number. Well names followed by (p) are proposed wells. The pink area represents a cautionary salinity class and the red area represents a threatened salinity class—continued.

over the model domain was 89 Mgal/d, based on 2000–04 land use without plantation-scale agriculture and 1926–2004 rainfall during simulation periods 2010–24 and 2030–39 (table 5). Injection of treated wastewater effluent was 7.0 Mgal/d after 30 years. A 5-yr drought within the 30-yr simulation was represented during simulation period 2025–29 using recharge conditions estimated with no agriculture and 1998–2002 rainfall (table 1). The period 1998–2002 had the lowest rainfall for any 5-yr period recorded on Maui (Engott and Vana, 2007). The recharge during this period was 65 Mgal/d. Withdrawal rates (table 8) were the same as for Scenario 2 for all wells. In this scenario, total withdrawal after 30 years averaged 11.20 Mgal/d throughout the Lahaina Aquifer Sector. This scenario is considered a severe one, because the 5-yr drought is not balanced in this simulation by any compensating wet years that would typically occur to balance out the long-term average during a 30-yr period.

Differences in salinities between the drought and the non-drought scenario are small after 30 years at most wells (fig. 35). Salinities are higher by as much as 1-2 percent seawater by the end of the drought at some of the wells but return to nearly the same salinities as during the non-drought condition (Scenario 2) by the end of the 30-year simulation. The largest long-term simulated salinity increases are at Honokōwai B and P-4, P-5, and P-6 wells in the Honokōwai Aquifer System, where the salinity increases by as much as 2-percent seawater salinity during the 5-yr drought. During the drought, the simulated salinity increases into the threatened class at 6 wells and into the cautionary class at 9 wells. Six of the wells in which salinities increase into the cautionary class during the drought are wells in which salinities remained in the acceptable class during the non-drought scenario. The amount of withdrawn water in which salinities are either threatened or cautionary after 30 years, expressed as a percent of total withdrawal, for each of the

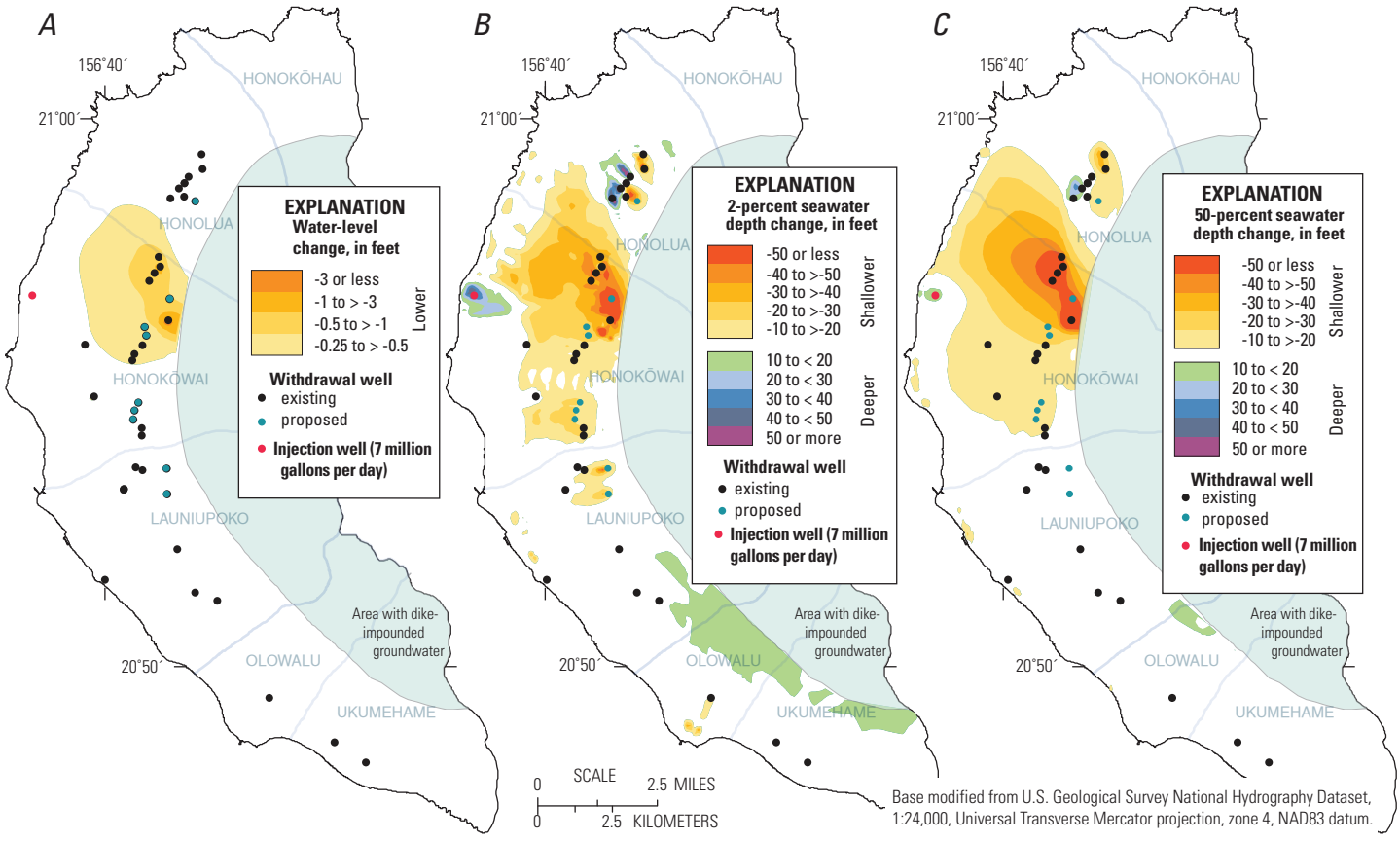

Figure 31. Simulated change (relative to end of Scenario 2) in (*A*) water level, (*B*) 2-percent seawater salinity depth, and (*C*) 50-percent seawater salinity depth after 30 years of withdrawal at full-build projected rates with long-term projected recharge of 89 Mgal/d (Scenario 4), Lahaina District, west Maui, Hawai'i. Well names shown on figure 25*D*.

four most-utilized aquifer systems is as follows: Honolua, 45 percent; Honokōwai, 62 percent; Launiupoko, 4 percent; Olowalu, 0 percent.

Model Limitations

The numerical model developed for this study simulates water levels and salinity on a regional scale and thus may not accurately predict either the pumped water level at an individual well or the salinity of water pumped from that well. These values, however, are still indicative of expected regional trends in water levels and salinity. The salinity of water pumped from a well may be controlled by local heterogeneities in the aquifer that are not represented in the model. The level of model discretization affects the numerical accuracy with which transport mechanisms are simulated. The model has several other limitations for predictive purposes because of the various assumptions made and possible uncertainties in input data. These limitations are discussed below.

Differences between measured and simulated water levels and salinity profiles are greater in some areas than in others, which may reflect uncertainties in the recharge or withdrawal estimates, boundary conditions, assigned parameter values in the model, or representations of the different hydrogeological features in the model. Recharge estimates are based on water-budget computations that could be improved with a better understanding of the spatial rainfall distributions, evapotranspiration, runoff, and land-cover characteristics in the study area. Improved recharge estimates in the study area will lead to better estimates for parameter values in the numerical groundwater model and greater confidence in model simulation results. Withdrawals represented in the model were based on available

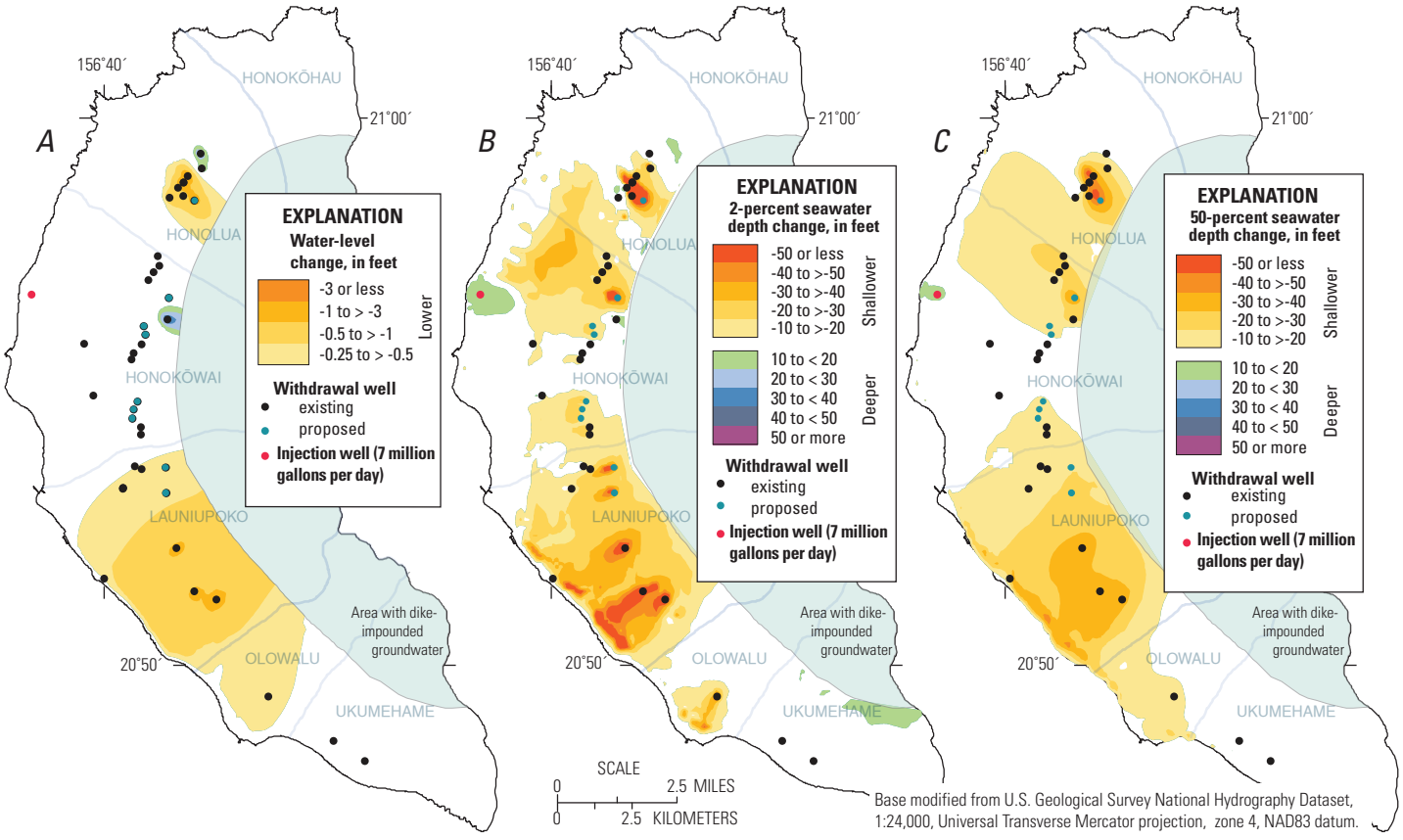

Figure 32. Simulated change (relative to end of historical simulation) in (*A*) water level, (*B*) 2-percent seawater salinity depth, and (*C*) 50-percent seawater salinity depth after 30 years of withdrawal at maximized rates and acceptable salinity with long-term projected recharge of 89 Mgal/d (Scenario 5), Lahaina District, west Maui, Hawai‘i. Well names shown on figure 25*E*.

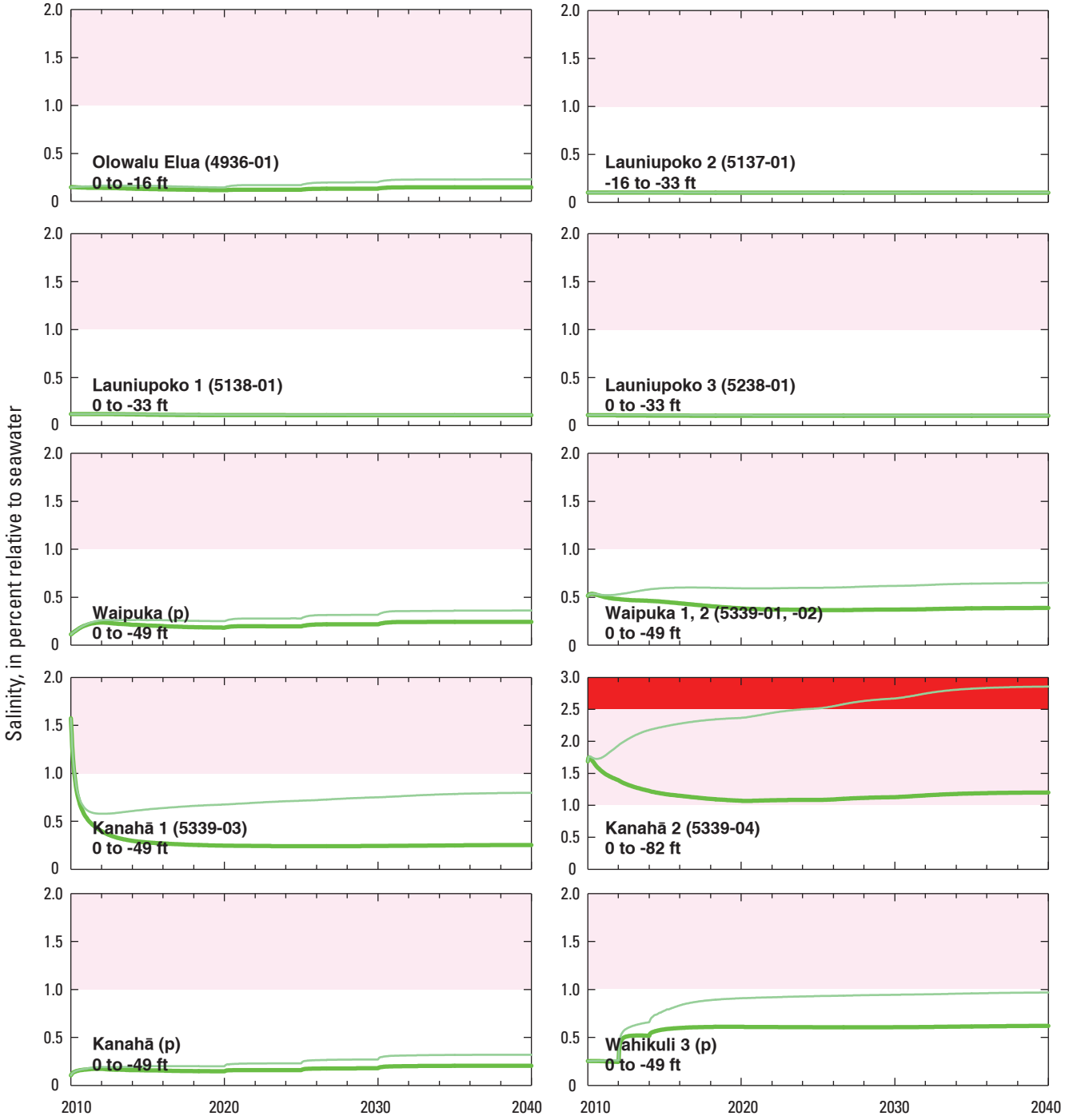

Figure 33. Simulated salinity data for Scenario 6 (dark green lines) for the period 2010–2039 assuming projected pumping rates at selected wells in the Lahaina Aquifer Sector and full streamflow restoration compared to Scenario 2 (light green lines), west Maui, Hawai‘i. For each well shown, the simulated salinity is for the deepest node representing the well. The depths of the nodes used are shown under each well name and number. Well names followed by (p) are proposed wells. The pink area represents a cautionary salinity class and the red area represents a threatened salinity class.

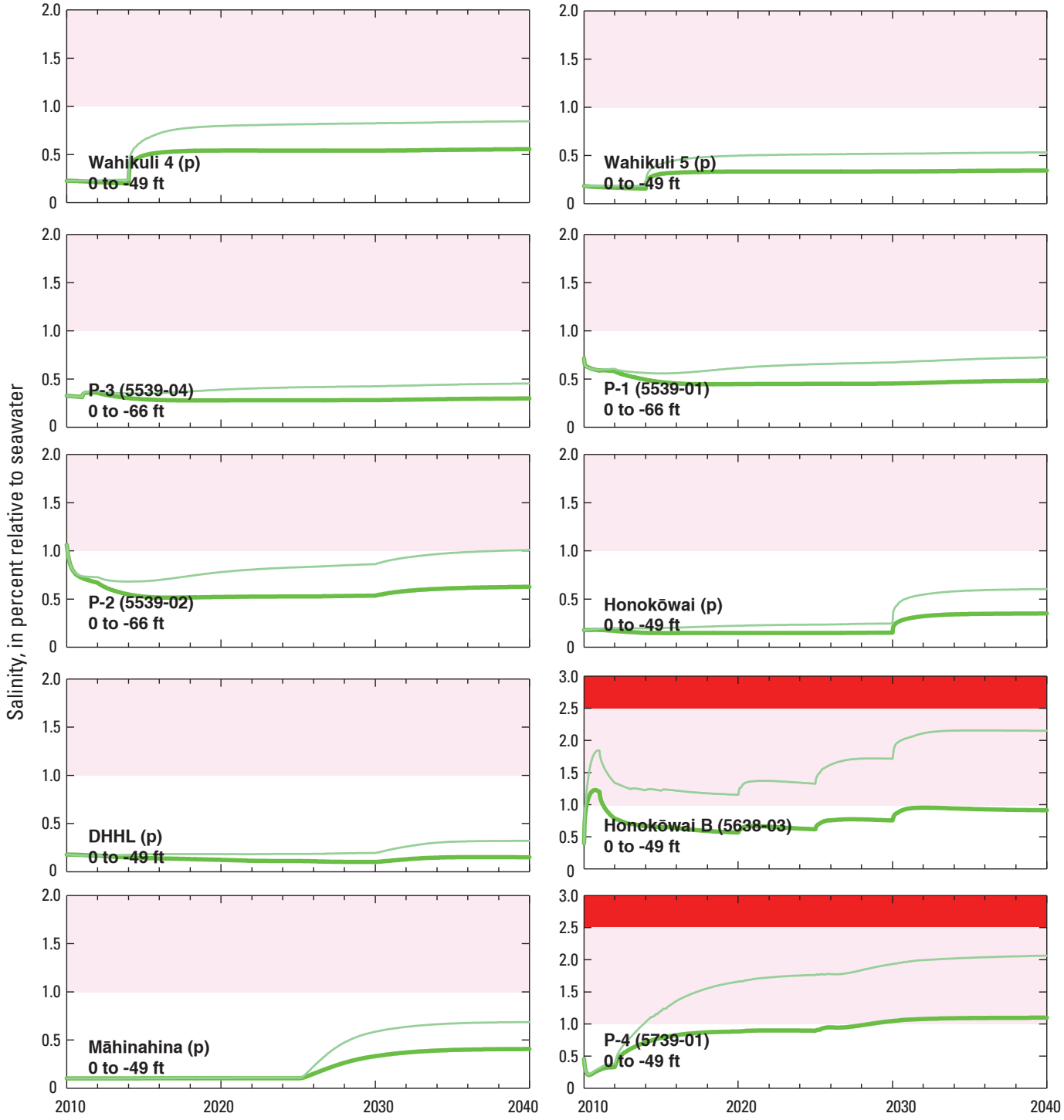

Figure 33. Simulated salinity data for Scenario 6 (dark green lines) for the period 2010–2039 assuming projected pumping rates at selected wells in the Lahaina Aquifer Sector and full streamflow restoration compared to Scenario 2 (light green lines), west Maui, Hawai‘i. For each well shown, the simulated salinity is for the deepest node representing the well. The depths of the nodes used are shown under each well name and number. Well names followed by (p) are proposed wells. The pink area represents a cautionary salinity class and the red area represents a threatened salinity class—continued.

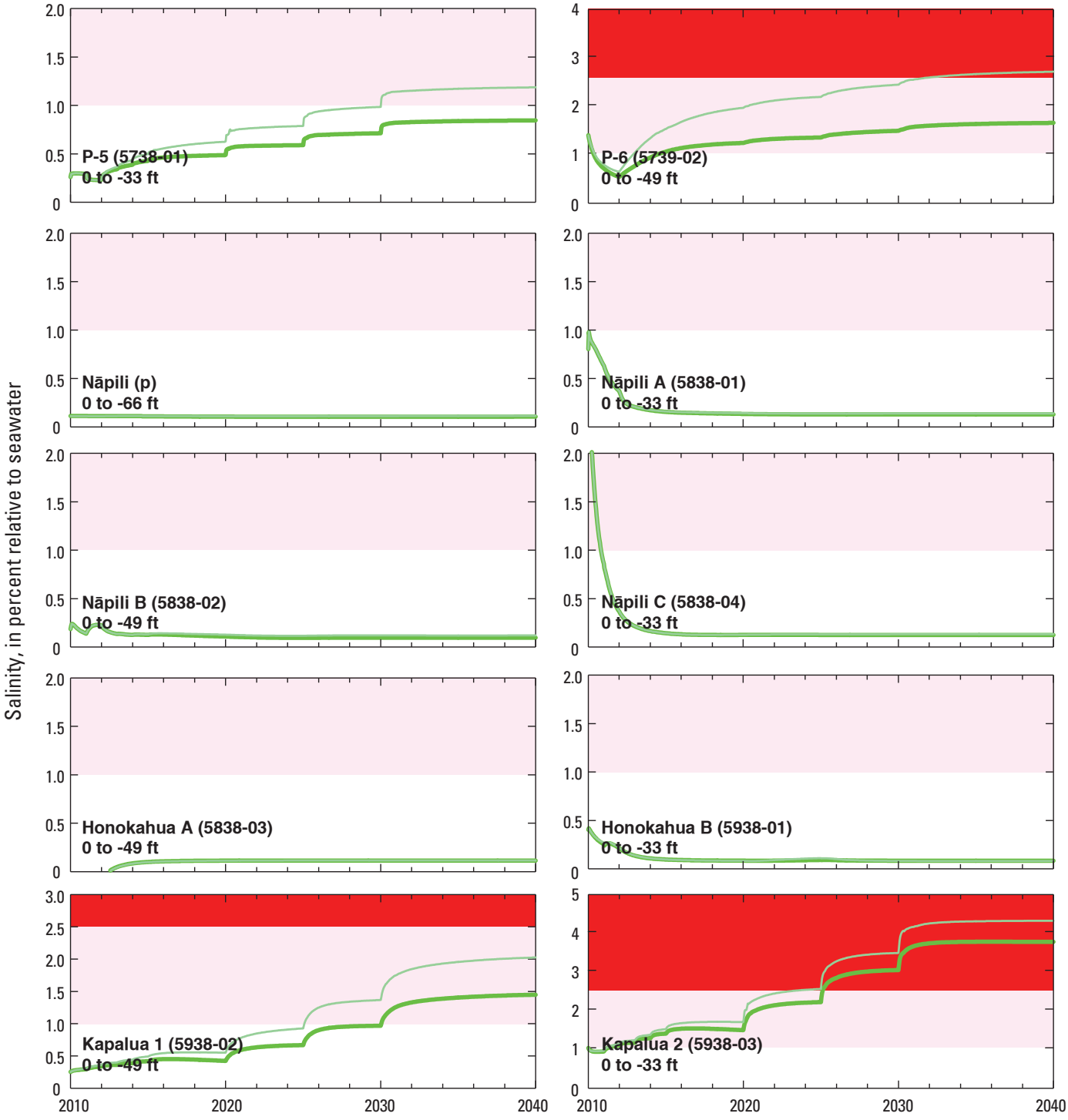

Figure 33. Simulated salinity data for Scenario 6 (dark green lines) for the period 2010–2039 assuming projected pumping rates at selected wells in the Lahaina Aquifer Sector and full streamflow restoration compared to Scenario 2 (light green lines), west Maui, Hawai‘i. For each well shown, the simulated salinity is for the deepest node representing the well. The depths of the nodes used are shown under each well name and number. Well names followed by (p) are proposed wells. The pink area represents a cautionary salinity class and the red area represents a threatened salinity class—continued.

information. Unreported withdrawals and uncertainties in reported withdrawals that cannot be quantified also affect the accuracy of model results.

The distributions of parameter values assigned in the model were kept simple to avoid creating an overly complex model that could not be justified on the basis of existing information. Heterogeneity in the groundwater system likely exists but is poorly understood. Values assigned to model parameters initially were based on existing estimates and subsequently adjusted to simulate historical head and salinity observations. Some of these parameter values, however, particularly dispersion coefficients, may be poorly known. Simulation results, especially those for pumped water salinity, are particularly sensitive to the dispersion coefficients used in the model. Therefore, further quantification of these values in future investigations would be useful to improve confidence that the model accurately predicts pumped-water salinity.

The geometrical representation of the possible valley-fill barriers and caprock also were simplified for the model. The geometric definition of the valley-fill barriers, especially in the Launiupoko and Olowalu Aquifer Systems, could be improved by using surface geophysical techniques in conjunction with drilling additional monitor wells within the valleys. For this study, the coastal caprock was represented as a homogeneous zone of relatively low permeability. High-permeability zones likely exist within the caprock, but they are poorly understood and were not represented in the model. Confidence in model simulation results can be improved by addressing the limitations described in this section. In particular, improved estimates of the distribution of model parameters likely will lead to better model reliability. Despite these limitations, the model developed for this study and used for the simulations described above does an acceptable job of predicting future conditions and regional trends for several scenarios of interest.

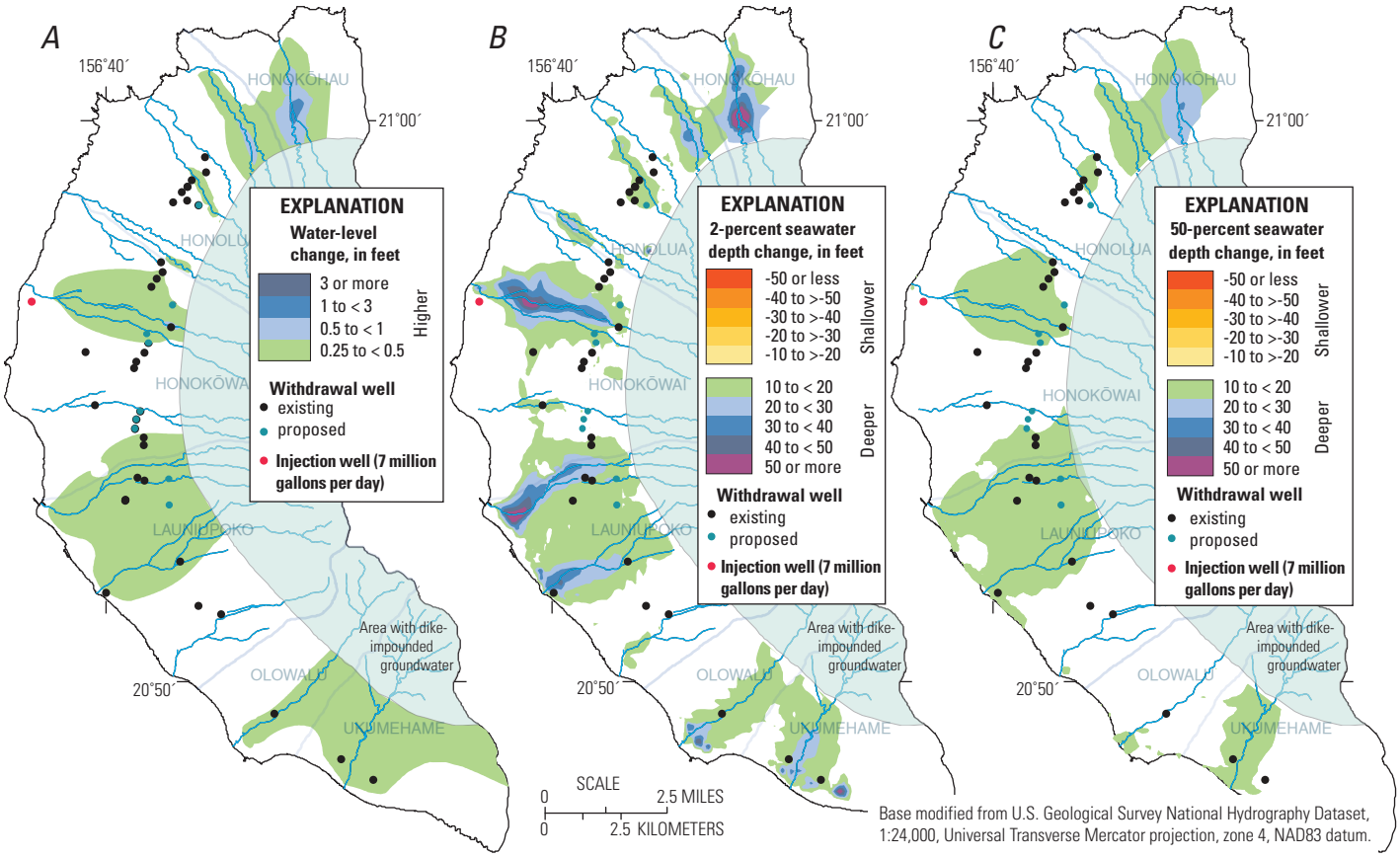

Figure 34. Simulated change (relative to end of Scenario 2) in (*A*) water level, (*B*) 2-percent seawater salinity depth, and (*C*) 50-percent seawater salinity depth after 30 years of withdrawal at projected rates with long-term projected recharge of 89 Mgal/d and restored streamflow of 16 Mgal/d (Scenario 6), Lahaina District, west Maui, Hawai‘i.

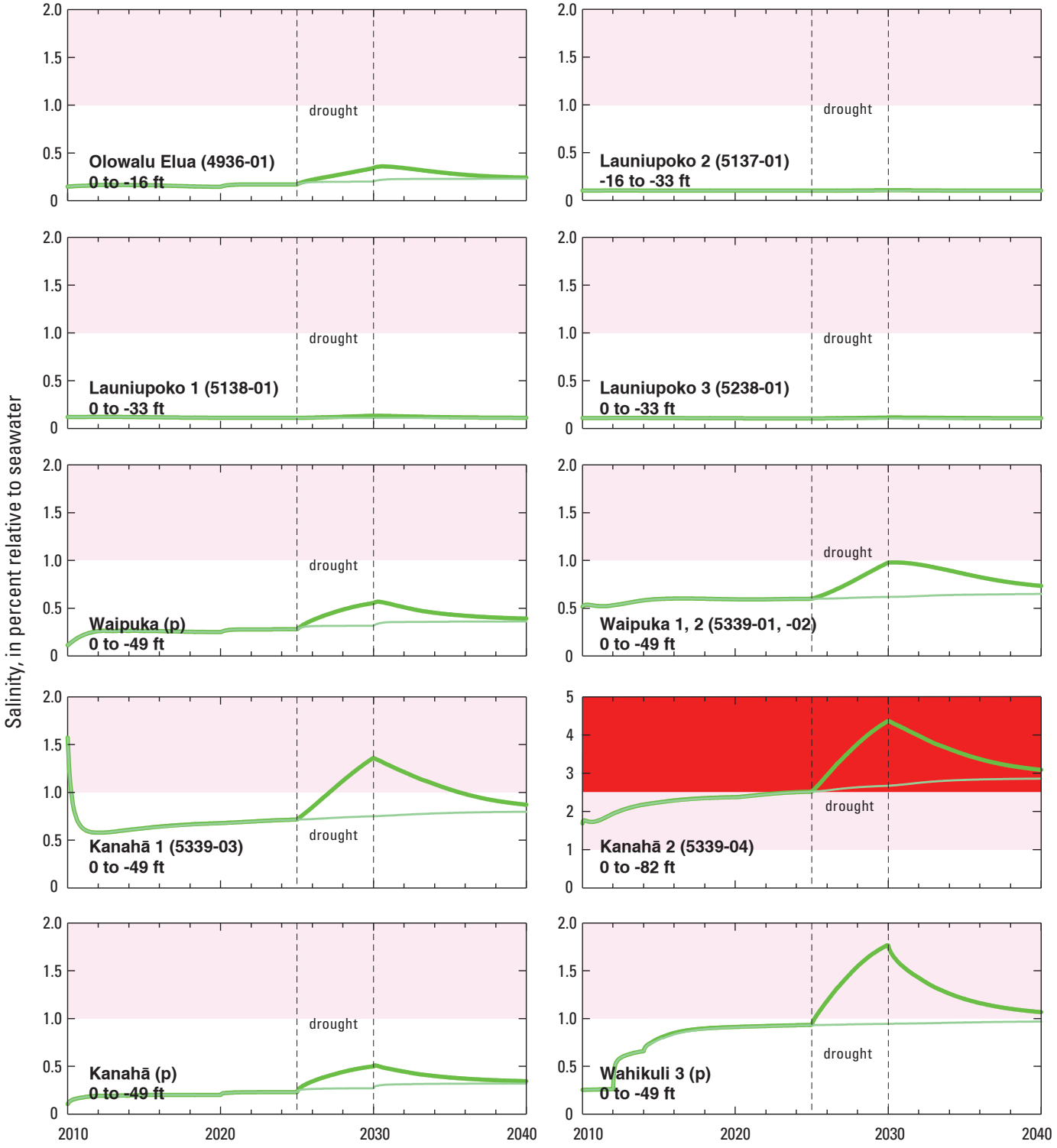

Figure 35. Simulated salinity data for Scenario 7 (dark green lines) for the period 2010–2039 assuming projected pumping rates at selected wells in the Lahaina Aquifer Sector compared to Scenario 2 (light green lines), west Maui, Hawai'i. For each well shown, the simulated salinity is for the deepest node representing the well. The depths of the nodes used are shown under each well name and number. Well names followed by (p) are proposed wells. The pink area represents a cautionary salinity class and the red area represents a threatened salinity class.

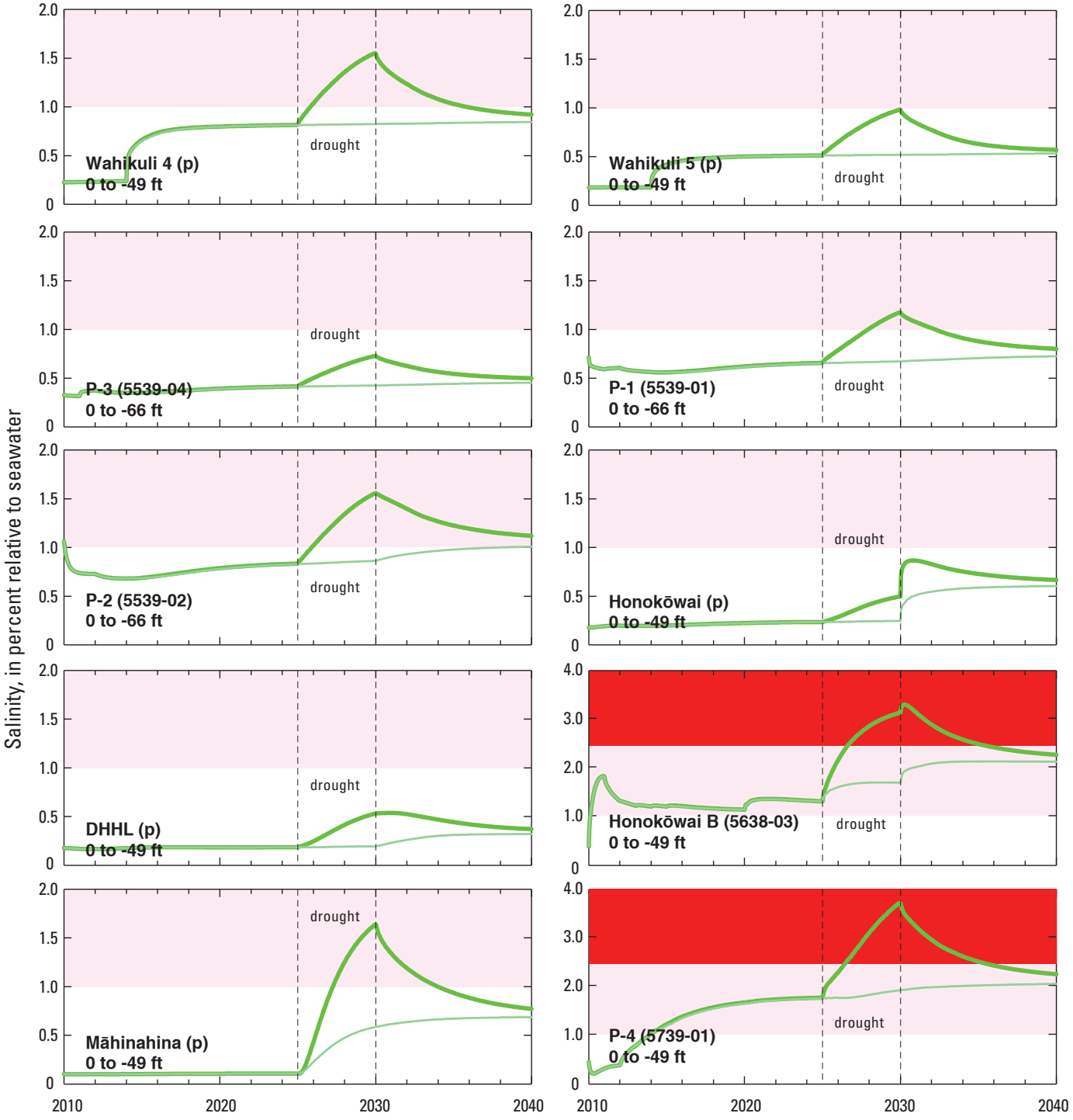

Figure 35. Simulated salinity data for Scenario 7 (dark green lines) for the period 2010–2039 assuming projected pumping rates at selected wells in the Lahaina Aquifer Sector compared to Scenario 2 (light green lines), west Maui, Hawai‘i. For each well shown, the simulated salinity is for the deepest node representing the well. The depths of the nodes used are shown under each well name and number. Well names followed by (p) are proposed wells. The pink area represents a cautionary salinity class and the red area represents a threatened salinity class—continued.

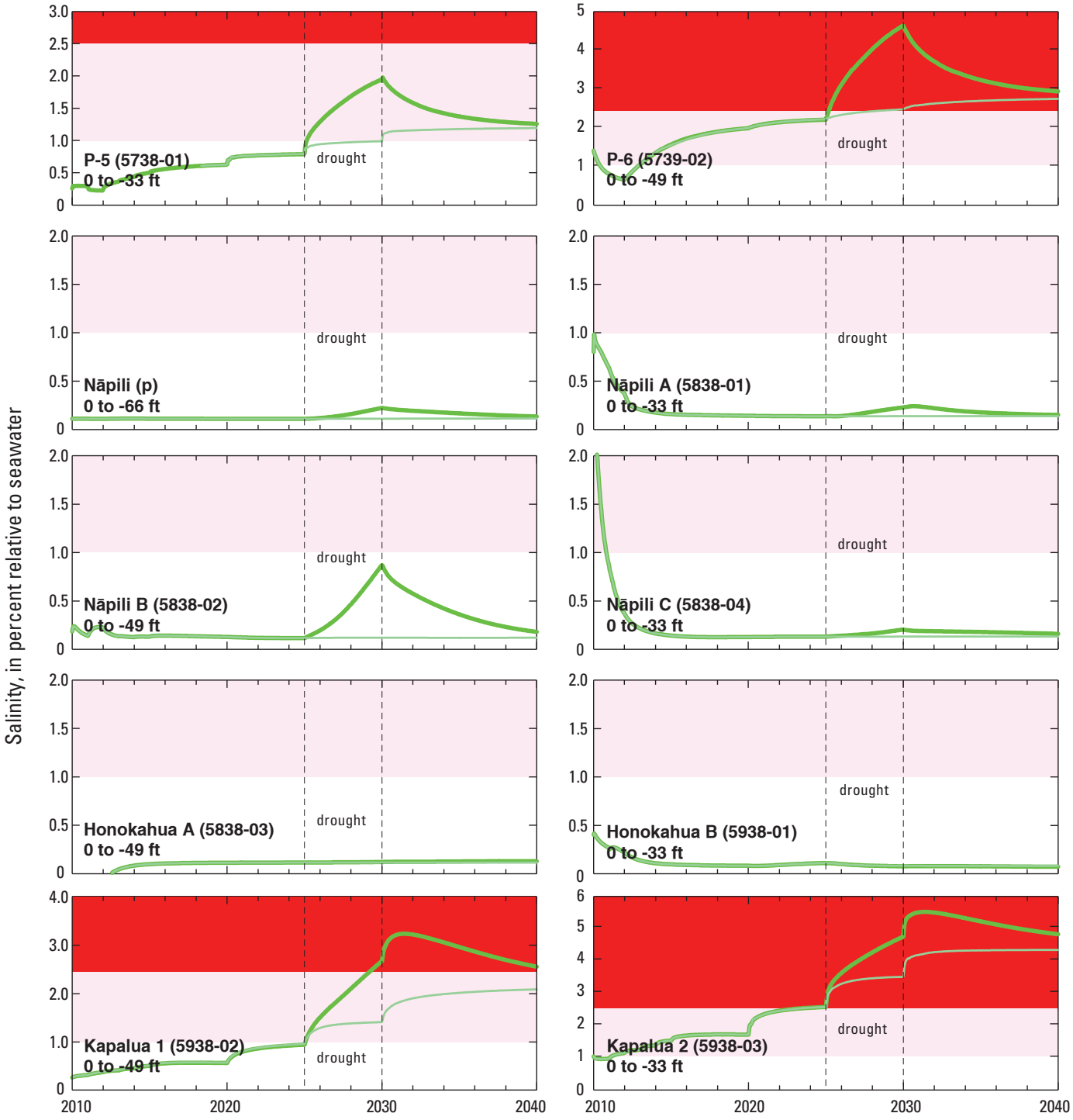

Figure 35. Simulated salinity data for Scenario 7 (dark green lines) for the period 2010–2039 assuming projected pumping rates at selected wells in the Lahaina Aquifer Sector compared to Scenario 2 (light green lines), west Maui, Hawai‘i. For each well shown, the simulated salinity is for the deepest node representing the well. The depths of the nodes used are shown under each well name and number. Well names followed by (p) are proposed wells. The pink area represents a cautionary salinity class and the red area represents a threatened salinity class—continued.

Summary

Demand for groundwater provided by the Maui County Department of Water Supply (MDWS) in the Lahaina area of west Maui is estimated to increase from about 2.1 Mgal/d in 2007 to 3.5 Mgal/d in 2030. Accounting for groundwater pumped by several private water systems in the area, the total demand for groundwater is expected to increase from 5.8 Mgal/d in 2007 to 11.1 Mgal/d in 2030. However, the amount of groundwater that is available in the Lahaina area to meet future water demands is uncertain. In response to reduced recharge and increased withdrawals from the freshwater lens of the Lahaina area, the chloride concentrations of water pumped from wells has increased. Chloride concentrations in water pumped from several MDWS wells occasionally exceeds 250 mg/L. The potential rise in the transition zone between freshwater and saltwater, the consequent increase in chloride concentrations in pumped water, and the large increase in expected withdrawals have led to concern over the long-term sustainability of withdrawals from existing wells in the Lahaina area. The objective of this 4-year study, begun in 2008, is to estimate the effects of several hypothetical withdrawal scenarios within the Lahaina area, using a numerical groundwater flow and transport model, on water levels, the transition zone between freshwater and saltwater, and surface-water/groundwater interactions.

Average withdrawals from the Lahaina Aquifer Sector during 2000–08 were about 4 Mgal/d from public and private wells. Most streams on West Maui Volcano receive groundwater discharge from the dike-impounded water body; however, much of this water is diverted for offstream uses. Total average base flow during 1913–2005 upstream of any diversions from the 9 gaged streams in the study area was about 35 Mgal/d.

A three-dimensional numerical groundwater model capable of simulating density-dependent solute transport was developed as part of this study. The model used published estimates for most of the hydraulic conductivity, storage, and dispersivity values of the materials, principally volcanic rocks, in which the water occurs. Simulated water levels, pumped-well water salinities, and salinity profiles generally were in agreement with measured water levels, salinities, and salinity profiles from representative wells in the modeled area during 1926–2008.

The numerical model constructed for this study was used to quantify changes in groundwater level and salinity for various withdrawal and recharge scenarios during the period 2010–39. Scenarios included groundwater withdrawal at 2008–09 rates and locations with average recharge, and withdrawal at redistributed rates and locations with average recharge, and with and without treated wastewater injection at the Lahaina Sewage Treatment Plant (STP). Simulation results from the 2008–09 withdrawal scenario (6.3 Mgal/d from 21 wells) indicate the following for the Lahaina Aquifer Sector:

- average water levels decrease about 0.5–1 ft and the transition zone becomes 20–40 ft shallower after 30 years, mainly in the Honokōwai Aquifer System, and
- 2 wells have simulated salinity values that increase into the threatened class (salinity greater than 2.5 percent seawater) and 4 wells have simulated salinity values that increase into the cautionary class (salinity between 1.0 and 2.5 percent seawater) after 30 years.

Three scenarios were used to investigate the results of projected groundwater withdrawals and proposed wells on the hydrologic system. The three scenarios are (1) projected rates and locations based on the most likely estimate of future conditions, (2) the same conditions as (1) without wastewater injection, and (3) a maximum build-out projection. Simulation results from the most likely projected withdrawal scenario (11.2 Mgal/d from 28 wells including 10 proposed wells) indicate the following:

- average water levels decrease about 0.5–1 ft and the transition zone becomes 20–40 ft shallower after 30 years, mainly in the Honokōwai Aquifer System, however, the freshwater lens became slightly thicker in the area of the Lahaina STP injection and downgradient of the Nāpili wells in the Honolua Aquifer System where withdrawal was decreased, and
- 4 wells have simulated salinity values that increase into the threatened class and 5 wells have simulated salinity values that increase into the cautionary class after 30 years.

The same withdrawal scenario was simulated without injection of 7 Mgal/d of treated wastewater at the Lahaina Sewage Treatment Plant. The injected freshwater acts as a hydrologic barrier, therefore when the injection is stopped, salinities increase in pumped wells upgradient of the injection site by as much as 1-percent seawater salinity over 30 years. Salinity increases from the cautionary to threatened class at two wells and from acceptable to cautionary in one well. This is an increase of cautionary and threatened yield of 0.46 Mgal/d because of the removal of the injection source. Simulation results from the projected full-build withdrawal scenario (17.1 Mgal/d from 28 wells including 10 proposed wells) indicate the following:

- average water levels decrease by as much as 3 ft and the transition zone becomes more than 50 ft shallower after 30 years, mainly in the Honokōwai Aquifer System and the southern part of the Honolua Aquifer System, and
- 7 wells have simulated salinity values that increase into the threatened class and 9 wells have simulated salinity values that increase into the cautionary class after 30 years.

A scenario in which groundwater withdrawal was redistributed in an attempt to maximize withdrawal and maintain acceptable salinities was determined using the numerical model in an iterative manner. Redistributed withdrawals at existing wells were combined with withdrawal

from the proposed new well sites. The redistribution simulates 20.7 Mgal/d of withdrawal from 26 wells or well fields in the Lahaina Aquifer Sector. Simulation results from this scenario indicate the following:

- average water levels decrease by about 0.5–1 ft and the transition zone becomes 20–50 ft shallower after 30 years, mainly in the Launiupoko Aquifer System near the proposed wells, and
- all wells have simulated salinities in the acceptable class after 30 years.

A scenario showing the effects of additional recharge caused by restoring flow to losing stream sections indicates that the salinity of water in many of the pumped wells decreases relative to the scenario without restored streamflow due to thickening of the freshwater body. Wells in stream valleys along losing stream reaches are most likely to have salinity decreases. A scenario including a 5-yr drought showed salinities are higher by as much as 1-2 percent seawater salinity by the end of the drought at some of the wells but return to nearly the same salinities as during the prior non-drought condition after ten additional years of average future recharge.

The numerical model developed for this study simulates water levels and salinity on a regional scale and thus may not accurately predict either the pumped water level at an individual well or the salinity of water pumped from that well, but these values are still indicative of expected regional trends in water levels and salinity. Salinity of water pumped from a well may be controlled by local heterogeneities in the aquifer that are not represented in the model. The model has several other limitations for predictive purposes because of the various assumptions used and possible uncertainties in input data. Model reliability can be improved as the understanding of groundwater recharge, the distribution of the aquifer hydraulic values, and the geometry of the sedimentary layers and valley-fill barriers become better known through additional data collection.

References Cited

Blumenstock, D.I., and Price, Saul, 1967, Climates of the States-Hawaii: U.S. Department of Commerce, Climatography of the United States, no. 60–51, 27 p.

Bowles, S.P., 1970, Storm runoff disposal wells at Kahului, Maui: A report for Kahului Development Co., July 1970.

Burnham, W.L., Larson, S.P., and Cooper, H.H., Jr., 1977, Distribution of injected wastewater in the saline lava aquifer, Wailuku-Kahului wastewater treatment facility, Kahului, Maui, Hawaii: U.S. Geological Survey Open-File Report 77–469, 58 p.

Commission on Water Resource Management, 2008, Mahinahina Deep Monitor Well, Maui (5739-03), Chart showing the elevation of the midpoint and top of the transition zone over time, accessed June 25, 2008, at http://hawaii.gov/dlnr/cwrm/monitoringdata/dmw_mahinahina.pdf.

Engott, J.A., and Vana, T.T., 2007, Effects of agricultural land-use changes and rainfall on ground-water recharge in central and west Maui, Hawai‘i, 1926–2004: U.S. Geological Survey Scientific Investigations Report 2007–5103, 56 p.

Fontaine, R.A., 2003, Availability and distribution of base flow in lower Honokohau Stream, Island of Maui, Hawaii: U.S. Geological Survey Water-Resources Investigations Report 03-4060, 37 p.

Freeze, R.A., and Cherry, J.A., 1979, Groundwater: Englewood Cliffs, N.J., Prentice-Hall, Inc., 604 p.

Giambelluca, T.W., Nullet, M.A., and Schroeder, T.A., 1986, Rainfall atlas of Hawai‘i: State of Hawai‘i, Department of Land and Natural Resources, Division of Water and Land Development, Report R76, 267 p.

Gingerich, S.B., 2008, Ground-water availability in the Wailuku area, Maui, Hawai‘i: U.S. Geological Survey Science Investigations Report 2008–5236, 95 p.

Gingerich, S.B., and Oki, D.S., 2000, Ground water in Hawaii: U.S. Geological Survey Fact Sheet FS 126–00, 6 p.

Gingerich, S.B., and Voss, C.I., 2005, Three-dimensional variable-density flow simulation of a coastal aquifer in southern Oahu, Hawaii, USA: Hydrogeology Journal, v. 13, p. 436–450.

Harbaugh, A.W., 1990, A computer program for calculating subregional water budgets using results from the U.S. Geological Survey modular three-dimensional ground-water flow model: U.S. Geological Survey Open-File Report 90–392, 46 p.

Harbaugh, A.W., Banta, E.R., Hill, M.C., and McDonald, M.G., 2000, MODFLOW-2000, the U.S. Geological Survey modular ground-water model—user guide to modularization concepts and the ground-water flow process: U.S. Geological Survey Open-File Report 00–92, 121 p.

Huber, R.D., and Adams, W.M., 1971, Density logs from underground gravity surveys in Hawaii: University of Hawai‘i Water Resources Research Center Technical Report no. 45, 39 p.

Hunt, C.D., Jr., 2007, Ground-water nutrient flux to coastal waters and numerical simulation of wastewater injection at Kihei, Maui, Hawaii: U.S. Geological Survey Scientific Investigations Report 2006–5283, 69 p.

Ishizaki, Kenneth, Burbank, N.C., Jr., and Lau, L.S., 1967, Effects of soluble organics on flow through thin cracks of basaltic lava: University of Hawai‘i Water Resources Research Center Technical Report no. 16, 56 p.

Langenheim, V.A.M., and Clague, D.A., 1987, The Hawaiian-Emperor volcanic chain, part II, stratigraphic framework of volcanic rocks of the Hawaiian Islands, chap. 1 *of* Decker, R.W., Wright, T.L., and Stauffer, P.H., eds., Volcanism in Hawaii: U.S. Geological Survey Professional Paper 1350, v. 1, p. 55–84.

Liu, C.C.K., 2006, Analytical groundwater flow and transport modeling for the estimation of the sustainable yield of Pearl Harbor Aquifer *for* Hawai‘i Department of Land and Natural Resources State Commission on Water Resources Management Project Report PR-2006-06, 58 p.

Macdonald, G.A., Abbott, A.T., and Peterson, F.L., 1983, Volcanoes in the sea, the geology of Hawaii (2d ed.): Honolulu, Hawai‘i, University of Hawai‘i Press, 517 p.

McCandless, J.S., 1936, Development of artesian well water in the Hawaiian Islands, 1880–1936: Honolulu, Hawai‘i, 79 p.

McDougall, Ian, 1964, Potassium-argon ages from lavas of the Hawaiian Islands: Geological Society of American Bulletin, v. 75, p. 107–128.

Meyer, William, and Presley, T.K., 2001, The response of the Iao aquifer to ground-water development, rainfall, and land-use practices between 1940 and 1998, island of Maui, Hawaii: U.S. Geological Survey Water-Resources Investigations Report 00–4223, 60 p.

Meyer, William, and Souza, W.R., 1995, Factors that control the amount of water that can be diverted to wells in a high-level aquifer, *in* Hermann, Raymond, Back, William, Sidle, R.C., and Johnson, A.I., eds., Water resources and environmental hazards: emphasis on hydrologic and cultural insight in the Pacific Rim: Proceedings of the American Water Resources Association Annual Summer Symposium, Honolulu, Hawai‘i, June 25-28, 1995, p. 207–216.

Miller, M.E., 1987, Hydrogeologic characteristics of central Oahu subsoil and saprolite; implications for solute transport: University of Hawai‘i at Mānoa M.S. thesis, 231 p.

Mink, J.F., and Lau, L.S., 1980, Hawaiian groundwater geology and hydrology, and early mathematical models: University of Hawai‘i Water Resources Research Center Technical Memorandum Report no. 62, 74 p.

National Oceanic and Atmospheric Administration, 2009, Historic tide data, last accessed June 16, 2009, at http://tidesandcurrents.noaa.gov/data_menu.shtml?stn=1615680%20Kahului,%2HI&type=Historic+Tide+Data.

Naughton, J.J., Macdonald, G.A., and Greenberg, V.A., 1980, Some additional potassium-argon ages of Hawaiian rocks; the Maui Volcanic Complex of Molokai, Maui, Lanai, and Kahoolawe: Journal of Volcanology and Geothermal Research, v. 7, p. 339–355.

Nichols, W.D., Shade, P.J., and Hunt, C.D., 1996, Summary of the Oahu, Hawaii regional aquifer-system analysis: U.S. Geological Survey Professional Paper 1412–A, 61 p.

Oki, D.S., 2005, Numerical simulation of the effects of low-permeability valley-fill barriers and the redistribution of ground-water withdrawals in the Pearl Harbor Area, Oahu, Hawaii: U.S. Geological Survey Scientific Investigations Report 2005–5253, 111 p.

Oki, D.S, Souza, W.R., Bolke, E.L., and Bauer, G.R., 1998, Numerical analysis of the hydrogeologic controls in a layered coastal aquifer system, Oahu, Hawaii, USA: Hydrogeology Journal, v. 6, no. 2, p. 243–263.

Paillet, F.L., Williams, J.H., Oki, D.S., and Knutson, K.D., 2002, Comparison of formation and fluid-column logs in a heterogeneous basalt aquifer: Ground Water, v. 40, no. 6, p. 577–585.

Peterson, F.L., and Sehgal, M.M., 1974, Determining porosity with neutron logs from Hawaiian basaltic aquifers: University of Hawai‘i Water Resources Research Center Technical Report no. 80, 37 p.

Poeter, E.P., Hill, M.C., Banta, E.R., Mehl, Steffen, and Christensen, Steen, 2005, UCODE_2005 and Six Other Computer Codes for Universal Sensitivity Analysis, Calibration, and Uncertainty Evaluation: U.S. Geological Survey Techniques and Methods 6–A11, 283 p.

R.M. Towill Corporation, 1978, Feasibility study, surface water impoundment/recharge Pearl Harbor basin Oahu, Hawaii, variously paginated.

Rotzoll, K., 2010, Effects of groundwater withdrawal on borehole flow and salinity measured in deep monitor wells in Hawai‘i—implications for groundwater management: U.S. Geological Survey Scientific Investigations Report 2010–5058, 42 p.

Rotzoll, K., El-Kadi, A.I., and Gingerich, S.B., 2007, Estimating hydraulic properties of volcanic aquifers using constant-rate and variable-rate aquifer tests: Journal of the American Water Resources Association v. 43, no. 2, p. 334–345.

Rotzoll, K., Oki, D.S., and El-Kadi, A.I., 2010, Changes of freshwater-lens thickness in basaltic islands aquifers overlain by thick coastal sediments: Hydrogeology Journal, v. 18, no. 6, p. 1425–1436.

Sherrod, D.R., Nishimitsu, Yoshitomo, and Tagami, Takahiro, 2003, New K-Ar ages and the geologic evidence against rejuvenated-stage volcanism at Haleakalā, East Maui, a postshield-stage volcano of the Hawaiian island chain: Geological Society of America Bulletin, v. 115, no. 6, p. 683–694.

Souza, W.R., 1981, Ground-water status report, Lahaina District, Maui, Hawaii: U.S. Geological Survey Open-File Report 81–549, 2 sheets.

Souza, W.R., and Voss, C.I., 1987, Analysis of an anisotropic coastal aquifer system using variable-density flow and solute transport simulation: Journal of Hydrology, v. 92, p. 17–41.

State of Hawai‘i, 2008, Hawaii Water Plan, Water Resource Protection Plan, June 2008: Commission on Water Resource Management, Department of Land and Natural Resources, variously paginated.

State of Hawai‘i, 2010, Wailuku Water Company and HC&S to release water in Waihee River and Waiehu Stream: Department of Land and Natural Resources News Release NR01-100 released August 2, 2010, at http://hawaii.gov/dlnr/chair/pio/nr/2010/NR10-100.pdf/view.

State of Hawai‘i Department of Business, Economic Development, & Tourism, 2011, Research and data highlights released June 7, 2011, at http://hawaii.gov/dbedt/info/census/Census_2010/Info_release/2010_Census_Report_3_Informational_Release.pdf.

Stearns, H.T., and Macdonald, G.A., 1942, Geology and ground-water resources of the island of Maui, Hawaii: Hawai‘i Division of Hydrography Bulletin 7, 344 p.

Takasaki, K.J., 1978, Summary appraisals of the nation’s ground-water resources–Hawaii region: U.S. Geological Survey Professional Paper 813–M, 29 p.

Taylor, L.A., Eakins, B.W., Carignan, K.S., Warnken, R.R., Sazonova, T., and Schoolcraft, D.C., 2008, Digital elevation model of Lahaina, Hawaii—Procedures, data sources and analysis: NOAA Technical Memorandum NESDIS NGDC-10, National Geophysical Data Center, Boulder, Colorado, 19 p. at http://gcmd.nasa.gov/records/NOAA-NMMR_gov.noaa.ngdc.mgg.dem.tigp_hi_lahaina.html]

U.S. Environmental Protection Agency, 2011, Secondary Drinking Water Regulations: Guidance for Nuisance Chemicals, accessed July 29, 2011, at http://water.epa.gov/drink/contaminants/secondarystandards.cfm.

U.S. Geological Survey, 2006, Recent hydrologic conditions, Iao and Waihee aquifer areas, Maui, Hawaii, accessed November 27, 2006, at http://hi.water.usgs.gov/iao/iao_summary.htm.

U.S. Geological Survey, 2010, National Water Information System data available on the World Wide Web (Water Data for the Nation), accessed June 10, 2010, at http://waterdata.usgs.gov/nwis/inventory?agency_code=USGS&site_no=205655156412501.

U.S. Geological Survey, 2011, Recent hydrologic conditions, Hawaii, accessed March 4, 2011, at http://hi.water.usgs.gov/recent/hawaii/puukukui.html.

Voss, C.I., and Provost, A.M., 2002 (Version of June 2, 2008), SUTRA, A model for saturated-unsaturated variable-density ground-water flow with solute or energy transport: U.S. Geological Survey Water-Resources Investigations Report 02–4231, 270 p.

Wentworth, C.K., 1938, Geology and ground water resources of the Palolo-Waialae District; Honolulu, Hawaii: Honolulu Board of Water Supply, 274 p.

Wentworth, C.K., 1951, Geology and ground-water resources of the Honolulu-Pearl Harbor area, Oahu, Hawaii: Honolulu Board of Water Supply, 111 p.

Winston, R.B., and Voss, C.I., 2003, SutraGUI, a graphical-user interface for SUTRA, a model for ground-water flow with solute or energy transport: U.S. Geological Survey Open-File Report 03–285, 114 p., at http://water.usgs.gov/nrp/gwsoftware/sutra.html].

Yamanaga, George, and Huxel, C.J., 1969, Preliminary report on the water resources of the Lahaina District, Maui: State of Hawai‘i, Department of Land and Natural Resources, Division of Water and Land Development, Circular C51, 47 p.

Yamanaga, George, and Huxel, C.J., 1970, Preliminary report on the water resources of the Wailuku area, Maui: State of Hawai‘i, Department of Land and Natural Resources, Division of Water and Land Development, Circular C61, 43 p.

This page left intentionally blank.

Appendixes

Appendix A. Wells in the study area with stratigraphic information, Lahaina District, west Maui, Hawai‘i

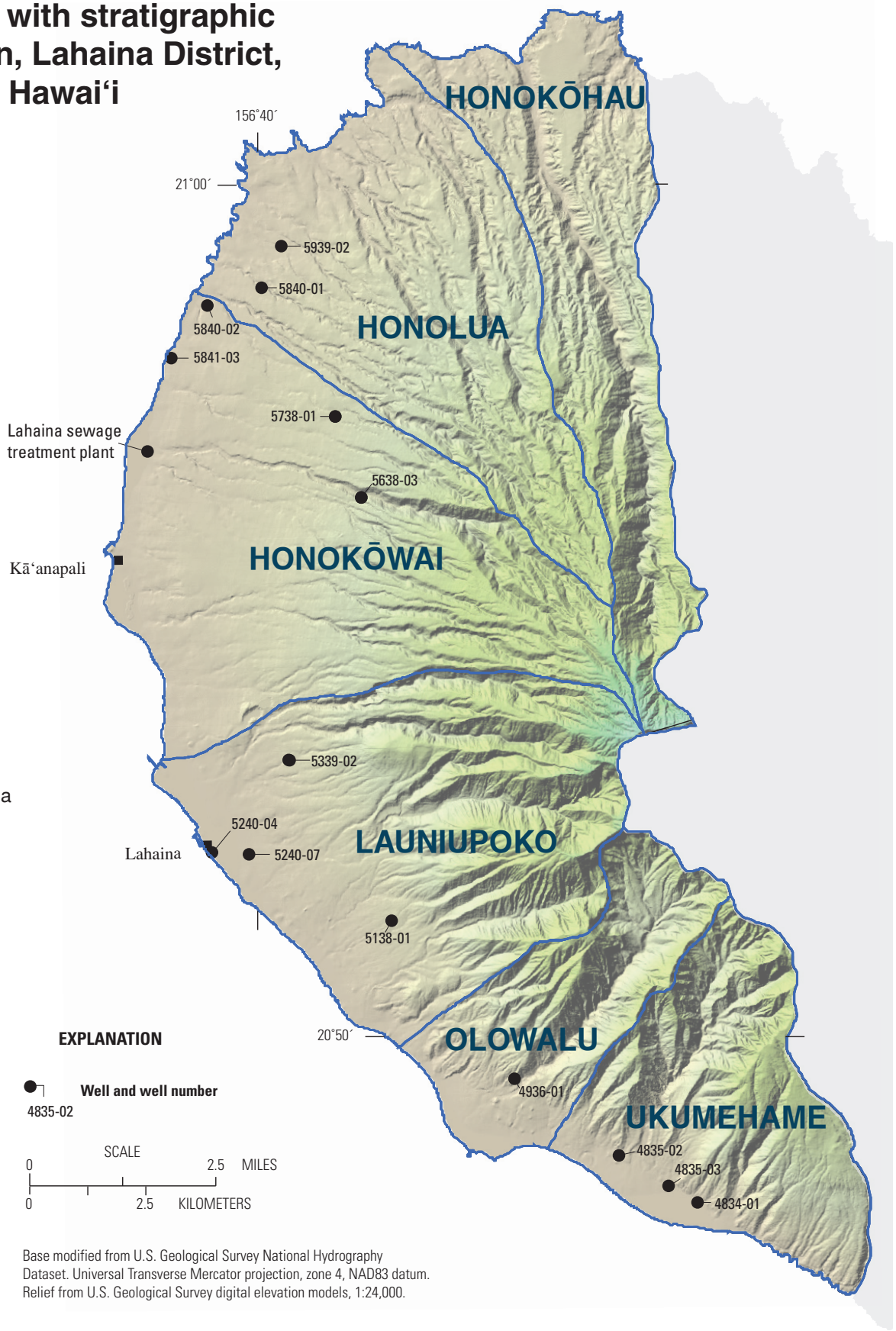

Figure A1. Wells in the study area with stratigraphic information, Lahaina District, west Maui, Hawai‘i.

Base modified from U.S. Geological Survey National Hydrography Dataset. Universal Transverse Mercator projection, zone 4, NAD83 datum. Relief from U.S. Geological Survey digital elevation models, 1:24,000.

Table A1. Wells in the study area with stratigraphic information, Lahaina District, west Maui, Hawai‘i.

[Altitude relative to mean sea level; CWRM, State of Hawai‘i Department of Land and Natural Resources Commission on Water Resource Management; USGS, U.S. Geological Survey Pacific Islands Water Science Center; <, deeper than]

Well number	Local well name	Altitude of top of Wailuku Basalt (feet)	Reference
4834-01	Environmental	22	CWRM well completion report
4835-02	Sugar Way 1	133	CWRM well completion report
4835-03	Sugar Way 2	< -27	CWRM well completion report
4936-01	Olowalu ‘Elua	135	CWRM well completion report
5138-01	Launiupoko 1	566	unpublished driller's log in USGS files
5240-04	Lahaina	-45	unpublished driller's log in USGS files
5240-07	Lahaina Park	-5	CWRM well completion report
5339-02	Waipuka 2	435	unpublished driller's log in USGS files
5638-03	Honokōwai B	785	CWRM well completion report
5738-01	P-5	884	CWRM well completion report
5840-01	‘Alaeloa	175	State of Hawaii (1965)
5840-02	Kahana Ridge	24	CWRM well completion report
5841-03	Shoemaker	4	CWRM well completion report
5939-02	Nāpili Park	132	CWRM well completion report
5641*01	Lahaina Sewage Treatment Plant 1	-52	unpublished driller's log in USGS files

Appendix B. Updated groundwater-recharge estimates for the Lahaina District, west Maui, Hawai‘i.

Groundwater recharge for central and west Maui, including the Lahaina District, was estimated by Engott and Vana (2007) for six time periods spanning 1926–004. These estimates incorporated historical rainfall and accounted for changes in land-cover and agricultural irrigation practices. Recharge also was estimated for several hypothetical rainfall and land-cover scenarios, including drought conditions and cessation of plantation-scale agriculture. The scenario without plantation-scale agriculture assumed all former sugarcane or pineapple fields were “cropland and pasture” and no irrigation was applied. Modifications to the water-budget model in Engott and Vana (2007) were made for this study to (1) give better consideration to canopy-interception processes in forests, (2) distinguish between native and alien forest, and (3) account for differences in the transpiration properties of forests depending on their location with respect to the fog zone. Discussed below are the salient changes made to the water-budget model and the resulting new groundwater-recharge estimates used in this study.

Refined Conceptual Model

A refined conceptual model was created that considers the differences between forested and non-forested land covers (fig. B1). For forest and non-forest areas (fig. B2), the conceptual model employs a plant-root zone reservoir; however, the model for forest areas includes a second reservoir consisting of the forest canopy. Net precipitation, which is the output from the canopy reservoir that becomes input to the plant-root zone reservoir, is calculated using a relation to fog interception and rainfall that is developed on the basis of results from published studies. Canopy evaporation is then calculated as the difference between the combined rainfall and fog interception volume and net precipitation.

Model Calculations

Changes to the model calculations reflect the changes to the conceptual model for forested areas. Model subareas with forested land cover are treated differently than in Engott and Vana (2007). Specifically, the interim moisture storage is computed using net precipitation.

For each subarea at the start of each day, the model calculates interim moisture storage. Interim moisture storage is the amount of water that enters the plant-root zone for the current day plus the amount of water already in the zone from the previous day. For non-forest subareas, it is given by the equation:

$$X_i = P_i + F_i + I_i + W_i - R_i + S_{i\text{-}1}, \quad (1a)$$

where:

X_i = interim moisture storage for current day [L],

P_i = rainfall for current day [L],

F_i = fog interception for current day [L],

I_i = irrigation for current day [L],

W_i = excess water from the impervious fraction of an urban area distributed over the pervious fraction [L],

R_i = runoff for current day [L],

$S_{i\text{-}1}$ = moisture storage at the end of the previous day (i-1) [L], and

i = subscript designating current day.

For forest subareas, interim moisture storage is given by the equation:

$$X_i = (NP)_i - R_i + S_{i-1}, \quad (1b)$$

where:

$(NP)_i$ = net precipitation for current day [L].

For forest subareas, net precipitation is computed as the sum of rainfall and fog interception less canopy evaporation, which is the amount of water from rainfall and fog that collects on the leaves, stems, and trunks of trees and subsequently evaporates. The equation is:

$$(NP)_i = P_i + F_i - (CE)_i, \quad (2)$$

where:

$(CE)_i$ = canopy evaporation for the current day [L].

The remainder of the equations in the Model Calculations section of Engott and Vana (2007) are unchanged.

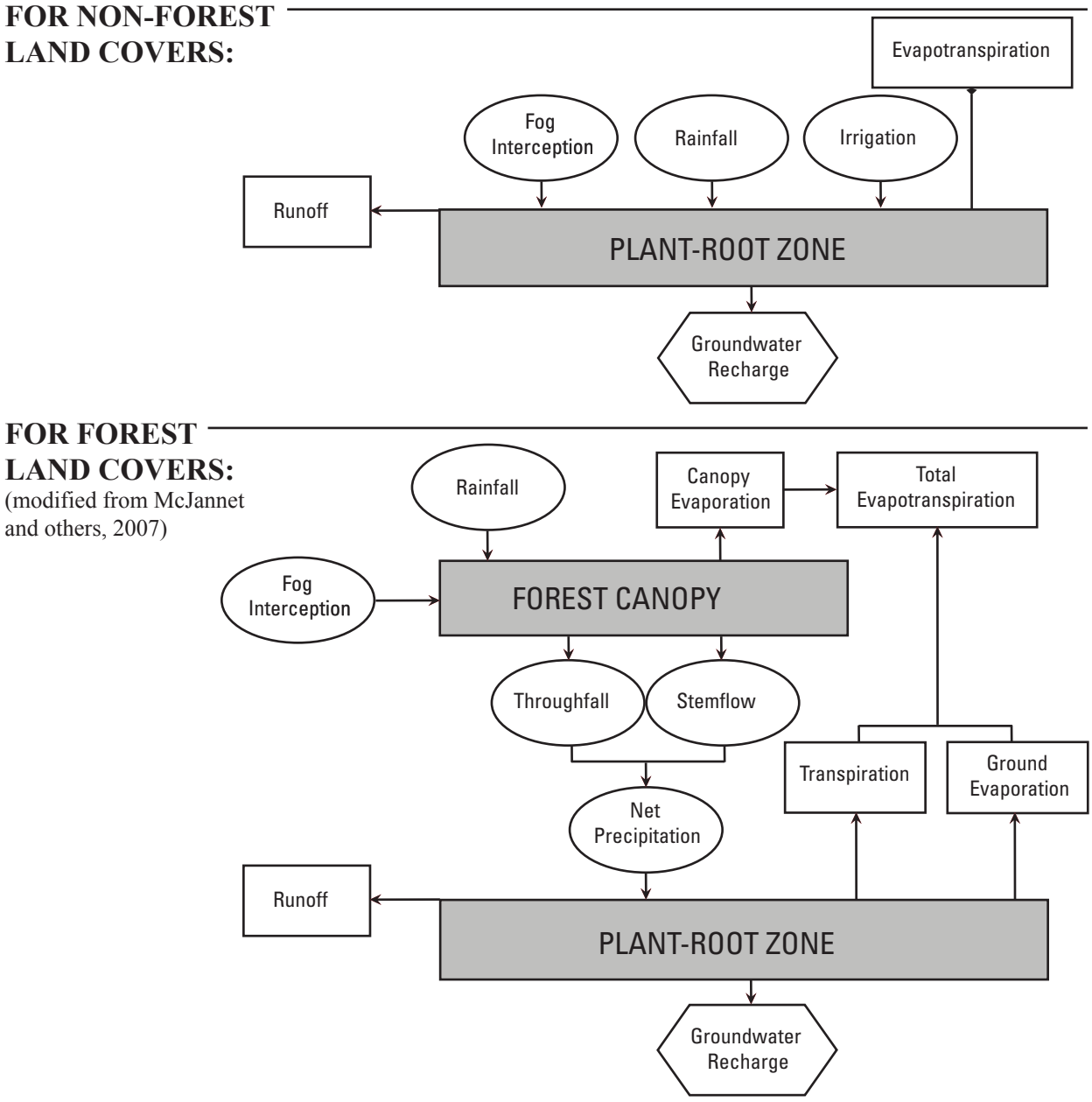

Figure B1. Generalized water-budget flow diagrams for forest and non-forest land covers.

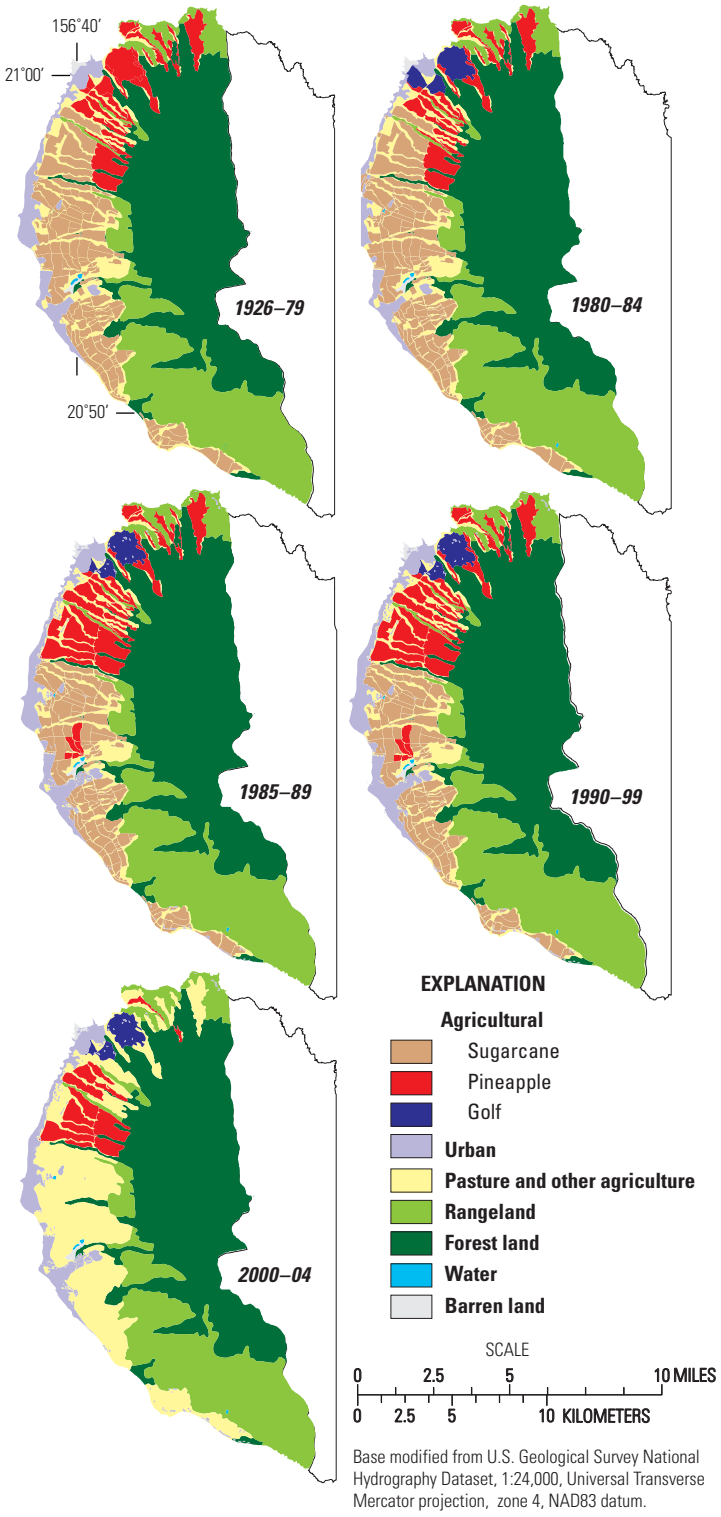

Figure B2. Land use during 1926–2004 in the Lahaina District, west Maui, Hawai‘i (modified from Engott and Vana, 2007).

Fog Interception

Engott and Vana (2007) limited the area in which fog contributed to the water budget to the windward side of the West Maui Volcano, above an elevation of 2,000 ft. However, their model considered only fog drip, which is fog intercepted by vegetation that subsequently drips or flows down branches or stems to the ground. With the addition of the forest-canopy reservoir, the new model handles fog differently. The new model requires an estimation of fog interception, rather than fog drip.

Fog interception occurs through the processes of turbulent diffusion and gravitational sedimentation of droplets onto vegetative surfaces, mainly leaves or needles (Bruijnzeel and others, 2005). Rates of fog interception are highly site dependent and influenced by meteorological and biotic variables, including the duration and frequency of fog periods, wind speed and direction, liquid water content of fog, and structural characteristics of the forest, such as height, size, spatial pattern, and physical characteristics of leaves and epiphytes (Walmsley and others, 1996; Bruijnzeel and others, 2005; Villegas and others, 2007). The quantification of fog interception is a notoriously complex endeavor and is the subject of continuing research, in Hawai‘i and worldwide. In water budgets, fog interception is commonly applied spatially within defined fog zones by using a relation to rainfall. One common method of estimating this relation is to compare the amount of cloud water collected in a mechanical fog gage to the amount of rainfall collected in a rain gage in the same area during concurrent periods.

Giambelluca and Nullet (1991) describe the fog zone in Hawai‘i as existing between about 600 and 2,400 meters (1,968 and 7,874 ft) above mean sea level. For the new water-budget model of the Lahaina Area, the lower extent of the fog zone is set at 2,000 ft. No upper limit on the elevation of the fog zone is needed, as the maximum elevation of the study area is only 5,788 ft, The ratio of fog interception to rainfall is set at 0.2 within the entire fog zone. This value reflects the middle of the range (0.11 to 0.29) given in Juvik and Ekern (1978, p. 46) for a transect of fog gages on the leeward side of Mauna Loa on the island of Hawai‘i.

Distinguishing Between Native and Alien Forest

For this study, the “forest land” land-cover category in Engott and Vana (2007) is divided between native forest and alien forest. In general, previous water budgets for the Hawaiian Islands (see for example, Izuka and others, 2005; Engott and Vana, 2007) placed all forested areas into a single land-cover category, failing to account for non-uniformity in forest structure and species. Owing to recent, ongoing studies of Hawaiian forest hydrology (Santiago and others, 2000; Giambelluca and others, 2009a; Giambelluca and others, 2009b; Kagawa and others, 2009), it has become feasible to

attempt to distinguish differences in water-budget parameters among different, albeit broad, categories of forest structure and species. Examination of the USGS GAP land-cover map (U.S. Geological Survey, 2006), which distinguishes between native and alien forest, shows that the boundary between native and alien forest generally is at an elevation of about 2,000 ft, with native forest existing at the higher elevations. Accordingly, the land-cover map in Engott and Vana (2007) was changed to account for the two different forest types. For this study, forest below 2,000 ft is considered alien forest, and forest at 2,000 ft and higher is considered native.

Evapotranspiration in Forested Areas

The evapotranspiration (ET) component of the water budget is treated differently for this study compared to that in Engott and Vana (2007). Evapotranspiration is a collective term for all of the evaporative processes in a plant-soil system. These processes can be grouped into 3 main types: (1) canopy evaporation, which is evaporation of intercepted rain and fog from the vegetation surface; (2) ground evaporation, which is evaporation from the soil surface and overlying litter and mulch layers; and (3) transpiration, the process by which soil moisture taken up by vegetation is eventually evaporated as it exits at plant pores (Viessman and Lewis, 2003, p. 143).

Historically, hydrologists have had difficulty distinguishing among the different processes and have simply combined them. Water budgets for Hawai‘i have treated ET similarly (for example, Giambelluca, 1983; Izuka and others, 2005; and Engott and Vana, 2007). A more rigorous treatment of ET may be appropriate for some areas because the various ET processes tend to operate on much different time scales and vary in relative importance according to prevailing meteorological conditions and land-cover setting. Canopy and ground evaporation operate on the order of hours, whereas transpiration operates on the order of weeks or longer, depending on soil depth (Savenije, 2004).

Canopy evaporation can be very important in forests. Because of the height of trees, turbulent diffusion is much more efficient at removing intercepted water from forests than from other land-cover types, Shuttleworth (1993) contends that the enhanced evaporation rate from wet canopy makes realistic estimates of ET from forests possible only if transpiration and canopy evaporation are evaluated separately. For this study, ET in forests is calculated by separately estimating canopy evaporation and combined ground evaporation and transpiration. These two terms are then added together to yield a total ET rate. For all other land covers, ET is calculated using the approach in Engott and Vana (2007), which is a more traditional approach that is commonly used in agricultural practice and other water budgets for Hawai‘i. No separate estimates of canopy evaporation and combined ground evaporation and transpiration are made for non-forested areas. The concept of potential ET, combined with soil-moisture limiting, is used to estimate ground evaporation and transpiration in forests and total ET for all other land covers. Canopy evaporation in forests is estimated using data from published studies.

Canopy Evaporation and Net Precipitation

As rain falls on a vegetated surface, a fraction of the droplets will strike and collect on the leaves, trunks, or stems of the vegetation in a process known as canopy interception. Additional moisture from fog interception may also enhance the volume of this collected water, which commonly is called “canopy storage.” Canopy storage is partitioned into 3 fractions: (1) that which remains on the vegetation and is evaporated after or during rainfall, called “canopy evaporation” in this report; (2) that which flows to the ground via trunks or stems, commonly called “stemflow;” and (3) that which drips from the canopy and falls to the ground between the various components of the vegetation (Crockford and Richardson, 2000). The fraction of rain that does not contact vegetation on the way to the ground combined with the fraction described in (3) commonly is called “throughfall.” The amount of water that reaches the soil surface, commonly called “net precipitation,” is the sum of throughfall and stemflow. Canopy interception takes place in all vegetated land covers, but research primarily has been limited to forests. Direct measurements of canopy evaporation are very difficult to obtain and rarely attempted. Instead, it is far more common for researchers to collect net precipitation on the floor of a forest, beneath the canopy, and compare it to rainfall collected contemporaneously above the forest canopy or in a nearby open field. Therefore, net precipitation commonly is reported as a percentage of rainfall, regardless of whether fog interception is occurring in the forest. In areas where fog interception takes place, it is possible for net precipitation to be greater than 100 percent of rainfall.

For this study, net precipitation in forests was estimated using published studies listed on figure B3. Nearly one-half of the sites investigated in these studies are in Hawai‘i—17 of 36. The rest of the sites are in similar tropical locations. For forests outside of the fog zone, the average net-precipitation value of 29 non-fog forest sites, 73.45 percent of rainfall, was used. For forests in the fog zone, a linear regression was applied to net-precipitation and fog-interception data (fig. B2). For the point on the graph where fog interception equals zero (the y-intercept), the aforementioned average net-precipitation value of the 29 non-fog forest sites was used. The regression line was forced through this value. This same method was used by Engott (2011) to estimate net precipitation on the island of Hawai‘i. As expected, net precipitation increases with increasing fog interception. The linear relation is strong, as shown by a coefficient of determination (R^2) of 0.895. However, a large gap exists in the data between the highest fog-interception site and the second-highest site. More data from sites where fog interception is between about 30 in/yr and 90 in/yr would increase confidence in the regression.

Pan Coefficients

Evidence exists that forests frequently affected by low clouds and fog transpire less water than forests in drier areas because of lower canopy conductances (Bruijnzeel and Veneklaas, 1998). Accordingly, the two forest categories are divided into fog and

non-fog subcategories on the basis of whether they are inside or outside the fog zone. It happens that the elevation of the lower extent of the fog zone and the border between native and alien forest coincide at 2,000 ft. Hence, for the purposes of this study, all native forest is inside the fog zone and all alien forest is outside the fog zone.

Giambelluca and others (2009b) examined the evaporation and energy balance of a closed *Metrosideros polymorpha* (ohia) native forest, the most common forest type on the island of Maui. The site is located on the island of Hawai‘i in the fog zone at an elevation of about 4,000 ft. They estimated an annual total ET rate of 1,232 mm (48.5 in). To separate the combined transpiration and ground-evaporation component from this total ET estimate, which is necessary for the water-budget model, an estimate of canopy evaporation at the site was made on the basis of modeled fog interception and the relation between net precipitation and fog interception discussed in the Canopy Evaporation and Net Precipitation section of this appendix. The canopy-evaporation estimate was then subtracted from total ET estimated by Giambelluca and others (2009b). This approach yielded a combined transpiration and ground-evaporation rate of about 24.2 in. According to Ekern and Chang (1985), mean annual pan evaporation at the study site is about 55 inches, implying a pan coefficient for combined transpiration and ground evaporation of 0.44 in native fog forest.

Santiago and others (2000) measured sapflow to estimate transpiration in a closed *M. Polymorpha* forest on East Maui. They reported transpiration rates at three, non-waterlogged sites that were 79 to 89 percent of Penman-Monteith evaporation during the 5 days with the highest evaporative demand. Adding the estimated rate of daily ground evaporation of 0.10 mm (0.004 in) reported by Jordan and Heuveldop (1981) for tropical rainforest in Venezuela, results in values ranging from 81 to 95 percent of Penman-Monteith evaporation. Converting to pan evaporation by using 0.85 as a ratio of Penman-Monteith evaporation to pan evaporation yields pan coefficients for combined transpiration and ground evaporation ranging from 0.69 to 0.81, with an average value of 0.74 for the three sites. Although it was not explicitly stated in Santiago and others (2000), it could be assumed that during these 5-day periods the presence of fog was minimal. In a different study, Giambelluca and others (2009a) measured sapflow to estimate transpiration in a native *M. Polymorpha* forest on the island of Hawai‘i during periods of wet and dry canopy. The mean transpiration rate during periods when the canopy was partially wet was reported to be 47 percent of transpiration during dry-canopy periods. If it is assumed that the result is representative of transpiration in native fog forests (partially wet canopy) and transpiration in native non-fog forests (dry canopy), then the pan coefficient for native non-fog forest could be computed from the pan coefficient for native fog forest (0.44) by dividing it by 0.47. The resulting value is 0.94. In the water-budget model, 0.84 was used as the combined transpiration and ground-evaporation pan coefficient for native non-fog forest. This is the average of the values derived from the studies of Santiago and others (2000) and Giambelluca and others (2009a).

In general, invasive alien species of trees consume more water through ET than do native species (Calder and Dye, 2001). On leeward Mauna Loa, Kagawa and others (2009) reported transpiration rates, as measured by sapflow, in an alien *Eucalyptus Saligna* plantation and an alien *Fraxinus uhdei* (tropical ash) forest that were about 1.3 and 2.5 times

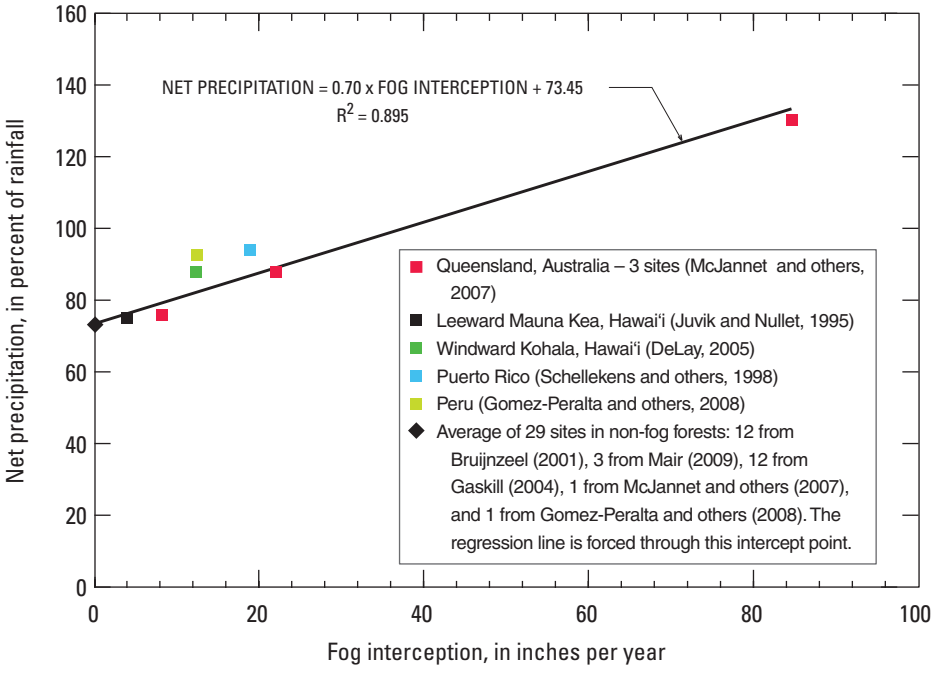

Figure B3. Analysis of the linear relation between net precipitation and fog interception in forests, based on data from studies in Hawai‘i and similar tropical locations around the world.

the rate in a native *M. Polymorpha* forest, respectively. The pan coefficient used in the model for alien forest inside the fog zone is 0.88, twice the pan coefficient for native forest inside the fog zone (0.44 x 2). This is also the pan coefficient used for mixed alien/native forest inside the fog zone. Outside the fog zone, the pan coefficient for these two forest types is 1.68 (0.84 x 2).

Updated Recharge Estimates

Updated recharge estimates generally are lower than the estimates from Engott and Vana (2007) (table B1). For each historical and hypothetical land-cover and rainfall scenario, total recharge for the entire Lahaina Area is lower by 2.50 to 9.86 percent. However, in 3 of the 5 aquifer systems that make up the Lahaina Area, updated recharge is higher for some scenarios.

The difference in recharge estimates is distributed spatially for the 2000–2004 land-cover and rainfall scenario (fig. B4). The spatial distribution of recharge change for this scenario is fairly representative of all scenarios. Change in recharge is limited to forested areas. Below the fog zone, where forests are assumed to consist of alien species for this study, updated recharge estimates are lower. In the fog zone, where forests are assumed to consist of native species, updated recharge estimates are higher in all but a few small areas.

Table B1. Updated groundwater-recharge estimates for each aquifer system in the Lahaina District, west Maui, Hawai'i, and the change in recharge estimates relative to Engott and Vana (2007).

[Aquifer systems from State of Hawai'i Commission on Water Resource Management (1990); LU1, 1926–79 land use and 1926–2004 rainfall; LU2, 2000–04 land use and 1926–2004 rainfall; LU3, 2000–04 land use without plantation-scale agriculture and 1926–2004 rainfall; LU2 drght, 2000-04 land use and 1998–2002 rainfall (drought condition); LU3 drght, 2000–04 land use without plantation-scale agriculture and 1998–2002 rainfall (drought condition); values of decreased recharge estimates are shown in red]

Groundwater-recharge estimate, in million gallons per day

Aquifer system	Historical land cover and rainfall						Hypothetical land cover and rainfall				
	1926–79	1980–84	1985–89	1990–94	1995–99	2000–04	LU1	LU2	LU3	LU2 drght	LU3 drght
Honokōhau	27.73	30.82	38.86	32.55	25.62	23.27	28.27	27.50	27.50	23.32	23.25
Honolua	23.54	26.92	32.41	26.45	20.79	16.60	24.14	21.05	19.06	15.94	13.94
Honokōwai	63.13	39.35	46.70	41.36	36.64	28.48	63.00	32.35	29.07	26.89	23.27
Launiupoko	51.02	41.68	48.3	41.2	34.74	25.27	51.57	33.61	33.94	25.58	25.72
Olowalu	17.78	17.73	18.89	18.65	13.78	9.94	18.08	14.47	14.53	10.18	10.21
Ukumehame	15.85	16.16	18.10	15.91	11.97	9.79	15.99	13.60	13.64	8.64	8.65
Total	199.04	172.66	203.25	176.13	143.54	113.35	201.06	142.59	137.73	110.55	105.05

Change in groundwater-recharge estimate relative to Engott and Vana (2007), in percent

Aquifer system	Historical land cover and rainfall						Hypothetical land cover and rainfall				
	1926–79	1980–84	1985–89	1990–94	1995–99	2000–04	LU1	LU2	LU3	LU2 drght	LU3 drght
Honokōhau	-17.80	-19.30	-18.94	-18.17	-15.58	-15.48	-17.95	-18.37	-17.94	-13.14	-13.17
Honolua	-18.24	-19.79	-20.26	-18.66	-16.80	-16.21	-18.35	-20.49	-22.75	-13.74	-15.41
Honokōwai	0.21	- 0.58	- 2.38	2.21	1.41	2.34	0.16	0.25	9.00	2.63	17.07
Launiupoko	1.06	0.56	- 0.76	1.74	2.37	4.32	0.99	1.48	2.35	4.13	5.58
Olowalu	-11.17	-13.11	-12.79	-13.80	-13.17	-12.65	-11.19	-13.60	-12.87	-13.66	-12.95
Ukumehame	- 2.82	- 4.02	- 3.40	- 3.94	- 3.03	- 2.14	- 2.96	- 3.45	- 0.49	- 2.23	1.64
Total	- 6.26	- 9.14	- 9.86	- 8.01	- 6.56	- 6.15	- 6.41	- 8.83	- 7.18	- 5.29	- 2.50

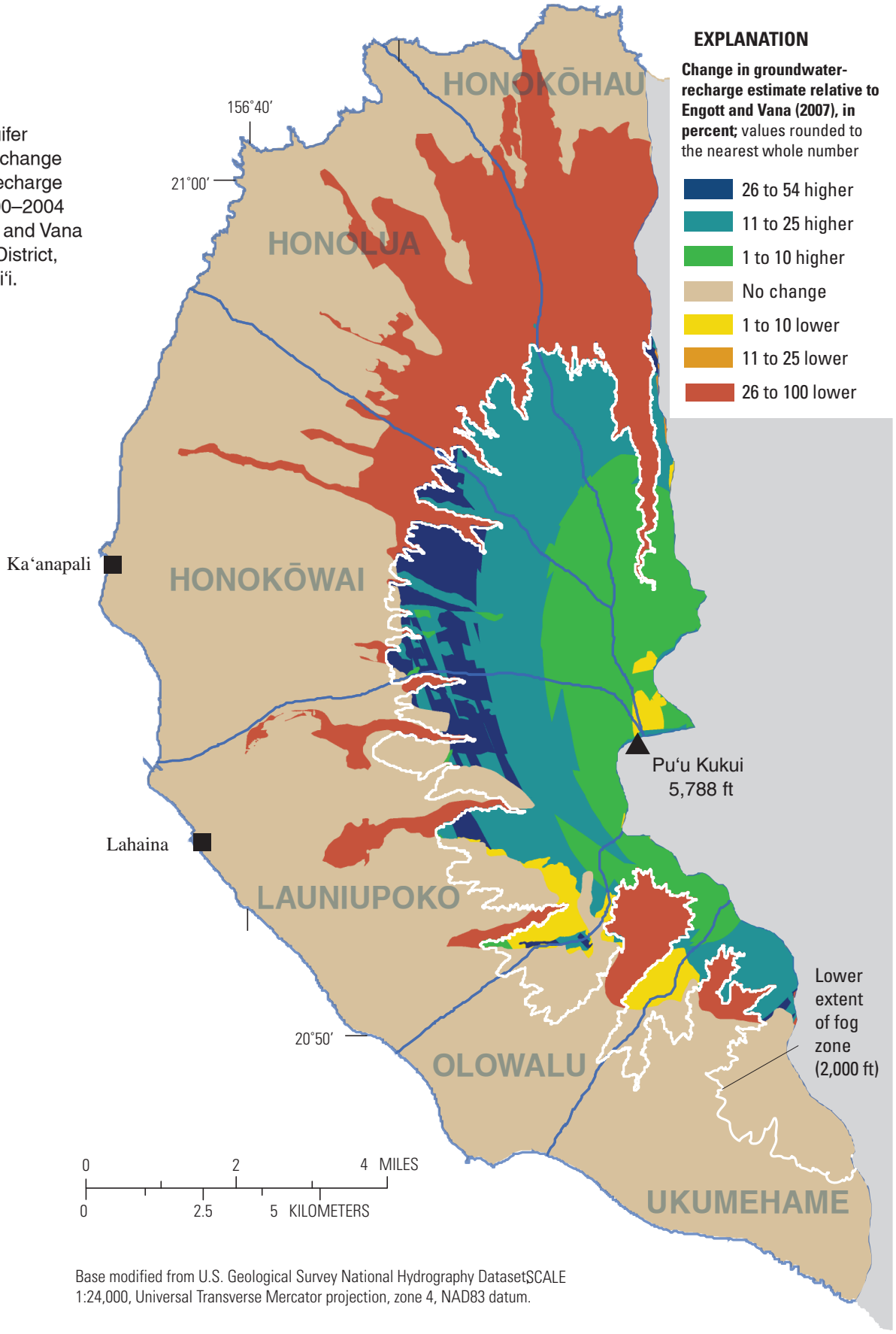

Figure B4. Aquifer systems and the change in groundwater-recharge estimates for 2000–2004 relative to Engott and Vana (2007), Lahaina District, west Maui, Hawai‘i.

Base modified from U.S. Geological Survey National Hydrography DatasetSCALE 1:24,000, Universal Transverse Mercator projection, zone 4, NAD83 datum.

References Cited

Bruijnzeel, L.A., 2001, Hydrology of tropical montane cloud forests: a reassessment: Land Use and Water Resources Research, v. 1, p. 1.1–1.18.

Bruijnzeel, L.A., and Veneklaas, E.J., 1998, Climatic conditions and tropical montane forest productivity: the fog has not lifted yet: Ecology, v. 79, no. 1, p. 3–9.

Bruijnzeel, L.A.S., Eugster, Werner, and Burkard, Reto, 2005, Fog as a hydrologic input, chap. 38 *of* Anderson, M.G., ed., Encyclopedia of Hydrological Sciences: Hoboken, New Jersey, John Wiley and Sons, Ltd., p. 559–582.

Calder, Ian, and Dye, Peter, 2001, Hydrological impacts of invasive alien plants: Land Use and Water Resources Research, v. 1, p. 8.1–8.12.

Commission on Water Resource Management, 1990, Water resources protection plan, June 1990: Hawai‘i Department of Land and Natural Resources, 2 v.

Crockford, R.H., and Richardson, D.P., 2000, Partitioning rainfall into throughfall, stemflow and interception: effect of forest type, ground cover and climate: Hydrological Processes, v. 14, p. 2903–2920.

DeLay, J.K., 2005, Canopy water balance on an elfin cloud forest at Alakahi, Hawai‘i: Honolulu, University of Hawai‘i, M.S. thesis, 78 p.

Ekern, P.C., and Chang, J.H., 1985, Pan evaporation: State of Hawai‘i, 1894–1983: State of Hawai‘i, Department of Land and Natural Resources, Division of Water and Land Development, Report R74, 172 p.

Engott, J.A., 2011, A water-budget model and assessment of groundwater recharge for the Island of Hawai‘i: U.S. Geological Survey Scientific Investigations Report 2011–5078, 53 p.

Engott, J.A., and Vana, T.T., 2007, Effects of agricultural land-use changes and rainfall on ground-water recharge in central and west Maui, Hawai‘i, 1926–2004: U.S. Geological Survey Scientific Investigations Report 2007–5103, 56 p.

Gaskill, T.G.R., 2004, Hydrology of forest ecosystems in the Honouliuli preserve: implications for groundwater recharge and watershed restoration: Honolulu, University of Hawai‘i, Ph.D. dissertation, 177 p.

Giambelluca, T.W., 1983, Water balance of the Pearl Harbor-Honolulu basin, Hawai‘i, 1946–1975: University of Hawai‘i Water Resources Research Center Technical Report no. 151, 151 p.

Giambelluca, T.W., and Nullet, Dennis, 1991, Influence of the trade-wind inversion on the climate of a leeward mountain slope in Hawaii: Climate Research, v. 1, p. 207–216.

Giambelluca, T.W., Delay, J.K., Takahashi, M., Mudd, R.G., Huang, M., Asner, G.P., Martin, R.E., and Nullet, M.A., 2009a, Effects of canopy wetness on evapotranspiration in native and invaded tropical montane cloud forest in Hawai‘i: American Geophysical Union, Fall Meeting 2009, abstract #H31G-01.

Giambelluca, T.W., Martin, R.E., Asner, G.P., Huang, Maoyi, Mudd, R.G., Nullet, M.A., DeLay, J.K., and Foote, David, 2009b, Evaporation and energy balance of native wet montane cloud forest in Hawai‘i: Agricultural and Forest Meteorology, v. 149, no. 2, p. 230–243.

Gomez-Peralta, Daniel, Oberbauer, S.F., McClain, M.E., and Philippi, T.E., 2008, Rainfall and cloud-water interception in tropical montane forests in the eastern Andes of central Peru: Forest Ecology and Management, v. 255, p. 1315–1325.

Izuka, S.K., Oki, D.S., and Chen, C., 2005, Effects of irrigation and rainfall reduction on ground-water recharge in the Lihue Basin, Kauai, Hawaii: U.S. Geological Survey Scientific Investigations Report 2005–5146, 48 p.

Jordan, C.F., and Heuveldop, J., 1981, The water budget of an Amazonian rain forest: Acta Amazonica, v. 11, p. 87–92.

Juvik, J.O., and Ekern, P.C., 1978, A climatology of mountain fog on Mauna Loa, Hawaii Island: University of Hawai‘i Water Resources Research Center Technical Report no. 118, 63 p.

Juvik, J.O., and Nullet, Dennis, 1995, Relationships between rainfall, cloud-water interception, and canopy throughfall in a Hawaiian montane forest, chap. 11 *of* Hamilton, L.S., Juvik, J.O., and Scatena, F.N., eds., Tropical Montane Cloud Forests: New York, Springer-Verlag, p. 165–182.

Kagawa, Aurora, Sack, Lawren, Duarte, Ka‘eo, and James, Shelley, 2009, Hawaiian native forest conserves water relative to timber plantation: Species and stand traits influence water use: Ecological Applications, v. 19, no. 6, p. 1429–1443.

Mair, Alan, 2009, Effects of rainfall variability and groundwater pumping on streamflow in the upper Mākaha Valley: Honolulu, University of Hawai‘i, Ph.D. dissertation, 200 p.

McJannet, David, Wallace, Jim, Fitch, Peter, Disher, Mark, and Reddell, Paul, 2007, Water balance of tropical rainforest canopies in north Queensland, Australia: Hydrological Processes, v. 21, p. 3473–3484.

Santiago, L.S., Goldstein, Guillermo, Meinzer, F.C., Fownes, J.H., and Muller-Dombois, Dieter, 2000, Transpiration and forest structure in relation to soil waterlogging in a Hawaiian montane cloud forest: Tree Physiology, v. 20, no. 10, p. 673–681.

Savenije, H.H.G., 2004, The importance of interception and why we should delete the term evapotranspiration from our vocabulary: Hydrological Processes, v. 18, p. 1507–1511.

Schellekens, J., Bruijnzeel, L.A. Wickel, A.J., Scatena, F.N., and Silver, W.L., 1998, Interception of horizontal precipitation by elfin cloud forest in the Luquillo Mountains, eastern Puerto Rico, *in* Schemenauer, R.S., and Bridgman, H.A., eds., First international conference on fog and fog collection: Ottawa, ICRC, p. 29–32.

Shuttleworth, W.J., 1993, Evaporation, chap. 4 *of* Maidment, D.R., ed., Handbook of hydrology: New York, McGraw-Hill, p. 4.1–4.53.

U.S. Geological Survey, 2006, A GAP analysis of Hawaii: U.S. Geological Survey, The Hawaii GAP Analysis Project, at http://gapanalysis.nbii.gov/portal/community/GAP_Analysis_Program/ Communities/GAP_Home/.

Viessman, Warren, Jr., and Lewis, G.L., 2003, Introduction to hydrology, (5th ed.): Upper Saddle River, N.J., Prentice Hall, 612 p.

Villegas, J.C., Tobon, Conrado, and Breshears, D.D., 2007, Fog interception by non-vascular epiphytes in tropical montane cloud forests: dependencies on gauge type and meteorological conditions: Hydrological Processes, v. 22, no. 14, p. 2484–2492.

Walmsley, J.L., Schemenauer, R.S., and Bridgman, H.A., 1996, A method for estimating the hydrologic input from fog in mountainous terrain: Journal of Applied Meteorology, v. 35, no. 12, p. 2237–2249.

Appendix C. Monthly groundwater withdrawals during 1900–2008 from wells in west Maui, Hawai‘i

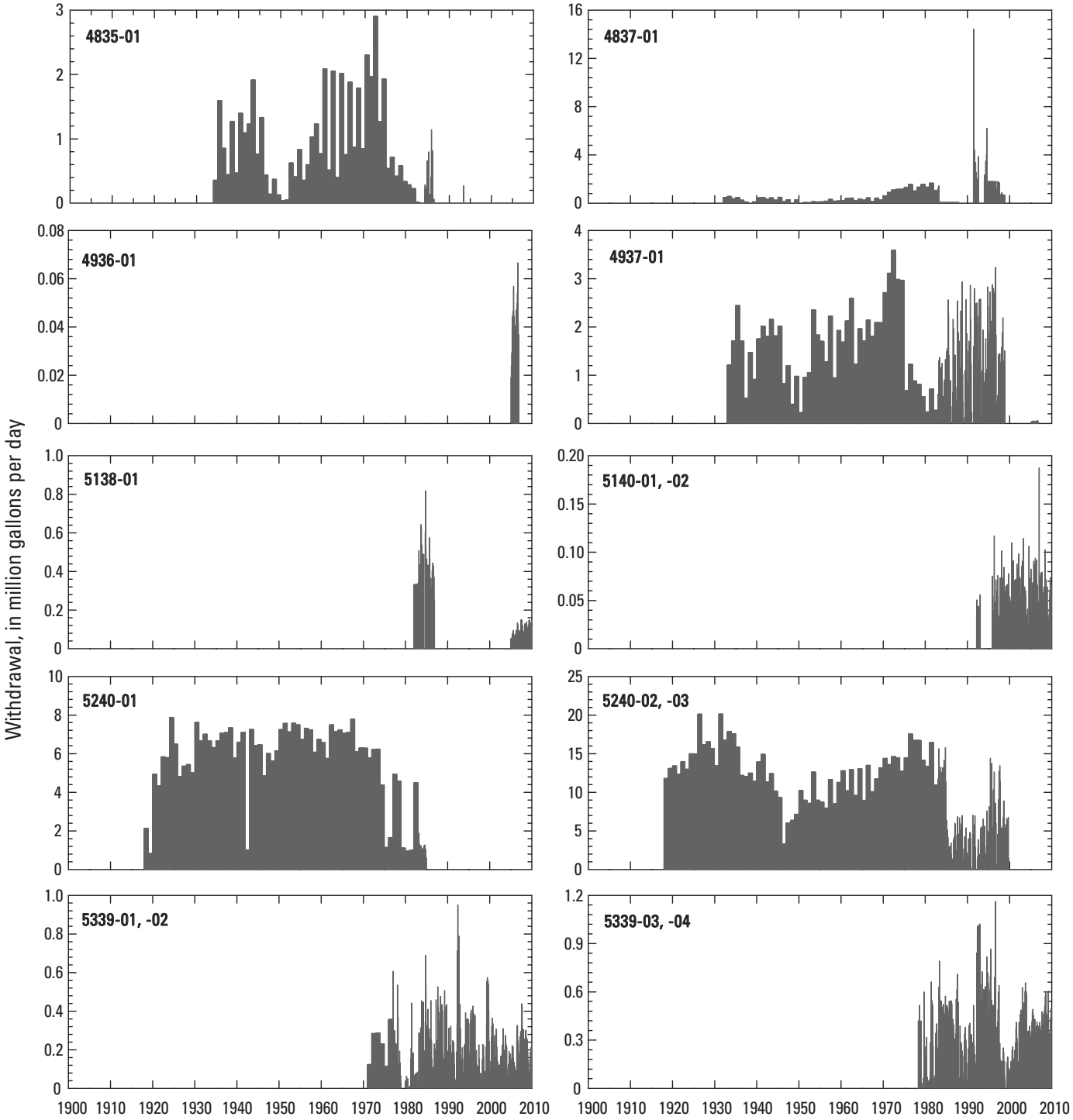

Figure C1. Groundwater withdrawal data for wells in the study area, Lahaina District, west Maui, Hawai‘i.

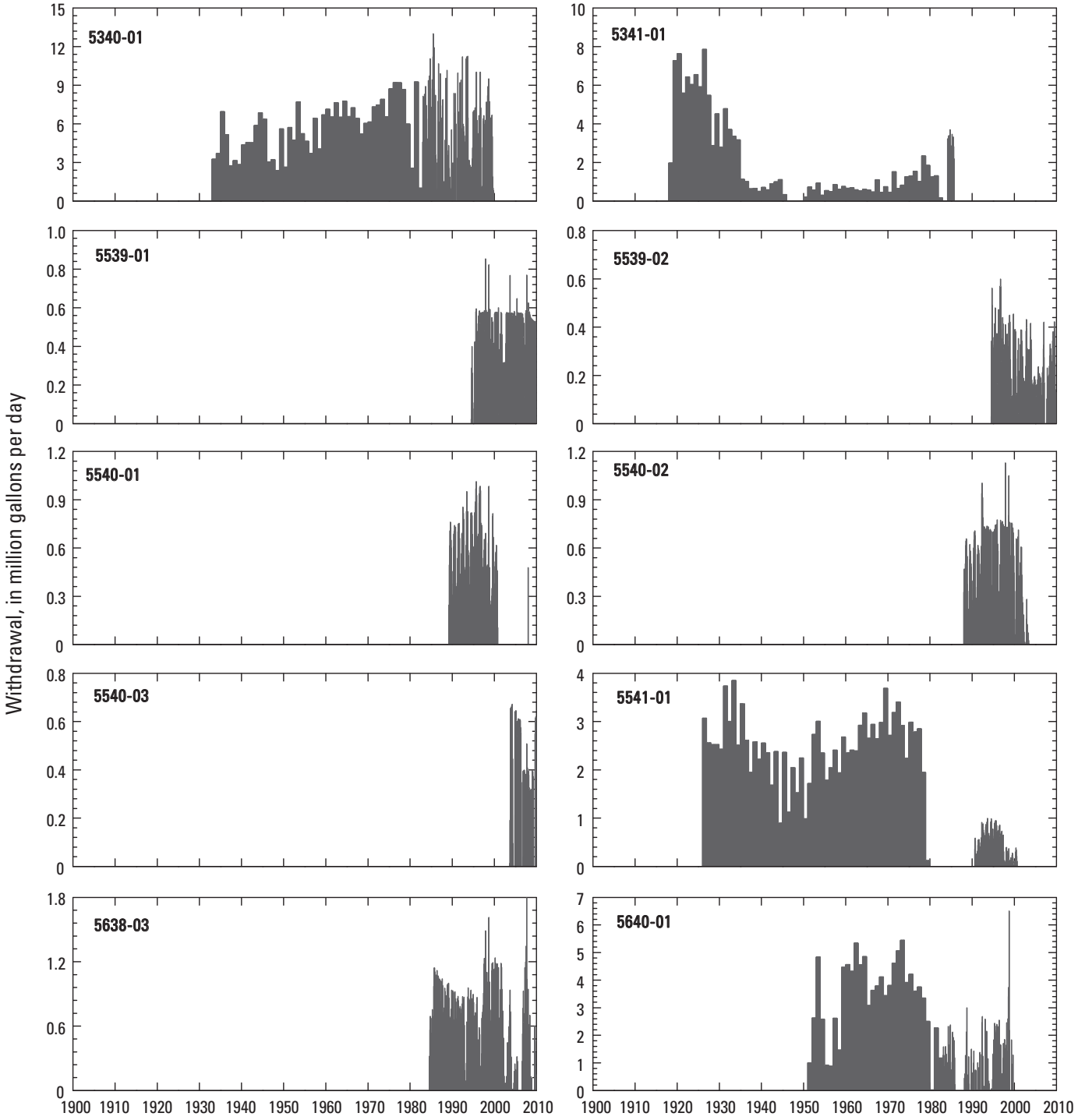

Figure C1. Groundwater withdrawal data for wells in the study area, Lahaina District, west Maui, Hawai'i—continued.

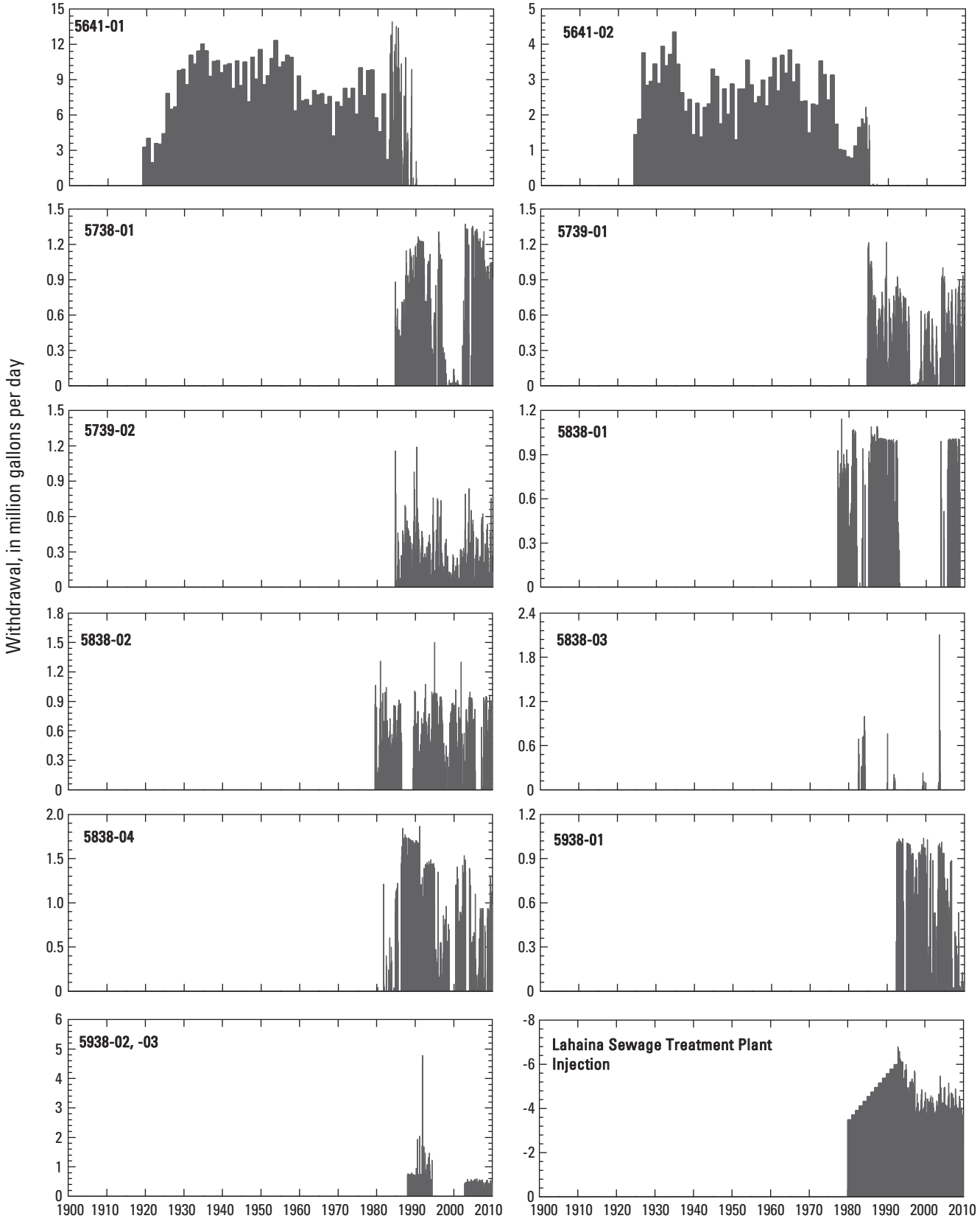

Figure C1. Groundwater withdrawal data for wells in the study area, Lahaina District, west Maui, Hawai‘i—continued.

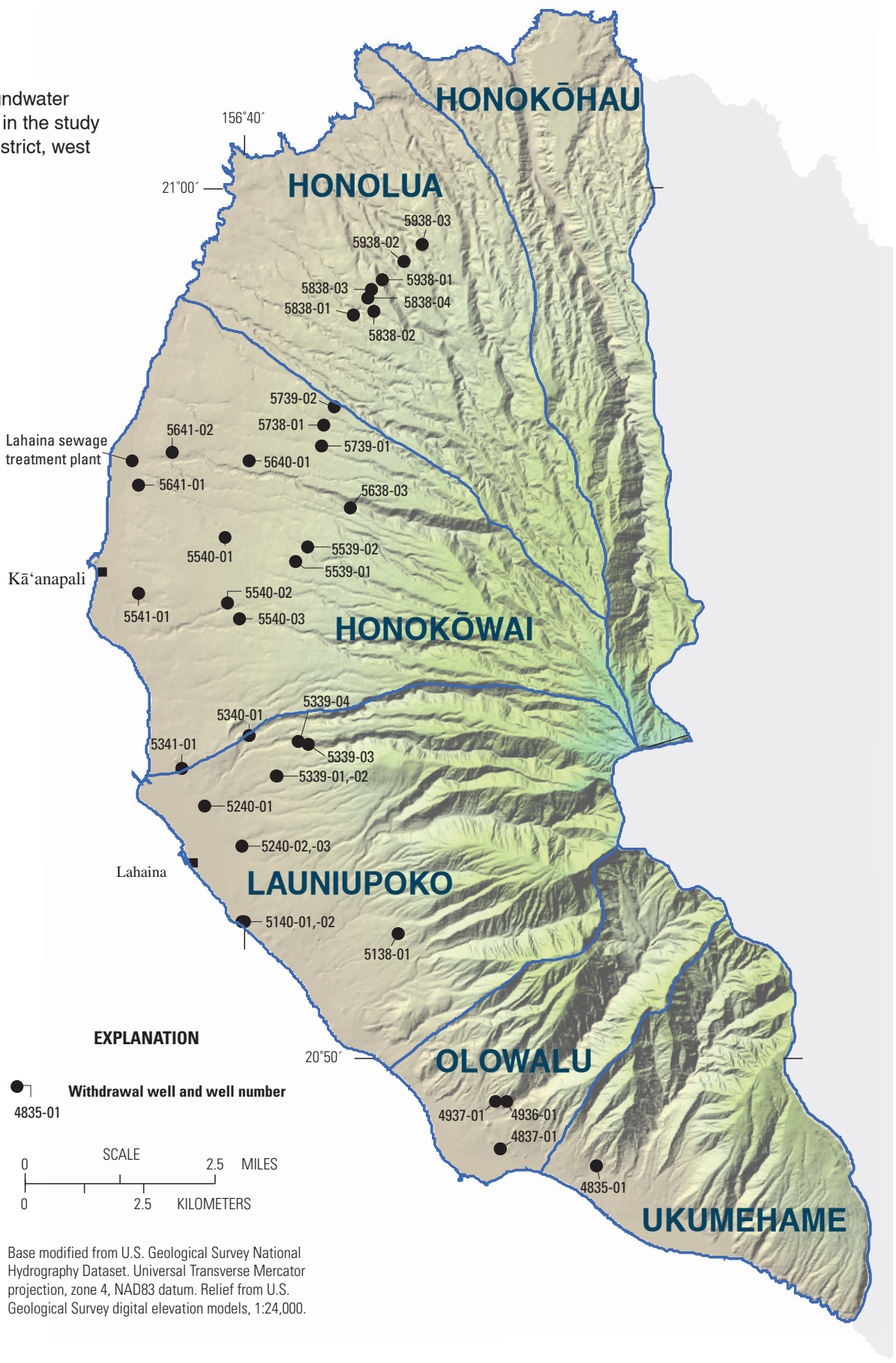

Figure C2. Groundwater withdrawal wells in the study area, Lahaina District, west Maui, Hawai‘i.

Base modified from U.S. Geological Survey National Hydrography Dataset. Universal Transverse Mercator projection, zone 4, NAD83 datum. Relief from U.S. Geological Survey digital elevation models, 1:24,000.

Appendix D. Properties of pumped wells in the study area, Lahaina District, west Maui, Hawai‘i.

Table D1. Properties of pumped wells in the Lahaina District, west Maui, Hawai‘i.

[nr, not reported; --, not applicable; Maui-type shafts are generally open from above the water table to several feet below the water table; Data from State of Hawai‘i Department of Land and Natural Resources Commission on Water Resource Management well database and U.S. Geological Survey Pacific Islands Water Science Center well files; length of shafts reported in Stearns and Macdonald (1942)]

Well number	Well name	Year drilled	Altitude of top of open interval (feet relative to sea level)	Altitude of bottom of open interval (feet relative to sea level)	Length of horizontal shaft (feet)
4835-01	Pump P (shaft)	1934	nr	nr	428
4837-01	Pump O (shaft)	1905	nr	nr	670
4936-01	Olowalu	1999	-6	-24	--
4937-01	Pump N (shaft)	1933	nr	nr	239
5137-01	Launiupoko 2	2000	-4	-35	--
5138-01	Launiupoko 1	1979	1	-44	--
5238-01	Launiupoko 3	2002	7	-48	--
5140-01	Puamana 1	1987	-3	-31	--
5140-02	Puamana 2	1987	-12	-45	--
5240-01	Pump C (shaft)	1897	nr	nr	768
5240-03	Pump B (shaft)	1897	nr	nr	1,094
5339-01	Waipuka 1	1962	4	-57	--
5339-03	Kanahā 1	1977	1	-52	--
5339-04	Kanahā 2	1974	3	-92	--
5340-01	Pump M (shaft)	1933	nr	nr	3,801
5341-01	Pump L (shaft)	1897	nr	nr	215
5439-01	Wahikuli 1	1992	5	-60	--
5439-02	Wahikuli 2	1993	1	-65	--
5539-01	P-1	1990	-1	-61	--
5539-02	P-2	1991	0	-63	--
5540-01	Pu‘ukoli‘i	1968	0	-28	--
5540-02	Hāhākea 1	1971	0	-20	--
5540-03	Hāhākea 2	1971	0	-20	--
5541-01	Pump G (shaft)	1923	nr	nr	187
5638-03	Honokōwai B	1976	10	-43	--
5640-01	Pump R (shaft)	1952	nr	nr	nr
5641-01	Pump D (shaft)	1897	nr	nr	1,561
5641-02	Pump F (shaft)	1921	nr	nr	--
5738-01	P-5	1982	4	-36	--
5739-01	P-4	1982	3	-54	--
5739-02	P-6	1982	1	-47	--
5838-01	Nāpili A	1971	0	-33	--
5838-02	Nāpili B	1972	1	-32	--
5838-03	Honokahua A	1978	0	-31	--
5838-04	Nāpili C	1979	-1	-21	--
5938-01	Honokahua B	1987	0	-20	--
5938-02	Kapalua 1	1989	13	-54	--
5938-03	Kapalua 2	1991	-2	-42	--
5641*1	Lahaina Injection 1	1979	-53	-168	--
5641*2	Lahaina Injection 2	1979	-55	-150	--
5641*3	Lahaina Injection 3	1985	-80	-200	--
5641*4	Lahaina Injection 4	1985	-79	-229	--

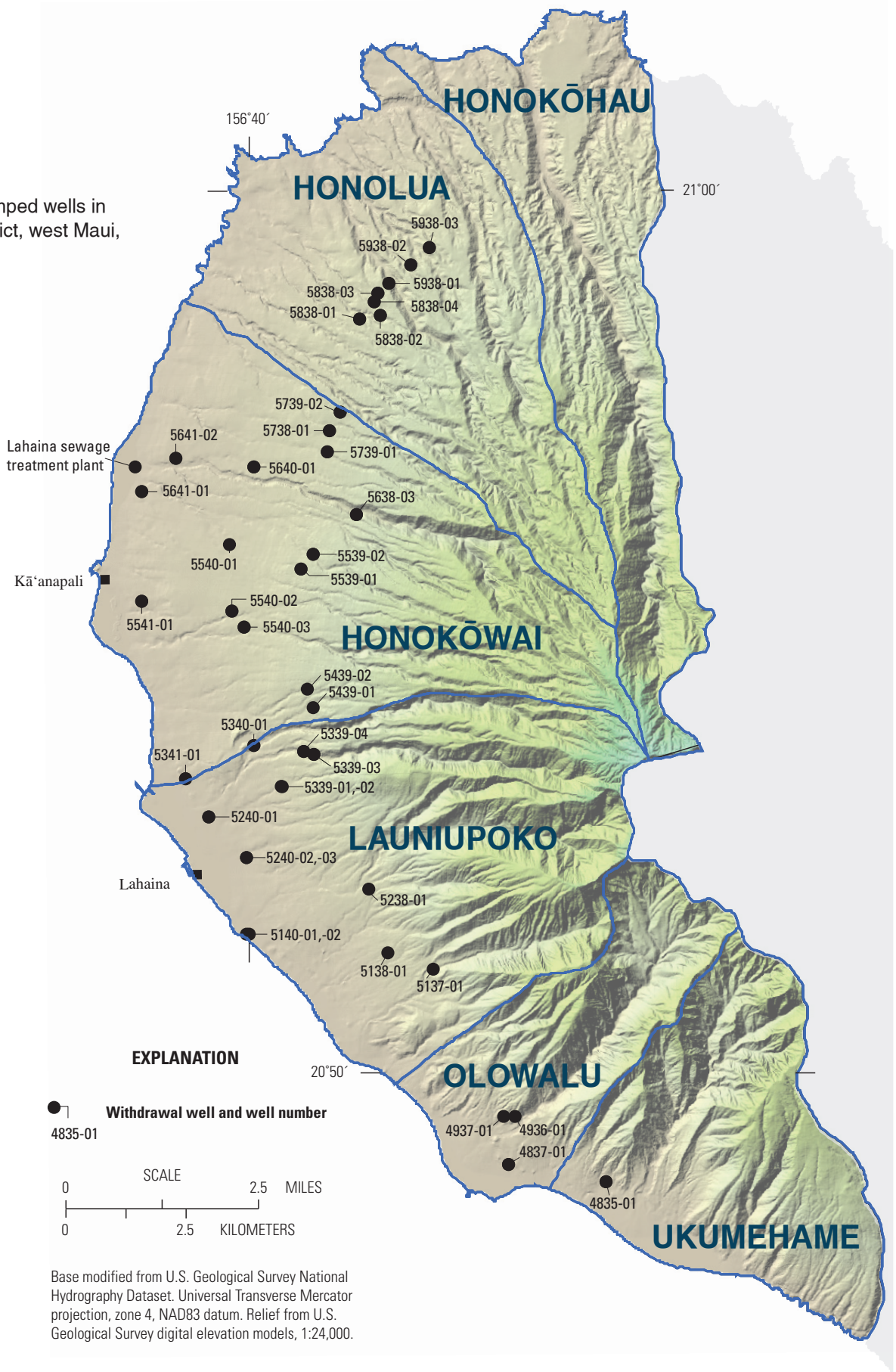

Figure D1. Pumped wells in the Lahaina District, west Maui, Hawai‘i.

Base modified from U.S. Geological Survey National Hydrography Dataset. Universal Transverse Mercator projection, zone 4, NAD83 datum. Relief from U.S. Geological Survey digital elevation models, 1:24,000.

Produced in the Western Region, Menlo Park, California
Manuscript approved for publication, December 16, 2011
Layout by Jeanne S. DiLeo